

Inhibition of tyrosinase-induced enzymatic browning by sulfite and natural alternatives

Tomas F.M. Kuijpers

Thesis committee

Promotor

Prof. Dr H. Gruppen
Professor of Food Chemistry
Wageningen University

Co-promotor

Dr J-P. Vincken
Assistant professor, Laboratory of Food Chemistry
Wageningen University

Other members

Prof. Dr M.A.J.S van Boekel, Wageningen University
Dr H.T.W.M. van der Hijden, Unilever R&D, Vlaardingen, The Netherlands
Dr C.M.G.C. Renard, INRA, Avignon, France
Prof. Dr H. Hilz, Hochschule Bremerhaven, Germany

This research was conducted under the auspices of the Graduate School VLAG (Advanced studies in Food Technology, Agrobiotechnology, Nutrition and Health Sciences).

Inhibition of tyrosinase-induced enzymatic browning by sulfite and natural alternatives

Tomas F.M. Kuijpers

Thesis

submitted in fulfilment of the requirements for the degree of doctor
at Wageningen University
by the authority of the Rector Magnificus
Prof. Dr M.J. Kropff,
in the presence of the
Thesis Committee appointed by the Academic Board
to be defended in public
on Friday 25 October 2013
at 4 p.m. in the Aula.

Tomas F.M. Kuijpers

Inhibition of tyrosinase-mediated enzymatic browning by sulfite and natural alternatives

136 pages

PhD thesis, Wageningen University, Wageningen, NL (2013)
With references, with summaries in English and Dutch

ISBN: 978-94-6173-668-0

ABSTRACT

Although sulfite is widely used to counteract enzymatic browning, its mechanism has remained largely unknown. We describe a double inhibitory mechanism of sulfite on enzymatic browning, affecting both the enzymatic oxidation of phenols into *o*-quinones, as well as the non-enzymatic reactions of these *o*-quinones into brown pigments. The non-enzymatic step is inhibited by formation of addition products of sulfite and *o*-quinones, sulfophenolics. Sulfonated derivatives of chlorogenic acid were found in sulfite-treated potato juice, and their structure was confirmed by mass spectrometry and nuclear magnetic resonance spectroscopy. Sulfonation of chlorogenic acid was demonstrated to occur via tyrosinase-catalyzed *o*-quinone formation. Tyrosinase activity was also irreversibly inactivated, in a relative slow time-dependent way. Simultaneous treatment of tyrosinase with sulfite and competitive inhibitors of tyrosinase did not result in irreversible inactivation, indicating that sulfite acts in the active site of tyrosinase. LC-MS analysis of protease digests of sulfite-treated tyrosinase indicated that inactivation occurred via covalent modification of a single amino acid residue in the active site, most likely a copper-coordinating histidine residue, which is conserved in all PPOs.

As the use of sulfite is controversial, we investigated the effect of potential natural inhibitors of enzymatic browning. Two different polyphenol oxidases (PPOs) were used to screen 60 plant extracts for potential inhibitors. PPOs were found to respond differently to these extracts: an extract that inhibited one PPO could activate the other. This suggests that natural alternatives to replace more generic anti-browning agents, such as sulfite, are PPO specific.

TABLE OF CONTENTS

Abstract		
Chapter 1	General introduction	1
Chapter 2	New insights into an ancient anti-browning agent: formation of sulfo-phenolics in sodium hydrogen sulfite treated potato extracts	17
Chapter 3	Inhibition of enzymatic browning of chlorogenic acid by sulfur-containing compounds	35
Chapter 4	The anti-browning agent sulfite inactivates mushroom tyrosinase through covalent modification of the copper-B site	55
Chapter 5	Potato and mushroom polyphenol oxidase activities are differently modulated by natural plant extracts	75
Chapter 6	General discussion	93
Summary		107
Samenvatting		111
Acknowledgements		115
About the author		119

Chapter 1

General introduction

Enzymatic browning in foods occurs through the oxidation of phenolic compounds by polyphenol oxidases. Brown discoloration is a major quality issue in the processing of foods, mainly fruits and vegetables (e.g. apples (1), potatoes (2)), but also shrimps (3) and mushrooms (4), and accounts for large economic losses in food industry (5). Besides its general detrimental effect, enzymatic browning is a desired effect in some other food processes, for example the enzymatic fermentation of tea (6) and cocoa (7).

CHARACTERISTICS OF POLYPHENOL OXIDASE

The nomenclature of different polyphenol oxidases (PPOs) is diffuse. Depending on the reactions catalyzed, they are categorized as cresolase, tyrosinase or monophenolase (PPOs that catalyze both *o*-hydroxylation and subsequent oxidation of monophenols and oxidation of *o*-diphenols) or as catecholase, catechol oxidase or diphenolase (PPOs that catalyze only oxidation of *o*-diphenols) (8, 9) (**Figure 1**). Although there are separate EC numbers for the *o*-hydroxylation and subsequent oxidation of monophenols (EC 1.14.18.1) and the oxidation of *o*-diphenols (EC 1.10.3.1), they are not consequently used. Tyrosinase, for instance, is sometimes indicated with EC 1.14.18.1 (10), and sometimes with EC 1.10.3.1 (11). Moreover, laccases (EC 1.10.3.2), enzymes that are capable of catalyzing the oxidation of both *o*-diphenols and *p*-diphenols, are considered to be PPOs by some, while others restrict the term PPO to enzymes having monophenolase or *o*-diphenolase activity (12). Structurally, laccases are different from other PPOs: laccases have two copper centers, one type-1 copper center and a combined type-2/type-3 copper center, while other PPOs have a single dinuclear type-3 copper center (13) (**Figure 2**). In this thesis, when the term PPO is used, it refers to type-3 copper proteins catalyzing the *o*-hydroxylation and subsequent oxidation of monophenols or the oxidation of *o*-diphenols.

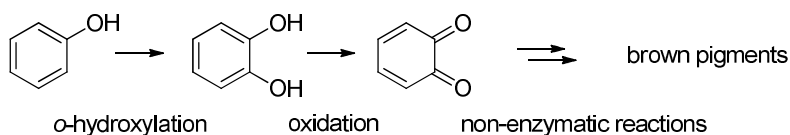


Figure 1. Schematic representation of enzymatic browning. *o*-Hydroxylation and oxidation are catalyzed by PPO. The *o*-quinones obtained participate in non-enzymatic reactions, resulting in formation of brown pigments.

PPOs are distributed widely in nature, and their function varies depending on species (14). For instance in plants PPO-catalyzed oxidation is thought to play a role in defense response against herbivores and pathogens (15), while in mammals it is responsible for initiating pigment formation (16), and in insects it is involved in sclerotization (17). The dinuclear type-3 copper center of PPO is highly conserved (18) and is also present in hemocyanins, oxygen carrier proteins in molluscs and arthropods (19). Under specific conditions,

hemocyanins also display phenol oxidase activity, suggesting that the protein structure around the copper center and the accessibility of the copper center can be modulated to facilitate oxidase activity (20-22). The two copper ions, Cu-A and Cu-B, in the type-3 copper center of PPO are each coordinated by three histidine residues. For several PPOs, a thioether has been found in the Cu-A binding site, a covalent bond between the thiol group of a cysteine and C ϵ 1 of the imidazole ring of one of the histidine residues coordinating Cu-A (**Figure 2**). This thioether is found in PPOs from different species, for instance grape (*Vitis vinifera*) (23), sweet potato (*Ipomoea batatas*) (24), mushroom (*Agaricus bisporus*) (25) and the fungus *Neurospora crassa* (26). A similar thioether has been found in several hemocyanins (27). It has been proposed that the formation of the thioether is catalyzed by presence of copper in the active site (23). The thioether is not essential for activity of PPOs in general, active PPOs without thioether bond in the Cu-A site have been described as well, for instance from the bacteria *Streptomyces castaneoglobosporus* (28) and *Bacillus megaterium* (29).

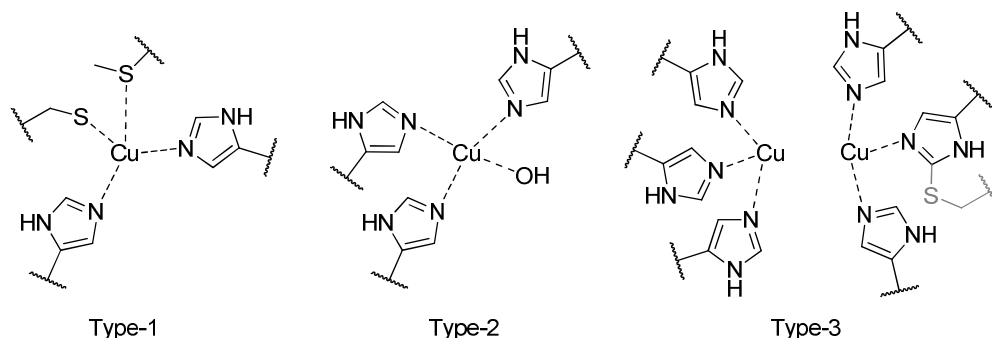


Figure 2. Schematic representation of type-1, type-2 and type-3 copper centers (adapted from (78)). In the type-3 copper center the His-Cys thioether that is found in some PPOs and hemocyanins is indicated in grey.

Catalytic mechanism of PPO

Depending on the oxidation states of the copper ions and the binding of oxygen to the copper ions, the active site of PPO is present in the met, oxy or deoxy state (**Figure 3**) (9). When present in the met state, the copper ions are in the Cu(II) oxidation state, with hydroxyl ligands bridging the two copper ions. In this state, an *o*-diphenol can bind. The *o*-diphenol is oxidized to an *o*-quinone, leaving the copper site in the reduced deoxy state, in which the copper ions are in the Cu(I) oxidation state. When present in the deoxy state, the copper ions can be oxidized by binding molecular oxygen, resulting in oxy PPO. When present in the oxy state, either an *o*-diphenol or a monophenol can bind. When an *o*-diphenol binds, it is oxidized, resulting in formation of an *o*-quinone and met PPO, after which the diphenolase cycle can start again. If a monophenol binds to oxy PPO, it is

o-hydroxylated and subsequently oxidized, resulting in an *o*-quinone and deoxy PPO. Deoxy PPO can be oxidized by molecular oxygen, resulting in oxy PPO, and either the mono or diphenolase cycle can be repeated. In the resting state, PPO is present predominantly in the met state, which causes the typical lag phase observed when assaying PPO activity on a monophenolic substrate. Whether a PPO has monophenolase or only diphenolase activity has been related to the amino acid residues surrounding the Cu-A binding site. It has been speculated that a phenylalanine shielding the Cu-A binding site prevents binding of monophenols to Cu-A, in this way blocking monophenolase activity (21,30).

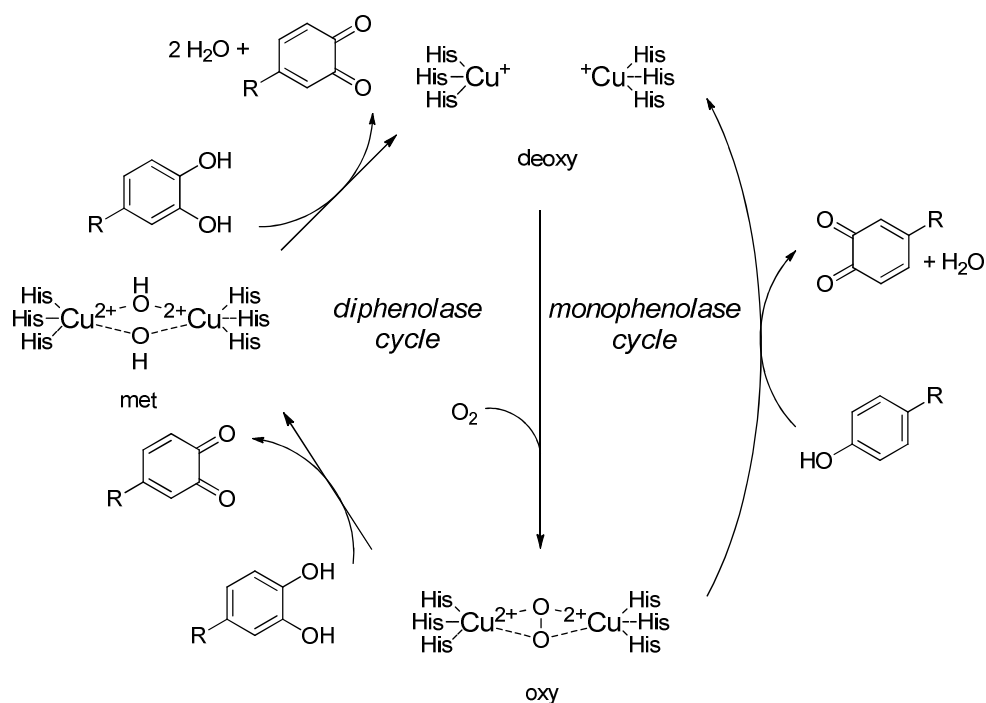


Figure 3. Schematic representation of the catalytic cycles of PPO for oxidation of *o*-diphenols and hydroxylation and subsequent oxidation of monophenols (adapted from (9)).

Quaternary structures of PPOs

To date, the crystal structures of several PPOs have been published. Although the type-3 copper center is conserved in all PPOs, the structure of the protein differs between PPOs from different sources. Some PPOs are monomers, e.g. grape and sweet potato PPO (23,24), while others are oligomeric, e.g. mushroom tyrosinase and *Streptomyces castaneoglobisporus* tyrosinase (28). Owing to its commercial availability, mushroom tyrosinase is one of the most studied PPOs. In solution, mushroom tyrosinase is a

heterotetramer, composed of two catalytically active subunits of 43 kDa (so-called heavy or H-chain), each containing a dinuclear type-3 copper center, and two smaller 14 kDa subunits (so-called light or L-chain), resulting in the quaternary structure H_2L_2 (31). In mushroom, six genes encoding the H-chain have been found, while only one gene encoding the L-chain has been identified (32-34). It is assumed that the L-chain can form the active tyrosinase tetramer with H-chains resulting from different genes. The function of the light chain, however, remains unknown (35-37).

FORMATION OF BROWN PIGMENTS

While referred to as enzymatic browning, the formation of brown pigments actually occurs through non-enzymatic reactions of the *o*-quinones resulting from PPO-catalyzed oxidation (**Figure 1**). The *o*-quinones are more reactive than their *o*-diphenolic precursors, and can polymerize with phenolics (38,39) or react with other compounds, for instance proteins or amino acids (40,41). These reactions result in a wide variety of dark colored products, which are often not well characterized. An exception to this is the formation of the mammalian pigment melanin, the metabolic pathway of which has been well described (**Figure 4**) (16,42). Tyrosinase hydroxylates tyrosine to 3,4-dihydroxyphenyl alanine (DOPA), which is subsequently oxidized to DOPAquinone. DOPAquinone can react further in two pathways, forming either pheomelanin or eumelanin. Addition of cysteine to DOPAquinone results in formation of pheomelanin, while ring closure with the amino group results in the formation of dopachrome, which can further react to eumelanin. The concentration and distribution of these two types of melanin determine the color of human skin, hair and eyes. The intermediate dopachrome is relatively stable, and has a characteristic red color (43), the accumulation of which can be easily monitored. Because of this, the conversion of tyrosine or DOPA to dopachrome is often used to assay PPO activity *in vitro*.

An example in which a much wider variety of reaction products is obtained is the fermentation of green tea to black tea. The relatively simple phenolic profile of green tea (44) is, via oxidation by PPO and laccase, converted to a variety of dark colored reaction products. It is estimated that several thousands of different products are formed (6), the characterization and classification of which is an ongoing endeavor (45-47). Reaction products are mainly classified as theaflavins which have relatively low molecular masses (up to 1000 g/mol) and thearubigens, polymeric polyphenols with higher molecular mass (6). PPO and laccase-catalyzed browning in tea is considered a positive effect, as it contributes to the formation of color and flavor of black tea. Similarly, during the fermentation of cocoa beans, PPO-catalyzed oxidation of phenolics contributes to color and flavor of the final cocoa products (7,48,49).

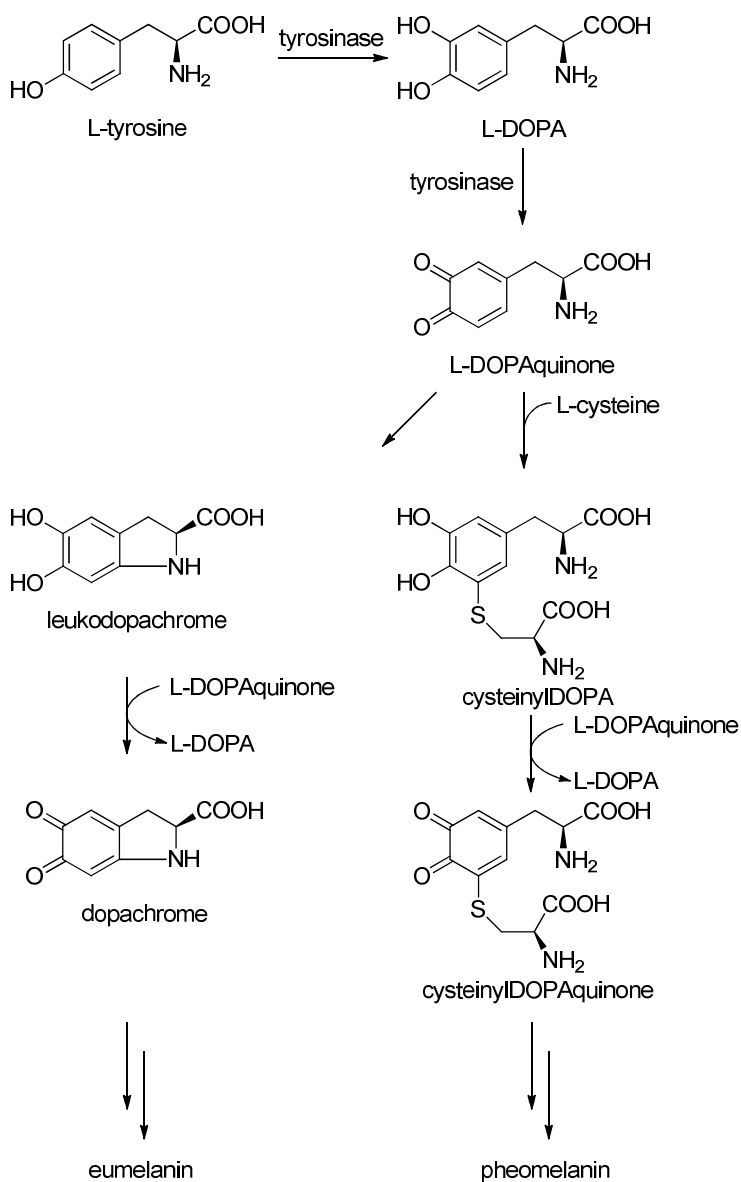


Figure 4. Formation of the mammalian pigments eumelanin and pheomelanin is initiated by the tyrosinase catalyzed hydroxylation and subsequent oxidation of L-tyrosine (adapted from (8, 16, 42).

For most other food products, enzymatic browning is considered a negative effect of processing. An example is the browning of potatoes, which is especially relevant for the large scale industrial processing of potatoes, in which starch and protein are extracted to

serve as food ingredients. Browning of the protein fraction can occur if PPO is not sufficiently inhibited. It was found that browning of potato protein occurred through covalent interactions with chlorogenic acid (50). Using model systems, covalent addition of chlorogenic acid to proteins has been demonstrated to proceed through PPO-catalyzed oxidation (41,51). Other examples include mushrooms, browning of which occurs as a result of bruising sustained during harvesting and post-harvest handling (52), and shrimps, which show discoloration as a result of PPO catalyzed oxidation of tyrosine during chilled storage (3,53).

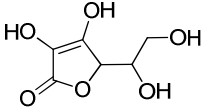
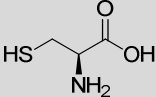
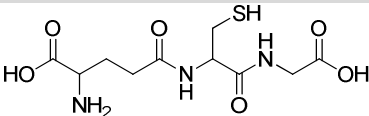
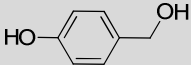
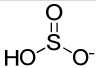
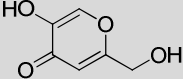
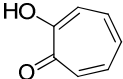
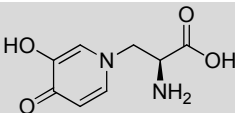
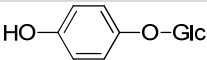
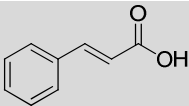
INHIBITION OF ENZYMATIC BROWNING

The fact that enzymatic browning in fact involves both enzymatic and non-enzymatic steps means that two main strategies can be applied to inhibit brown discoloration. First, the enzymatic action can be prevented by inhibiting or inactivating PPO, so that no reactive *o*-quinones are formed. A second approach is to prevent the *o*-quinones from reacting into brown pigments by using reducing compounds, that either reduce *o*-quinones back to their *o*-diphenolic precursors or form colorless addition products with *o*-quinones. For illustration, some examples of different inhibitors of browning are listed in **Table 1**.

The most common example of a reducing compound used to prevent enzymatic browning is ascorbic acid, which reduces *o*-quinones back to their *o*-diphenolic precursors (54). The *o*-diphenols can be oxidized again by PPO, illustrating the disadvantage of this method: the oxidation and subsequent reduction can only continue if ascorbic acid is still present. After depletion of ascorbic acid browning will still occur. Alternatively, reducing compounds that react with *o*-quinones to form phenolic addition products can be used to trap *o*-quinones. An example of the latter is cysteine, which reacts with *o*-quinones to form colorless addition products, which cannot be oxidized by PPO anymore (55). Interestingly, addition of cysteine to DOPAquinone also occurs in mammalian pigmentation, eventually leading to the formation of pheomelanin (**Figure 4**), which indicates that cysteine addition to *o*-quinones not necessarily prevents color formation in all cases.

Inhibiting the enzymatic formation of *o*-quinones can be accomplished by rendering PPO inactive by changing temperature or pH. However, this will not only affect PPO, also other properties of a product will be modified. Therefore, this approach is only useful in a limited number of cases. A more specific way of prevention of browning is inhibition of PPO with reversible or irreversible inhibitors. Numerous reversible inhibitors of PPO have been reported (56-59), which can inhibit PPO through competitive, non-competitive, uncompetitive or mixed type inhibition. For illustration, the structures, reported IC₅₀ values and type of inhibition of some inhibitors of mushroom tyrosinase are given (**Table 1**). As can be seen from the examples given, reported IC₅₀ values widely differ, and multiple mechanisms of inhibition have been proposed for some inhibitors. This indicates that it is difficult to compare different inhibitor studies with each other, and that probably the

Table 1. A selection of some common inhibitors of enzymatic browning. IC₅₀ values reported were determined using mushroom tyrosinase and L-tyrosine or L-DOPA as substrate.

Inhibitor (references)	IC ₅₀ (μM)	Type of inhibition
 Ascorbic acid (54)	-	Reduction of <i>o</i> -quinones
 L-cysteine (55)	-	Addition to <i>o</i> -quinones
 Glutathione (54)	-	Addition to <i>o</i> -quinones
 <i>p</i> -hydroxybenzyl alcohol (89)	351	Irreversible inactivation
 Sulfites (62,66,67)	-	Reduction of <i>o</i> -quinones Addition to <i>o</i> -quinones Inactivation of tyrosinase
 Kojic acid (79,80)	4.0-230	Competitive Noncompetitive Mixed
 Tropolone (81,82)	0.4-2.1	Mixed Competitive
 L-Mimosine (83,84)	3.7-340	Competitive
 Arbutin (85,86)	40-1113	Competitive
 Cinnamic acid (87,88)	700-2100	Mixed Competitive

method of assessing the PPO inhibitory potential of a compound is important for the outcome. A common structural feature of all inhibitors in **Table 1** seems to be a more or less planar ring, which is often substituted with a hydroxyl or a hydroxyl and adjacent carbonyl group. This planar structure might suggest that these compounds could act as substrate analogs, targeting the active site of PPO, which would fit with the reported competitive mode of inhibition proposed for all of these compounds. Of course structural prerequisites cannot be determined based on only a few structures. More promising in that respect are computational studies, in which the potential inhibitory effect of compounds is predicted based on their structure (60,61). Another possibility of inactivating PPO is by chelation of the copper ions from the active site. EDTA and citric acid have been reported to inhibit PPO in this way (62).

SULFITE AS AN INHIBITOR OF ENZYMATIC BROWNING

One of the most commonly used inhibitors of enzymatic browning is sulfite. Already in ancient times, sulfur was burned in wine barrels, resulting in deposition of sulfur dioxide on the wall of the barrel. Once filled with wine, the sulfur dioxide would dissolve, and give sulfite in solution (63). Nowadays, different sulfite salts are used as food additive, which when dissolved all result in a pH dependent mixture of SO_3^{2-} and HSO_3^- , with the bisulfite ion (HSO_3^-) being the major contributor in the pH range 3-7 (64,65). Remarkably, despite its longstanding use, the inhibitory mechanism of sulfite on enzymatic browning has not been fully explained yet. Different explanations have been suggested over the years, including irreversible inactivation of PPO (66), reduction of *o*-quinones to *o*-diphenols (62), and formation of addition products between sulfite and *o*-quinones (67).

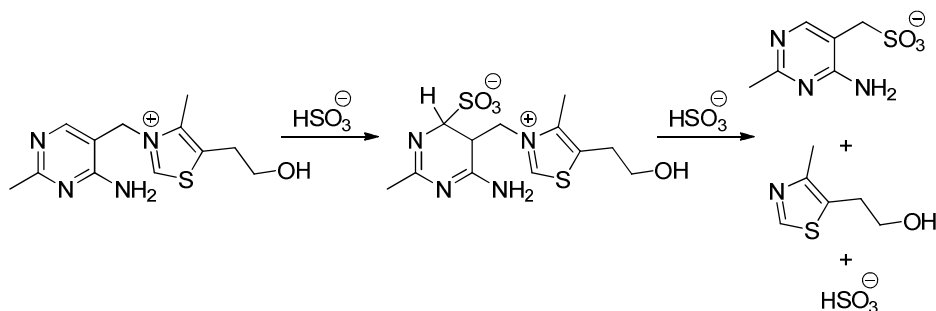


Figure 5. Proposed reaction of thiamine with sulfite (adapted from (74)).

The use of sulfites as a food additive is becoming increasingly controversial due to presumed health risks, such as allergies, resulting in skin rash (68) or even anaphylaxis (69), and adverse pulmonary reactions in asthmatic patients (70). These negative health

effects are doubted by others. For instance, some studies in which the often reported response of sulfite-sensitive individuals to wine was investigated did not find a correlation between sulfite and reported symptoms of sulfite-sensitivity (71,72). Another negative side effect of sulfite is its reaction with vitamin B1 (thiamine), the methylene bridge (between the pyrimidine and thiazole moiety) of which is cleaved by sulfite (**Figure 5**) (73-75). Because of these adverse effects of sulfite, its use is strictly regulated by European and US food laws. The use of sulfite is only permitted in selected food products, and maximum levels of sulfite are set for different product categories (76,77). For instance, in the European Union, sulfite can be used in red and white wine (up to 160 mg/L and 210 mg/L, respectively) and in dried fruits, such as apricots (2000 mg/kg) (77).

AIM AND OUTLINE OF THE THESIS

The use of sulfite as a food additive is controversial, and bound to strict regulations, and much research has been dedicated to finding new inhibitors of enzymatic browning. Surprisingly enough, despite its established use, the mechanism of browning inhibition by sulfite remains largely unknown, with different possible explanations proposed in literature. The aim of this thesis is to explain the inhibitory mechanism of sulfite on enzymatic browning in more detail, by investigating its effects on reaction products of enzymatic browning and tyrosinase activity. Furthermore, the possible influence of the source of PPO on the outcome of screening studies for PPO inhibitors is investigated by screening plant extracts using two different PPOs.

In **Chapter 2**, the effect of the enzymatic browning inhibitors ascorbic acid and sodium hydrogen sulfite on the phenolic composition of potato juice is compared. Using RP-UHPLC-PDA-MS sulfophenolics were found in sulfite-treated potato juice. Applying a model system, it was demonstrated that sulfonation occurred via tyrosinase-catalyzed *o*-quinone formation. The effect of sulfite in this model browning system was further investigated in **Chapter 3**. The effect of sulfite was compared to the effect of other sulfur-containing inhibitors of enzymatic browning. Besides tyrosinase-mediated formation of sulfophenolics, a time-dependent inhibition of tyrosinase activity was observed. This time-dependent inhibition was investigated in more detail in **Chapter 4**, where the irreversible inactivation of mushroom tyrosinase through covalent modification of a single amino acid residue in the active site is described. In **Chapter 5** potato PPO and mushroom tyrosinase were compared with respect to inhibition by plant extracts. The screening of a collection of plant extracts for inhibitory activities on both PPOs is described. Large differences in the effects of plant extracts on the different PPOs were found. In **Chapter 6** the implications of our findings are discussed. Additional experimental data on the possible formation of sulfophenolics in wine and a competition experiment for the addition of sulfite, cysteine and glutathione to enzymatically formed *o*-quinones is provided.

Furthermore, the possible extrapolation of the results found for the inhibition of tyrosinase-catalyzed browning by sulfite to other PPOs and laccases is discussed.

REFERENCES

1. Chow, Y.-N.; Louarme, L.; Bonazzi, C.; Nicolas, J.; Billaud, C., Apple polyphenoloxidase inactivation during heating in the presence of ascorbic acid and chlorogenic acid. *Food Chem.* **2011**, *129*, 761-767.
2. Marri, C.; Frazzoli, A.; Hochkoeppler, A.; Poggi, V., Purification of a polyphenol oxidase isoform from potato (*Solanum tuberosum*) tubers. *Phytochemistry* **2003**, *63*, 745-752.
3. Nirmal, N. P.; Benjakul, S., Effect of ferulic acid on inhibition of polyphenoloxidase and quality changes of Pacific white shrimp (*Litopenaeus vannamei*) during iced storage. *Food Chem.* **2009**, *116*, 323-331.
4. Jolivet, S.; Arpin, N.; Wichers, H. J.; Pellon, G., *Agaricus bisporus* browning: a review. *Mycol. Res.* **1998**, *102*, 1459-1483.
5. Vámos-Vigyázó, L.; Haard, N. F., Polyphenol oxidases and peroxidases in fruits and vegetables. *CRC Cr. Rev. Food Sci.* **1981**, *15*, 49-127.
6. Drynan, J. W.; Clifford, M. N.; Obuchowicz, J.; Kuhnert, N., The chemistry of low molecular weight black tea polyphenols. *Nat. Prod. Rep.* **2010**, *27*, 417-462.
7. Hansen, C. E.; del Olmo, M.; Burri, C., Enzyme activities in cocoa beans during fermentation. *J. Sci. Food Agric.* **1998**, *77*, 273-281.
8. Sánchez-Ferrer, Á.; Neptuno Rodríguez-López, J.; García-Cánovas, F.; García-Carmona, F., Tyrosinase: a comprehensive review of its mechanism. *Biochim. Biophys. Acta* **1995**, *1247*, 1-11.
9. Yoruk, R.; Marshall, M. R., Physicochemical properties and function of plant polyphenol oxidase: a review. *J. Food Biochem.* **2003**, *27*, 361-422.
10. Muñoz, E.; Avila, J. G.; Alarcón, J.; Kubo, I.; Werner, E.; Céspedes, C. L., Tyrosinase inhibitors from *Calceolaria integrifolia* s.l.: *Calceolaria talcana* aerial parts. *J. Agric. Food Chem.* **2013**, *61*, 4336-4343.
11. Li, J. L. Y.; Sulaiman, M.; Beckett, R. P.; Minibayeva, F. V., Cell wall peroxidases in the liverwort *Dumortiera hirsuta* are responsible for extracellular superoxide production, and can display tyrosinase activity. *Physiol. Plant.* **2010**, *138*, 474-484.
12. Ferrar, P. H.; Walker, J. R. L., Inhibition of diphenol oxidases: a comparative study. *J. Food Biochem.* **1996**, *20*, 15-30.
13. Claus, H., Laccases and their occurrence in prokaryotes. *Arch. Microbiol.* **2003**, *179*, 145-150.
14. Andreini, C.; Banci, L.; Bertini, I.; Rosato, A., occurrence of copper proteins through the three domains of life: a bioinformatic approach. *J. Proteome Res.* **2007**, *7*, 209-216.
15. Mayer, A. M., Polyphenol oxidases in plants and fungi: Going places? A review. *Phytochemistry* **2006**, *67*, 2318-2331.
16. del Marmol, V.; Beermann, F., Tyrosinase and related proteins in mammalian pigmentation. *FEBS Lett.* **1996**, *381*, 165-168.
17. Andersen, S. O., Insect cuticular sclerotization: A review. *Insect Biochem. Mol. Biol.* **2010**, *40*, 166-178.
18. van Gelder, C. W. G.; Flurkey, W. H.; Wichers, H. J., Sequence and structural features of plant and fungal tyrosinases. *Phytochemistry* **1997**, *45*, 1309-1323.
19. Aguilera, F.; McDougall, C.; Degnan, B., Origin, evolution and classification of type-3 copper proteins: lineage-specific gene expansions and losses across the Metazoa. *BMC Evol. Biol.* **2013**, *13*, 96.
20. Decker, H.; Schweikardt, T.; Nillius, D.; Salzbrunn, U.; Jaenicke, E.; Tuczec, F., Similar enzyme activation and catalysis in hemocyanins and tyrosinases. *Gene* **2007**, *398*, 183-191.

21. Decker, H.; Tuczec, F., Tyrosinase/catecholoxidase activity of hemocyanins: structural basis and molecular mechanism. *Trends Biochem. Sci* **2000**, *25*, 392-397.
22. Hristova, R.; Dolashki, A.; Voelter, W.; Stevanovic, S.; Dolashka-Angelova, P., o-Diphenol oxidase activity of molluscan hemocyanins. *Comp. Biochem. Phys. B* **2008**, *149*, 439-446.
23. Virador, V. M.; Reyes Grajeda, J. P.; Blanco-Labra, A.; Mendiola-Olaya, E.; Smith, G. M.; Moreno, A.; Whitaker, J. R., Cloning, sequencing, purification, and crystal structure of grenache (*Vitis vinifera*) polyphenol oxidase. *J. Agric. Food. Chem.* **2010**, *58*, 1189-1201.
24. Klabunde, T.; Eicken, C.; Sacchettini, J. C.; Krebs, B., Crystal structure of a plant catechol oxidase containing a dicopper center. *Nat. Struct. Biol.* **1998**, *5*, 1084-1090.
25. Ismaya, W. T.; Rozeboom, H. J.; Weijn, A.; Mes, J. J.; Fusetti, F.; Wichers, H. J.; Dijkstra, B. W., Crystal structure of *Agaricus bisporus* mushroom tyrosinase: Identity of the tetramer subunits and interaction with tropolone. *Biochemistry (Mosc)*. **2011**, *50*, 5477-5486.
26. Lerch, K., Primary structure of tyrosinase from *Neurospora crassa*. II. Complete amino acid sequence and chemical structure of a tripeptide containing an unusual thioether. *J. Biol. Chem.* **1982**, *257*, 6414-9.
27. Gielens, C.; Idakieva, K.; De Maeyer, M.; Van den Bergh, V.; Siddiqui, N. I.; Compennolle, F., Conformational stabilization at the active site of molluscan (*Rapana thomasiana*) hemocyanin by a cysteine-histidine thioether bridge: A study by mass spectrometry and molecular modeling. *Peptides* **2007**, *28*, 790-797.
28. Matoba, Y.; Kumagai, T.; Yamamoto, A.; Yoshitsu, H.; Sugiyama, M., Crystallographic evidence that the dinuclear copper center of tyrosinase is flexible during catalysis. *J. Biol. Chem.* **2006**, *281*, 8981-8990.
29. Sendovski, M.; Kanteev, M.; Ben-Yosef, V. S.; Adir, N.; Fishman, A., First structures of an active bacterial tyrosinase reveal copper plasticity. *J. Mol. Biol.* **2011**, *405*, 227-237.
30. Eicken, C.; Krebs, B.; Sacchettini, J. C., Catechol oxidase — structure and activity. *Curr. Opin. Struct. Biol.* **1999**, *9*, 677-683.
31. Strothkamp, K. G.; Jolley, R. L.; Mason, H. S., Quaternary structure of mushroom tyrosinase. *Biochem. Biophys. Res. Commun.* **1976**, *70*, 519-524.
32. Weijn, A.; Bastiaan-Net, S.; Wichers, H. J.; Mes, J. J., Melanin biosynthesis pathway in *Agaricus bisporus* mushrooms. *Fungal Genet. Biol.* **2012** in press
33. Wichers, H. J.; Recourt, K.; Hendriks, M.; Ebbelaar, C. E. M.; Biancone, G.; Hoerberichts, F. A.; Mooibroek, H.; Soler-Rivas, C., Cloning, expression and characterisation of two tyrosinase cDNAs from *Agaricus bisporus*. *Appl. Microbiol. Biotechnol.* **2003**, *61*, 336-341.
34. Wu, J.; Chen, H.; Gao, J.; Liu, X.; Cheng, W.; Ma, X., Cloning, characterization and expression of two new polyphenol oxidase cDNAs from *Agaricus bisporus*. *Biotechnol. Lett.* **2010**, *32*, 1439-1447.
35. Flurkey, W. H.; Inlow, J. K., Proteolytic processing of polyphenol oxidase from plants and fungi. *J. Inorg. Biochem.* **2008**, *102*, 2160-2170.
36. Inlow, J. K., Homology models of four *Agaricus bisporus* tyrosinases. *Int. J. Biol. Macromol.* **2012**, *50*, 283-293.
37. Schurink, M.; van Berkel, W. J. H.; Wichers, H. J.; Boeriu, C. G., Novel peptides with tyrosinase inhibitory activity. *Peptides* **2007**, *28*, 485-495.
38. Cheynier, V.; Owe, C.; Rigaud, J., Oxidation of grape juice phenolic compounds in model solutions. *J. Food Sci.* **1988**, *53*, 1729-1732.
39. Bernillon, S.; Guyot, S.; Renard, C. M. G. C., Detection of phenolic oxidation products in cider apple juice by high-performance liquid chromatography electrospray ionisation ion trap mass spectrometry. *Rapid Commun. Mass Spectrom.* **2004**, *18*, 939-943.
40. Prigent, S. V. E.; Voragen, A. G. J.; Li, F.; Visser, A. J. W. G.; van Koningsveld, G. A.; Gruppen, H., Covalent interactions between amino acid side chains and oxidation products of caffeoylquinic acid (chlorogenic acid). *J. Sci. Food Agric.* **2008**, *88*, 1748-1754.

41. Prigent, S. V. E.; Voragen, A. G. J.; Visser, A. J. W. G.; van Koningsveld, G. A.; Gruppen, H., Covalent interactions between proteins and oxidation products of caffeoylquinic acid (chlorogenic acid). *J. Sci. Food Agric.* **2007**, *87*, 2502-2510.
42. Seo, S.-Y.; Sharma, V. K.; Sharma, N., Mushroom tyrosinase: recent prospects. *J. Agric. Food. Chem.* **2003**, *51*, 2837-2853.
43. Winder, A. J.; Harris, H., New assays for the tyrosine hydroxylase and dopa oxidase activities of tyrosinase. *Eur. J. Biochem.* **1991**, *198*, 317-326.
44. Wu, C.; Xu, H.; Héritier, J.; Andlauer, W., Determination of catechins and flavonol glycosides in Chinese tea varieties. *Food Chem.* **2012**, *132*, 144-149.
45. Kuhnert, N.; Drynan, J. W.; Obuchowicz, J.; Clifford, M. N.; Witt, M., Mass spectrometric characterization of black tea thearubigins leading to an oxidative cascade hypothesis for thearubigin formation. *Rapid Commun. Mass Spectrom.* **2010**, *24*, 3387-3404.
46. Scoparo, C. T.; de Souza, L. M.; Dartora, N.; Sasaki, G. L.; Gorin, P. A. J.; Iacomini, M., Analysis of *Camellia sinensis* green and black teas via ultra high performance liquid chromatography assisted by liquid-liquid partition and two-dimensional liquid chromatography (size exclusion × reversed phase). *J. Chromatogr. A* **2012**, *1222*, 29-37.
47. Tanaka, T.; Kouno, I., Oxidation of tea catechins: Chemical structures and reaction mechanism. *Food Sci. Technol. Res.* **2003**, *9*, 128-133.
48. Misnawi; Selamat, J.; Bakar, J.; Saari, N., Oxidation of polyphenols in unfermented and partly fermented cocoa beans by cocoa polyphenol oxidase and tyrosinase. *J. Sci. Food Agric.* **2002**, *82*, 559-566.
49. Serra Bonvehi, J.; Ventura Coll, F., Evaluation of bitterness and astringency of polyphenolic compounds in cocoa powder. *Food Chem.* **1997**, *60*, 365-370.
50. Narváez-Cuenca, C.-E.; Vincken, J.-P.; Gruppen, H., Quantitative fate of chlorogenic acid during enzymatic browning of potato juice. *J. Agric. Food. Chem.* **2013**, *61*, 1563-1572.
51. Rawel, H. M.; Kroll, J.; Riese, B., Reactions of chlorogenic acid with lysozyme: physicochemical characterization and proteolytic digestion of the derivatives. *J. Food Sci.* **2000**, *65*, 1091-1098.
52. Weijn, A.; Tomassen, M. M. M.; Bastiaan-Net, S.; Wigham, M. L. I.; Boer, E. P. J.; Hendrix, E. A. H. J.; Baars, J. J. P.; Sonnenberg, A. S. M.; Wichers, H. J.; Mes, J. J., A new method to apply and quantify bruising sensitivity of button mushrooms. *LWT - Food Sci. Technol.* **2012**, *47*, 308-314.
53. Montero, P.; Ávalos, A.; Pérez-Mateos, M., Characterization of polyphenoloxidase of prawns (*Penaeus japonicus*). Alternatives to inhibition: additives and high-pressure treatment. *Food Chem.* **2001**, *75*, 317-324.
54. Nappi, A. J.; Vass, E., Chromatographic analyses of the effects of glutathione, cysteine and ascorbic acid on the monophenol and diphenol oxidase activities of tyrosinase. *J. Liq. Chromatogr.* **1994**, *17*, 793 - 815.
55. Richard, F. C.; Goupy, P. M.; Nicolas, J. J.; Lacombe, J. M.; Pavia, A. A., Cysteine as an inhibitor of enzymic browning. I. Isolation and characterization of addition compounds formed during oxidation of phenolics by apple polyphenol oxidase. *J. Agric. Food. Chem.* **1991**, *39*, 841-847.
56. Chang, T.-S., An updated review of tyrosinase inhibitors. *Int. Journal Mol. Sci.* **2009**, *10*, 2440-2475.
57. Kim, Y. J.; Uyama, H., Tyrosinase inhibitors from natural and synthetic sources: structure, inhibition mechanism and perspective for the future. *Cell. Mol. Life Sci.* **2005**, *62*, 1707-1723.
58. Loizzo, M. R.; Tundis, R.; Menichini, F., Natural and synthetic tyrosinase inhibitors as antibrowning agents: an update. *Compr. Rev. Food Sci. F.* **2012**, *11*, 378-398.
59. Parvez, S.; Kang, M.; Chung, H.-S.; Bae, H., Naturally occurring tyrosinase inhibitors: mechanism and applications in skin health, cosmetics and agriculture industries. *Phytother. Res.* **2007**, *21*, 805-816.

60. Casañola-Martín, G. M.; Marrero-Ponce, Y.; Khan, M. T. H.; Ather, A.; Khan, K. M.; Torrens, F.; Rotondo, R., Dragon method for finding novel tyrosinase inhibitors: Biosilico identification and experimental in vitro assays. *Eur. J. Med. Chem.* **2007**, *42*, 1370-1381.
61. Marrero-Ponce, Y.; Khan, M. T. H.; Casañola Martín, G. M.; Ather, A.; Sultankhodzhaev, M. N.; Torrens, F.; Rotondo, R., Prediction of tyrosinase inhibition activity using atom-based bilinear indices. *ChemMedChem* **2007**, *2*, 449-478.
62. Iyengar, R.; McEvily, A. J., Anti-browning agents: alternatives to the use of sulfites in foods. *Trends Food Sci. Technol.* **1992**, *3*, 60-64.
63. Bush, R. K.; Taylor, S. L.; Busse, W., A critical evaluation of clinical trials in reactions to sulfites. *J. Allergy Clin. Immunol.* **1986**, *78*, 191-202.
64. Green, L. F., Sulphur dioxide and food preservation--A review. *Food Chem.* **1976**, *1*, 103-124.
65. Guthrie, J. P., Tautomeric equilibria and pKa values for 'sulfurous acid' in aqueous solution: a thermodynamic analysis. *Can. J. Chem.* **1979**, *57*, 454-457.
66. Sayavedra-Soto, L. A.; Montgomery, M. W., Inhibition of polyphenoloxidase by sulfite. *J. Food Sci.* **1986**, *51*, 1531-1536.
67. Ferrer, O. J.; Otwell, W. S.; Marshall, M. R., Effect of bisulfite on lobster shell phenoloxidase. *J. Food Sci.* **1989**, *54*, 478-480.
68. Lester, M. R., Sulfite sensitivity: significance in human health. *J. Am. Coll. Nutr.* **1995**, *14*, 229-32.
69. Riggs, B. S.; Harchelroad Jr, F. P.; Poole, C., Allergic reaction to sulfiting agents. *Ann. Emerg. Med.* **1986**, *15*, 77-79.
70. Bush, R. K.; Taylor, S. L.; Holden, K.; Nordlee, J. A.; Busse, W. W., Prevalence of sensitivity to sulfiting agents in asthmatic patients. *Am. J. Med.* **1986**, *81*, 816-820.
71. Armentia, A., Adverse reactions to wine: think outside the bottle. *Curr. Opin. Allergy Cl.* **2008**, *8*, 266-269.
72. Vally, H.; Thompson, P. J.; Misso, N. L. A., Changes in bronchial hyperresponsiveness following high- and low-sulphite wine challenges in wine-sensitive asthmatic patients. *Clin. Exp. Allergy* **2007**, *37*, 1062-1066.
73. Combs Jr, G. F., Chapter 10 - Thiamin. In *The Vitamins (Fourth Edition)*, Academic Press: San Diego, CA, USA, 2012; pp 261-276.
74. Zoltewicz, J. A.; Kauffman, G. M.; Uray, G., A mechanism for sulphite ion reacting with vitamin B1 and its analogues. *Food Chem.* **1984**, *15*, 75-91.
75. Zoltewicz, J. A.; Uray, G., Thiamin: A critical evaluation of recent chemistry of the pyrimidine ring. *Bioorg. Chem.* **1994**, *22*, 1-28.
76. Timbo, B.; Koehler, K. M.; Wolyniak, C.; Klontz, K. C., Sulfites-a food and drug administration review of recalls and reported adverse events. *J. Food Prot.* **2004**, *67*, 1806-1811.
77. EC, Directive 95/2/EC. 1995.
78. Tepper, A. W. J. W. Structure and mechanism of the type-3 copper protein tyrosinase. PhD thesis, Leiden University, Leiden, The Netherlands, 2005.
79. Li, B.; Huang, Y.; Paskewitz, S. M., Hen egg white lysozyme as an inhibitor of mushroom tyrosinase. *FEBS Lett.* **2006**, *580*, 1877-1882.
80. Chen, J. S.; Wei, C.-i.; Rolle, R. S.; Otwell, W. S.; Balaban, M. O.; Marshall, M. R., Inhibitory effect of kojic acid on some plant and crustacean polyphenol oxidases. *J. Agric. Food. Chem.* **1991**, *39*, 1396-1401.
81. Flurkey, A.; Cooksey, J.; Reddy, A.; Spoonmore, K.; Rescigno, A.; Inlow, J.; Flurkey, W. H., Enzyme, protein, carbohydrate, and phenolic contaminants in commercial tyrosinase preparations: potential problems affecting tyrosinase activity and inhibition studies. *J. Agric. Food. Chem.* **2008**, *56*, 4760-4768.
82. Kahn, V.; Andrawis, A., Inhibition of mushroom tyrosinase by tropolone. *Phytochemistry* **1985**, *24*, 905-908.

83. Cabanes, J.; Garcia-Canovas, F.; Tudela, J.; Lozano, J. A.; García-Carmona, F., L-mimosine a slow-binding inhibitor of mushroom tyrosinase. *Phytochemistry* **1987**, *26*, 917-919.
84. Khan, K. M.; Maharvi, G. M.; Khan, M. T. H.; Jabbar Shaikh, A.; Perveen, S.; Begum, S.; Choudhary, M. I., Tetraketones: A new class of tyrosinase inhibitors. *Biorg. Med. Chem.* **2006**, *14*, 344-351.
85. Jones, K.; Hughes, J.; Hong, M.; Jia, Q.; Orndorff, S., Modulation of melanogenesis by aloesin: a competitive inhibitor of tyrosinase. *Pigment Cell Res.* **2002**, *15*, 335-340.
86. Jin, Y. H.; Lee, S. J.; Chung, M. H.; Park, J. H.; Park, Y. I.; Cho, T. H.; Lee, S. K., Aloesin and arbutin inhibit tyrosinase activity in a synergistic manner via a different action mechanism. *Arch. Pharm. Res.* **1999**, *22*, 232-236.
87. Lee, H.-S., Tyrosinase inhibitors of *Pulsatilla cernua* root-derived materials. *J. Agric. Food. Chem.* **2002**, *50*, 1400-1403.
88. Shi, Y.; Chen, Q.-X.; Wang, Q.; Song, K.-K.; Qiu, L., Inhibitory effects of cinnamic acid and its derivatives on the diphenolase activity of mushroom (*Agaricus bisporus*) tyrosinase. *Food Chem.* **2005**, *92*, 707-712.
89. Liu, S.-H.; Pan, I. H.; Chu, I. M., Inhibitory effect of *p*-hydroxybenzyl alcohol on tyrosinase activity and melanogenesis. *Biol. Pharm. Bull.* **2007**, *30*, 1135-1139.

New insights into an ancient anti-browning agent: formation of sulfo-phenolics in sodium hydrogen sulfite treated potato extracts

The effect of sodium hydrogen sulfite (NaHSO_3), used as anti-browning agent, on the phenolic profile of potato extracts was investigated. This extract was compared to one obtained in the presence of ascorbic acid. In the presence of ascorbic acid, two major compounds were obtained: 5-*O*-caffeoyl quinic acid (ChA) and 4-*O*-caffeoyl quinic acid. With NaHSO_3 , their 2'-sulfo-adducts were found instead, the structures of which were confirmed by nuclear magnetic resonance spectroscopy and mass spectrometry. Also, for minor caffeoyl derivatives and quercetin glycosides, the corresponding sulfo-adducts were observed. Feruloyl and sinapoyl derivatives were not chemically affected by the presence of NaHSO_3 . Polyphenol oxidase (PPO) was thought to be responsible for the formation of the sulfo-adducts. This was confirmed by preparing 2'-sulfo-5-*O*-caffeoyl quinic acid in a model system using ChA, sodium hydrogen sulfite and PPO. This sulfo-adduct exhibited a small bathochromic shift (λ_{max} 329 nm) compared to ChA (λ_{max} 325 nm), and a strong hypochromic shift with an extinction coefficient of $9,357 \pm 395 \text{ M}^{-1}\text{cm}^{-1}$ compared to $18,494 \pm 196 \text{ M}^{-1}\text{cm}^{-1}$, respectively. The results suggest that whenever NaHSO_3 is used as anti-browning agent, the *o*-quinone formed with PPO reacts with NaHSO_3 to produce sulfo-*o*-diphenol, which does not participate in browning reactions.

INTRODUCTION

Prevention of enzymatic browning is a major concern during starch production and retrieval of other valuable components from potato. Phenolic compounds are considered to be the main precursors of the brown pigments. They constitute an abundant group of secondary metabolites in potato. Caffeic acid, 5-*O*-caffeoyl quinic acid (chlorogenic acid, ChA), its isomers and rutin are representatives of hydroxycinnamic acids (HCAs), HCA conjugates (HCAs), and flavonols, commonly found in potato, respectively (1-3). The content of phenolic compounds varies over a wide range depending on several factors, e.g. variety. ChA and its isomers have been found in potato tubers to commonly range from 23 to 350 mg/100 g DW, caffeic acid from trace to 48 mg/100 g DW, and rutin from 0 to 19 mg/100 g DW (1-3).

The compounds mentioned can be oxidized by polyphenol oxidase (PPO) to produce *o*-quinones, which subsequently polymerize into brown-colored melanins (4,5). This oxidation can be prevented by the addition of ascorbic acid or sulfites/hydrogen sulfites. Although the FDA prohibits the use of sulfites on fruits and vegetables for the fresh market, they are allowed in minimally processed potatoes (6). Furthermore, they are commonly used in the potato starch industry, which, for example, in The Netherlands amounts to about 2.5×10^6 tons of starch potatoes annually (7).

The anti-browning effect of ascorbic acid has been associated with its ability to reduce quinones to their precursor phenolics and by lowering the pH with a concomitant inhibition of PPO activity (8). The sulfur-containing agents seem to control the browning reaction by irreversible inactivation of PPO, by reduction of the quinones to the original phenolic compounds (9), as well as by reacting with quinones to produce colorless compounds (10). The latter mechanism has been proposed based on UV-vis data only, without structural elucidation or quantification of the end products (10). Hence, information on the modification of the individual phenolic compounds is lacking to date.

Recently, we have reported a method for the identification of HCAs/HCAcs/DHCAcs in potato by reverse-phase ultrahigh performance liquid chromatography-diode array detection-mass spectrometry (RP-UHPLC-DAD-MSⁿ) (11), which is a useful tool for structural elucidation of a complex extract. In the present study, this method was employed to investigate how addition of sodium hydrogen sulfite upon extraction of potato affects the composition of phenolics in the extract. Extraction in the presence of ascorbic acid was used as reference to quantify the phenolic compounds in their unmodified state, as it inhibits enzymatic oxidation of phenolics that would otherwise occur.

MATERIALS AND METHODS

Chemicals

Caffeic acid, ferulic acid, sinapic acid, chlorogenic acid (ChA), ascorbic acid, sodium hydrogen sulfite (NaHSO₃), and mushroom tyrosinase were purchased from Sigma-Aldrich Chemie GmbH (Steinheim, Germany). *Neo*-ChA (3-*O*-caffeoyl quinic acid) and *crypto*-ChA (4-*O*-caffeoyl quinic acid) were from Phytolab (Vestenbergsgreuth, Germany). Rutin (quercetin-3-*O*-rutinoside) was from Merck (Darmstadt, Germany). UHPLC/MS grade acetonitrile (ACN) was purchased from Biosolve BV (Valkenswaard, The Netherlands). Water was obtained using a Milli-Q water purification system (Millipore, Billerica, MA, USA). All other chemicals were from Merck (Darmstadt, Germany).

Plant material

Potato tubers (Nicola variety) were purchased from a local supermarket in Wageningen, The Netherlands. Tubers were washed under tap water and then processed further.

Extraction of phenolic compounds

Two hundred grams of fresh potato was diced (0.3-0.5 cm thickness) and immediately homogenized in a household blender with the addition of 200 mL of aqueous solutions of 20,000 ppm ascorbic acid (extractant *A*) or 400 ppm NaHSO₃ (extractant *S*). Subsequently, the mixture was stirred for 10 min at 4 °C. Starch and fibers were allowed to settle for 20 min at 4 °C. After it was decanted, the solution was centrifuged (18,000 x g; 20 min; 4 °C). The precipitated material and the pellet from centrifugation were collected, combined, and re-extracted with 100 mL extractants *A* or *S*. When analyzed with RP-UHPLC-DAD-MSⁿ (see later), the fifth extraction yielded less than 1% of the 5-*O*-caffeoyl quinic acid and its derivatives, when compared to the summed up amount of the five extractions. Therefore, only the material from the first four extractions was combined. The extracts will be referred to as extracts *A* and *S*. The pH values of extracts *A* and *S* were 3.9 and 6.0, respectively. To remove proteins, the pH of extract *S* was adjusted to 4.0 by adding 100% acetic acid and left overnight at 4 °C. Extract *A* was kept overnight at 4 °C without addition of acetic acid. The resulting materials were centrifuged (18,000 x g; 20 min; 4 °C), and the supernatants were subsequently filtered through a 0.45 µm filter (Whatman, Scheicher & Schuell, Dassel, Germany). Aliquots (500 µL) of the extracts were ultrafiltrated using regenerated cellulose centrifugal filter units (Amicon ultra 0.5 mL, cut-off 10 kDa, Millipore) according to the instructions of the manufacturer. Filtrates were stored at -20 °C until further analysis. All extractions were done in triplicate.

Large-scale extraction was performed by processing 2 kg of fresh potato with 2 L of extractant *S* using identical conditions as with the 200 g fresh potato samples. After the

filtration step (0.45 μm filter), the protocol was modified as follows. The supernatant obtained after precipitation of proteins (pH 4.0) and centrifugation was ultrafiltrated at 4 $^{\circ}\text{C}$ using a 2.5 L Amicon ultrafiltration cell (Millipore) with a regenerated cellulose membrane (cut-off 10 kDa; Millipore). The system had a magnetic stirrer to minimize concentration polarization at the membrane and was pressurized (4 atm) with nitrogen. Low molecular weight polar compounds were removed from the ultrafiltrated liquid using solid-phase extraction with C18 35 mL/10 g Sep-Pak cartridges, according to the instructions of the manufacturer (Waters, Milford, MA, USA). The methanolic fraction was evaporated under reduced pressure, and the remaining water was removed by freeze-drying, yielding 768 mg powder. A quantity of 200 mg of powder was suspended in MQ water to 5 mg/mL, stirred for 10 min, and centrifuged (12,000 \times g; 5 min, 4 $^{\circ}\text{C}$). Subsequently, the resolubilised powder was fractionated by semipreparative RP-HPLC. Extraction for preparative purposes was performed once.

Semipreparative RP-HPLC

The resolubilized powder obtained from the large scale extraction from potato was fractionated by a Waters preparative HPLC system, using a semipreparative XTerra RP18 column (150 mm \times 19 mm; particle size 5 μm ; Waters) with an XTerra RP18 guard column (19 \times 10 mm i.d.; particle size 5 μm ; Waters). The solvents used were water/ACN/acetic acid (99:1:0.5, v/v/v) (eluent A) and ACN/acetic acid (100:0.5, v/v) (eluent B). The following elution program was used: 0-5 min, 0% B; 5-35 min, 0 to 26% B; 35-37 min, 26 to 100% B; 37-42 min, 100% B; 42-44 min, 100 to 0% B; 44-54 min, 0% B. Volumes of 10 mL of 5 mg/mL sample were injected. The flow rate was 12 mL/min. The eluate was monitored at 325 nm and fractions (3.4 mL) were obtained during the time span of 15-25 min of each run. On the basis of RP-UHPLC-DAD-ESI-MSⁿ, two pools (I and II) were made. ACN was removed by evaporation under vacuum and the remaining water was removed by freeze-drying. Two hundred milligrams of powder yielded 4.3 and 20.4 mg of pools I and II, respectively. RP-UHPLC-DAD-ESI-MSⁿ analysis revealed that pool I comprised **22** (purity 45%, w/w), with impurities of tryptophan (45%, w/w), and **23** (10%, w/w). In pool II, **23** was the major compound, with a purity of approximately 71% w/w, with tryptophan (28%, w/w) and **22** (1%, w/w) as the main impurities.

PPO-catalyzed preparation of 2'-sulfo-5-O-caffeoyl quinic acid in a model system and its purification

To establish whether PPO is essential to the formation of sulfo-phenolics, 5-O-caffeoyl quinic acid and sodium hydrogen sulfite were incubated with and without commercial PPO. Only in the presence of PPO, 2'-sulfo-5-O-caffeoyl quinic acid was found as the major reaction product (data not shown). Five hundred mL of an aqueous solution of 5-O-caffeoyl quinic acid (1 mM) were fully converted after incubation with NaHSO₃ (2 mM) and

mushroom tyrosinase (140 units/mL; PPO units according to supplier) at 20 °C during 2 h. The initial pH was adjusted to 6.5 by adding 0.1 M NaOH. The resulting material was purified by semi-preparative RP-HPLC, similarly as described above. One hundred seventy-seven milligrams of 5-*O*-caffeoyl quinic acid yielded 77 mg of 2'-sulfo-5-*O*-caffeoyl quinic acid as the major reaction product, with a purity of 97% (after peak area integration at 325 nm), having identical retention time, UV and MSⁿ data as **23**. An isomer of the major reaction product was the major impurity.

Determination of the molar extinction coefficient

On the basis of stock solutions of 10 mg/mL of 5-*O*-caffeoyl quinic acid and 2'-sulfo-5-*O*-caffeoyl quinic acid (obtained by PPO-catalyzed preparation), dilution series in MQ water were made. The absorbances at 325 nm of these dilutions were measured against MQ water in a 1 mL quartz cuvet. Temperature of the solutions was maintained at 20 °C. The molar extinction coefficients (ϵ) were calculated using $Abs = \epsilon * l * c$, in which Abs = absorbance at 325 nm, l = light path = 1 cm, c = concentration (M). Furthermore, wavelength scans were made from 200 to 600 nm. Measurements were performed with six independently prepared replications.

RP-UHPLC-DAD-ESI-MSⁿ analysis

Potato extracts, undiluted and 10x diluted, and reaction products synthesized in a model system with commercial PPO were analyzed using an Accela UHPLC system (Thermo Scientific, San Jose, CA, USA) equipped with a pump, an autosampler, cooled at 7 °C, and a photo-diode array detector (DAD), using a Hypersil gold RP column (150 mm x 2.1 mm i.d.; particle size 1.9 μ m; Thermo Scientific) at 30 °C. The eluents used were water/ACN/acetic acid (99:1:0.2, v/v/v) (eluent A) and ACN/acetic acid (100:0.2, v/v) (eluent B). The elution program was 0-5 min, 0% B; 5-23 min, 0 to 60% B; 23-24 min, 60 to 100% B; 24-27 min, 100% B; 27-28 min, 100 to 0% B; 28-35 min, 0% B. The flow rate was 400 μ L/min. Sample volumes of 5 μ L were injected. MSⁿ analysis was performed on a LTQ-XL (Thermo Scientific) using electrospray ionization (ESI). Detection was in the negative ion mode with a source voltage of 3.5 kV and an ion transfer tube temperature of 350 °C. The instrument was auto-tuned using ChA. A full-scan mass spectrum over a m/z range of 150-1500 was recorded. MS² spectra of extracts A and S were collected with a collision energy of 30% with the use of wideband activation, which ensures that both the parent ion and the subsequent water loss ion undergo fragmentation. The control of the instrument and data processing were done using Xcalibur 2.07 (Thermo Scientific). Annotation of HCAs was done according to previous work (11). Furthermore, retention times and spectroscopic data of 3-*O*-, 4-*O*-, and 5-*O*-caffeoyl quinic acid isomers, caffeic acid, and rutin were compared to standards. 5-*O*-Caffeoyl quinic acid was adopted as standard for the quantification of caffeoyl quinic acid isomers. 2'-Sulfo-5-*O*-caffeoyl quinic

acid, obtained with the commercial PPO, was used as standard for the quantification of sulfo-caffeoyl quinic acid isomers. Other minor caffeoyl derivatives, different to (sulfo-) caffeoyl quinic acid isomers, were quantified using caffeic acid, with application of a MW correction factor. Ferulic acid and sinapic acid were used as standards for the quantification of ferulic acid and sinapic acid containing compounds, respectively, with the use of MW correction factors ($MW_{\text{HCAc}}/MW_{\text{external standard}}$), assuming that the response of the HCAs is determined by the HCA moiety. All HCAs/HCAcs were quantified at 325 nm. Quercetin glycosides were quantified based on calibration curves with rutin at 360 nm, and MW correction factors were used when necessary. In all cases calibration curves were done at concentrations ranging from 0.05 to 30 $\mu\text{g/mL}$. Calibration curves with tryptophan (1 to 30 $\mu\text{g/mL}$) were carried out at 280 nm to calculate its content in pools I and II from the large scale potato extraction.

Nuclear magnetic resonance (NMR) spectroscopy

Samples were dissolved in 0.35 mL D_2O (99.9 atom%, Aldrich) and approximately 1 μL acetone was added to each sample as internal standard. NMR spectra were recorded at a probe temperature of 300 K on a Bruker Avance-III-600 spectrometer, equipped with a cryo-probe located at Biqualy (Wageningen, The Netherlands). ^1H Chemical shifts were expressed in ppm relative to internal acetone at 2.220 ppm. ^{13}C chemical shifts were expressed in ppm relative to internal acetone at 30.89 ppm. One- and two-dimensional correlation spectroscopy (COSY), total correlation spectroscopy (TOCSY), heteronuclear multiple bond correlation (HMBC), and heteronuclear multiple quantum coherence (HMQC) spectra were acquired using standard pulse sequences delivered by Bruker. For the ^1H -COSY and ^1H -TOCSY spectra, 400 experiments of four scans and 400 experiments of eight scans were recorded, resulting in measuring times of 1 h and 2 h, respectively. The mixing time for the TOCSY spectra was 100 ms. For the [$^1\text{H},^{13}\text{C}$]-HMBC and [$^1\text{H},^{13}\text{C}$]-HMQC spectra, 1024 experiments of 16 scans and 512 experiments of four scans, were recorded, resulting in measuring times of 8 h and 1.2 h, respectively.

Statistical analysis

Data are reported as the mean with their standard deviation. Quantities of phenolics obtained in extracts *A* and *S* were compared by means of the Student's *t*-test ($P < 0.05$).

RESULTS

Altered composition of potato phenolics upon use of NaHSO_3

When ascorbic acid or NaHSO_3 was used in the potato extract preparation, no visual browning was observed. In contrast, the omission of either ascorbic acid or NaHSO_3 led to

rapid browning of the suspension (no further data shown). Interestingly, different chromatographic profiles were observed when the extracts were obtained in the presence of ascorbic acid (**Figure 1A**) or NaHSO₃ (**Figure 1B**).

Ascorbic acid as anti-browning agent

The chromatogram was dominated by HCAs with 5-*O*-caffeoyl quinic acid (**3**) as the most abundant phenolic compound, followed by 4-*O*-caffeoyl quinic acid (**4**). From 12 identified compounds, 10 were HCA-containing compounds (caffeic acid-, ferulic acid- and sinapic acid-derivatives), including caffeic acid in the free form, and two quercetin glycosides. The retention times, spectroscopic data, and mass spectrometric data of **1-12** are given in **Table 1**. The spectroscopic and mass spectrometric data of the 10 HCAs/HCAcs were in agreement with previous work (11). Moreover, the retention times of 3-*O*-, 4-*O*-, 5-*O*-caffeoyl quinic acid isomers and that of caffeic acid matched with those of authentic standards.

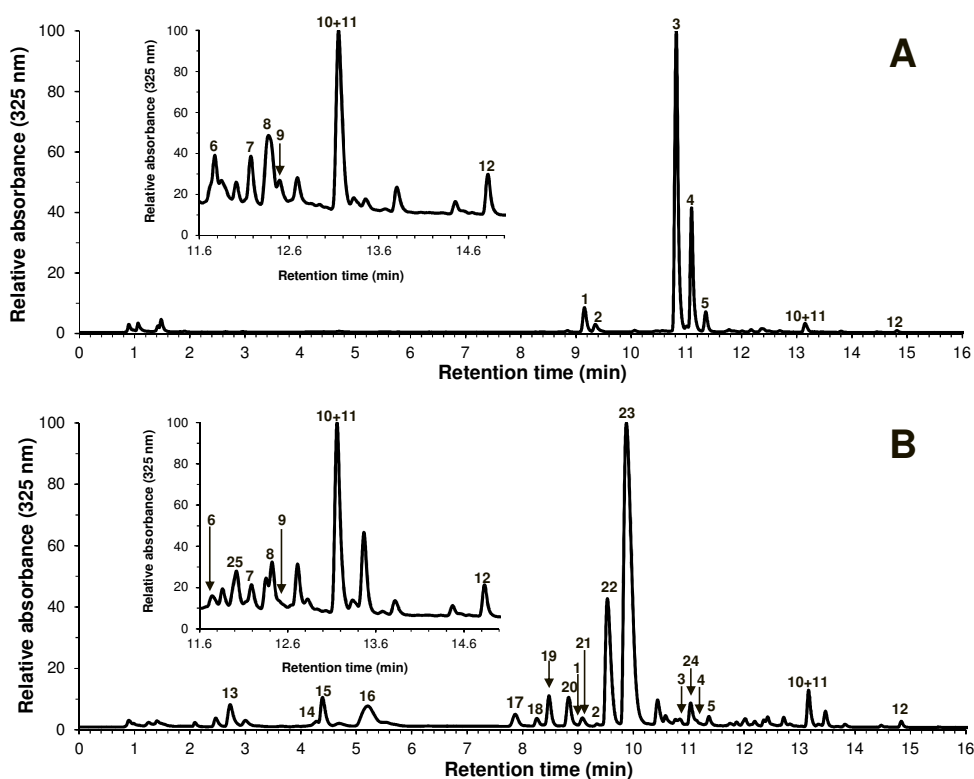


Figure 1. UHPLC chromatogram recorded at 325 nm of the potato extract prepared with the addition of (A) 20,000 ppm ascorbic acid or (B) 400 ppm NaHSO₃. The inserts are a zoom between 11.6 and 15.0 min.

Table 1. Retention times, MS, and UV data of HCAs/HCAcs and flavonols in potato.

#	RT (min)	MS (m/z)	MS ^{2a} (m/z)	UV λ_{\max} (nm)	Tentative identification
1	9.15	353	191 , <u>179</u> (45), 173 (3), <u>161</u> (1), <u>135</u> (8)	223, 240sh, 300sh, 324	3- <i>O</i> -Caffeoyl quinic acid ^b
2	9.35	249	249 , 207 (7), <u>161</u> (<1) <u>135</u> (23)	223, 293sh, 317	Caffeoyl putrescine
3	10.82	353	191 , <u>179</u> (3), 173 (<1), <u>161</u> (<1), <u>135</u> (<1)	223, 240sh, 305sh, 325	5- <i>O</i> -Caffeoyl quinic acid ^b
4	11.10	353	191 (21), <u>179</u> (59), 173 , <u>135</u> (8)	223, 240sh, 305sh, 326	4- <i>O</i> -Caffeoyl quinic acid ^b
5	11.35	179	<u>179</u> (86), <u>135</u> , <u>161</u> (<1)	224, 305sh, 323	Caffeic acid ^b
6	11.77	353	191 , <u>179</u> (4), 173 (<1), <u>161</u> (<1), <u>135</u> (1)	229, 240sh, 305sh, 325	Caffeoyl quinic acid isomer
7	12.18	445	385 , <u>223</u> (5), <u>205</u> (4), <u>179</u> (4)	225, 300sh, 330	Sinapoyl hexoside
8	12.37	367	<u>193</u> (9), 191 , 173 (37), <u>134</u> (<1)	214, 301sh, 324	5- <i>O</i> -Feruloyl quinic acid
9	12.50	625	505 (9), 463 (11), 445 (31), 301 (49), 300 , 271 (22), 255 (11), 179 (3), 151 (4) MS ³ 300 (28), 271 , 255 (46), 179 (2), 151 (4)	260, 300sh, 353	Quercetin-3- <i>O</i> -diglycoside
10	13.15	309	<u>193</u> , <u>178</u> (<1), <u>149</u> (<1), <u>134</u> (<1), 115 (<1)	225, 300sh, 326	Feruloyl malate ^c
11	13.22	609	301 , 300 (44), 271 (9), 255 (6), 179 (3) MS ³ (74), 179 , 151 (92)	259, 300sh, 351	Rutin ^{b,c}
12	14.82	429	385 (25), 249 , <u>223</u> (<1), <u>205</u> (44), <u>179</u> (21)	224, 311	Sinapoyl conjugate

^aBold numbers represent a relative abundance of 100%. In parentheses, the relative abundance is indicated. Values underlined are those that were diagnostic for the classification of compounds containing HCAs. In the case of quercetin glycosides MS³ of the 100% ion from MS² was included to provide extra information.

^bSimilar retention times, MS and UV data compared to authentic standards.

^cCoelution with other compounds. Peaks were resolved when the gradient was modified as follows: 0-5 min, 0% B; 5-23 min, 0 to 50% B; 23-24 min, 50 to 100% B; 24-27 min, 100% B; 27-28 min, 100 to 0% B; 28-35 min, 0% B at 40 °C, performed with eluents containing 0.1 instead of 0.2% HAc (Retention times of **10** and **11** were 12.98 and 13.20 min, respectively).

Two compounds were annotated as quercetin glycosides: Quercetin 3-*O*-diglycoside (**9**) and rutin (**11**). After MS fragmentation both compounds yielded the predominant ions m/z 300 ([M-2H-324][•]) and 301 ([M-H-324]⁻), which originated from homolytic and heterolytic cleavage of the glycosidic bond, respectively (3,12). Retention time and spectroscopic data of rutin were in accordance with those of the authentic compound. The C-3 substitution of quercetin with glucose in compound **9** has been previously described in potato (3). Furthermore, the presence of the ions m/z 505 and 445 during MS fragmentation was diagnostic for quercetin-*O*-dihexosides substituted at the C-3 position (12).

Table 2. Retention times, MS, and UV data of sulfo-HCAs/sulfo-HCAs/sulfo-flavonols in potato.

#	RT (min)	MS (m/z)	MS ^{2a} (m/z)	UV λ_{max} (nm)	Tentative identification
13	2.73	433	433(1), 415 (<1), 387 (3), 353 (80), 301 (2), 259 (13), 241 (44), 215 (3), 191 , 179 (6), 161 (34), 135 (1)	228, 246, 305sh, 327	O-Sulfate-caffeoyl quinic acid or sulfo-caffeoyl quinic acid
14	4.29	259	259 , 241(<1), 215 (13), 179 (47), 135 (13)	230, 250sh, 289, 323	Sulfo-caffeic acid isomer 1
15	4.39	433	433 (2), 415 (3), 387 (9), <u>353</u> (<1), 301 (2), 259 , 241 (12), 215 (38), 179 (1), 161 (9), 135 (3)	227, 245, 305sh, 327	Sulfo-caffeoyl quinic acid isomer 1
16	5.21	433	433 (3), 415 (3), 387 (18), <u>353</u> (<1), 301 (2), 259 (36), 241 , 215 (2), 179 (1), 161 (1), 135 (<1)	229, 250, 296, 324	Sulfo-caffeoyl quinic acid isomer 2
17	7.87	433	433 (1), 415 (<1), 387 (9), <u>353</u> (<1), 301 , 259 (3), 241 (6), 215 (<1), 179 (<1), 161 (<1), 135 (<1)	229, 245, 295, 324	Sulfo-caffeoyl quinic acid isomer 3
18	8.26	433	433 (1), 415 (2), 387 (3), <u>353</u> (<1), 301 , 259 (4), 241 (3), 215 (2), 179 (<1), 161 (2), 135 (1)	229, 291sh, 313	Sulfo-caffeoyl quinic acid isomer 4
19	8.48	329	329 (98), 249 , 241(80), 215 (6), 161 (34), 135 (4)	229, 291, 321	Sulfo-caffeoyl putrescine
20	8.83	433	433 (6), 415 (9), 387 (31), <u>353</u> (3), 301 (9), 259 , 241 (29), 215 (37), 191 (12), 179 (3), 161 (34), 135 (3)	228, 280sh, 315	Sulfo-caffeoyl quinic acid isomer 5
21	9.08	259	259 (6), 241(<1), 215 , 179 (1), 135 (2)	228, 281, 327	Sulfo-caffeic acid isomer 2
22	9.53	433	433 (<1), 415 (<1), 387 (2), <u>353</u> (<1), 301 , 259 (<1), 241 (2), 215 (1), 161 (1)	228, 240sh, 305sh, 329	2'-Sulfo-4-O-caffeoyl quinic acid
23	9.88	433	433 (9), 415 (9), 387 (38), 353 (<1), 301 (11), 259 , 241 (37), 215 (45), 191 (<1), 179 (<2), 161 (47), 135 (3)	224, 240sh, 305sh, 329	2'-Sulfo-5-O-caffeoyl quinic acid
24	11.04	705	543 (4), 525 (1), 381 , <u>301</u> (47), <u>271</u> (1)	229, 291sh, 318 ^b	Sulfo-quercetin-3-O- diglucoside
25	11.96	689	381 , <u>301</u> (53), <u>271</u> (1)	229, 259, 312 ^b	Sulfo-rutin

^aBold numbers represent a relative abundance of 100%. In brackets, the relative abundance is indicated. Values underlined are those that were diagnostic for the precursor compounds. Values in italic are those that were diagnostic for the assignment of SO₃ attached to the aromatic ring of caffeic acid or quercetin.

^bUV maxima data does agree with neither sulfo-quercetin nor with quercetin O-sulfate (13,14), probably due to co-elution.

NaHSO₃ as anti-browning agent

Compounds that were identified in extract A (**1-12**) were found in extract S as well, although in different relative quantities. Particularly 5-O-caffeoyl quinic acid and 4-O-caffeoyl quinic acid (**Figure 1A,B**) were much lower in extract S than in extract A.

Furthermore, about 18 new peaks were observed in extract *S*, of which 13 were tentatively identified (retention times, spectroscopic, and mass spectrometric data in **Table 2**). Compound **23** was the most abundant, followed by **22**.

The mass of the parent ions of the new compounds (**13-25**) revealed an increase of 80 a.m.u. (**Table 2**) when compared to the caffeoyl- and quercetin-containing compounds labeled **1-12** (**Table 1**), referred to in the text as precursor compounds. Eight isomers (**13, 15-18, 20, 22** and **23**) with MW of 434 were found, which represented the MW of caffeoyl quinic acid isomers plus 80 a.m.u. Similarly, MS analysis revealed that the MW of **19** matched with that of caffeoyl putrescine plus 80 a.m.u., **14** and **21** with a MW of caffeic acid plus 80 a.m.u., **24** with a MW of quercetin-3-*O*-diglucoside plus 80 a.m.u., and **25** with a MW of rutin plus 80 a.m.u. The extra 80 a.m.u. indicated that a SO₃ substituent is present in the molecules.

MS fragmentation and NMR spectroscopy of the two main SO₃H-caffeoyl quinic acids

Table 2 shows that **22** and **23** yielded, although in very low abundance, the ions m/z 353, 191, 179, 161 and 135, which are diagnostic for caffeoyl quinic acid isomers (**1, 3, 4** and **6**; **Table 1**). Moreover, MS fragmentation data (**Table 2**) revealed ions that indicate a SO₃H moiety linked to the caffeic acid moiety. The ions m/z 259 (SO₃H caffeic acid), m/z 241 (dehydrated SO₃H caffeic acid) and m/z 215 (decarboxylated SO₃H caffeic acid) were used as diagnostic tool for the linkage of the SO₃H group to the caffeic acid moiety and not to the quinic acid moiety. Other ions found for **22** and **23**, but not for caffeoyl quinic acid isomers, were: m/z 415 [M-H₂O-H]⁻, 387 [M-H₂O-CO-H]⁻ and 301 [M-C₅H₆O₃-H₂O-H]⁻. Interestingly, the ion m/z 259 was the most abundant for **23**, whereas for **22** the most abundant ion was m/z 301.

NMR spectroscopy was used to establish the position of the sulfite group on the caffeic acid moiety and the position of the ester linkage between caffeic acid and quinic acid. Interpretation of the 2D NMR spectra resulted in full assignment of both ¹H and ¹³C spectra for **22** and **23** (**Table 3**). In the caffeoyl ring the H-2' was missing when compared to 4-*O*- and 5-*O*-caffeoyl quinic acid, indicating that the SO₃H group must be attached to position C-2'. The carbon chemical shift of 125 ppm for C-2', assigned by a crosspeak in the HMBC between H-6' and C-2', was in accordance with a SO₃H group linked at position 2. In the HMBC of each compound, a crosspeak was assigned between a proton of quinic acid and C-9' of caffeic acid, indicating the linkage position of quinic acid. For **22** this was position 4. When compared to unsubstituted quinic acid, the downfield shift of 2.7 ppm for C-4, and upfield shifts of 2.4 and 2.0 ppm for C-3 and C-5, respectively, confirmed the linkage at position C-4 (*15*). For **23** a crosspeak between H-5 of quinic acid and C-9' of caffeic acid indicated C-5 as linkage position. This was also confirmed by a crosspeak in the HMBC between H-5 and C-1, which was not present in case of linkage at position C-4,

and by a downfield shift of 4.5 ppm for C-5 and upfield shifts of 3.4 and 3.6 ppm for C-4 and C-6, respectively, compared to unsubstituted quinic acid (15). Therefore, **22** was identified as 2'-SO₃H-4-O-caffeoyl quinic acid, and compound **23** as 2'-SO₃H-5-O-caffeoyl quinic acid.

Table 3. ¹H and ¹³C-NMR data of **22** and **23**.

Atom no	22				23			
	¹ H shift	multiplicity	J-coupling	¹³ C shift	¹ H shift	multiplicity	J-coupling	¹³ C shift
1	-	-	-	76.00	-	-	-	75.63
2	2.27	m		37.49	2.22	m		37.12
	2.11	m			2.10	m		
3	4.38	m		68.34	4.26	m		70.01
4	4.938	dd	9.1; 2.8	78.18	3.900	dd	8.5; 2.5	72.11
5	4.36	m		64.98	5.299	m		71.49
6	2.26	m		40.80	2.26	m		37.34
	2.12	m			2.14	m		
7	-	-	-	178.50	-	-	-	177.82
1'	-	-	-	125.24	-	-	-	125.11
2'	-	-	-	125.80	-	-	-	125.88
3'	-	-	-	143.21	-	-	-	143.14
4'	-	-	-	147.66	-	-	-	147.63
5'	7.027	d	8.4	118.35	6.974	d	8.4	118.21
6'	7.266	d	8.4	120.95	7.159	d	8.4	120.85
7'	8.493	d	15.7	144.66	8.436	d	15.7	144.45
8'	6.437	d	15.7	118.52	6.283	d	15.7	118.40
9'	-	-	-	168.90	-	-	-	168.77

Identification of minor SO₃H-phenolics based on MS fragmentation

Table 2 shows that the six minor SO₃H-caffeoyl quinic acid isomers yielded ions similar to those that were found for the two major SO₃H-caffeoyl quinic acid isomers (**22** and **23**), that is, the ions *m/z* 259 (SO₃H caffeic acid), 241 (dehydrated SO₃H caffeic acid) and 215 (decarboxylated SO₃H caffeic acid). The differences observed in the relative abundances of the ions among the six molecules suggest a distinctive effect of the position of the ester linkage between caffeic acid and quinic acid (16), as well as of the position of the SO₃H moiety. In the UV spectra there was a small bathochromic shift (maximum shift 5 nm) for **13**, **15**, **19**, **21**, **22** and **23**, if compared to the precursor compounds (those without the SO₃H group). On the contrary, there was a hypsochromic effect (maximum shift 10 nm) for **18** and **20**, if compared to precursor compounds. In literature, both bathochromic and hypsochromic spectral shifts have been reported upon nucleophilic attack of glutathione to caffeoyl-containing compounds (17, 18).

In our study the ion m/z 381, observed with both **24** and **25** (Table 2), demonstrated that the SO_3H was attached to the flavonoid skeleton and not to the saccharide moiety. The ions m/z 179 and 151, representing the A-ring moiety after C-ring cleavage of quercetin (19), were observed in **9** and **11** (Table 1) as well as in **24** and **25** (Table 2). The lack of ions m/z 179+80 and 151+80 in MS^n spectra of **24** and **25** suggested that the SO_3H group should be linked to ring B.

Extinction coefficient of sulfo-ChA and quantification of phenolics and sulfo-phenolics in potato extracts

The presence of the SO_3H moiety in 5-*O*-caffeoyl quinic acid caused a small bathochromic (λ_{max} shift from 325 to 329 nm) and a large hypochromic shift (Figure 2). The hypochromic shift effect was reflected in the extinction coefficient of 2'-sulfo-5-*O*-caffeoyl quinic acid ($9,357 \pm 395 \text{ M}^{-1}\text{cm}^{-1}$), which was half that of 5-*O*-caffeoyl quinic acid ($18,494 \pm 196 \text{ M}^{-1}\text{cm}^{-1}$). The extinction coefficient of 5-*O*-caffeoyl quinic acid was comparable to that reported in the literature ($18,130 \pm 242 \text{ M}^{-1}\text{cm}^{-1}$) (20).

Quantification of the (modified) HCAs/HCAcs/flavonols obtained in the presence of NaHSO_3 revealed that most chlorogenic acid isomers were modified (less than 1%, w/w, of total chlorogenic acid isomers were found as such), accounting for 95% (w/w) of all phenolic compounds. The content of sulfo-chlorogenic acid isomers obtained in the presence of NaHSO_3 was $113 \pm 25 \text{ mg}/100 \text{ g}$ potato DW, which corresponds to $102 \pm 20 \text{ mg}$ total chlorogenic acid isomers/100 g potato DW, a quantity that is well within the range of total chlorogenic acid isomers found in potato (1,2,11). Surprisingly, the total amount of

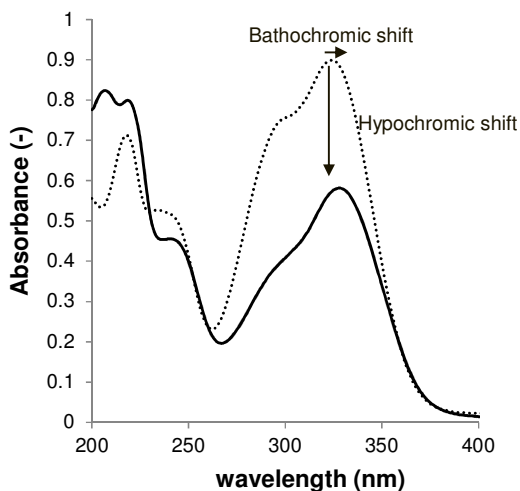


Figure 2. UV spectra of 0.05 mM 2'-sulfo-5-*O*-caffeoyl quinic acid (solid line) and 0.05 mM 5-*O*-caffeoyl quinic acid (dotted line).

chlorogenic acid isomers obtained in the presence of ascorbic acid was lower (60 ± 6 mg/100 g potato DW, $P < 0.05$) than that obtained in the presence of NaHSO_3 . Although the amount of ascorbic acid was nonlimiting, as judged by UHPLC-DAD-ESI-MSⁿ (data not shown), it might be that ascorbic acid competes with proteins in reacting with ChA quinone, by which ChA and ChA-protein complexes are formed, respectively. The latter are not analyzed by our method.

DISCUSSION

For the first time, molecular evidence of reaction products upon addition of NaHSO_3 as antibrowning agent against PPO during food processing is provided. Two new major compounds were identified as 2'-sulfo-5-*O*-caffeoyl quinic acid and 2'-sulfo-4-*O*-caffeoyl quinic acid, whereas several other minor compounds were tentatively assigned as positional isomers of sulfo-caffeoyl quinic acid, sulfo-caffeoyl putrescine, sulfo-caffeic acid isomers and sulfo-quercetin-3-*O*-glycosides. Our results suggest that whenever sodium hydrogen sulfite is used as antibrowning agent during fruit and vegetable processing, one can expect *o*-diphenolics to react into sulfo-*o*-diphenolics, which might change their nutritional and sensory properties.

Structural elucidation of the SO_3H -containing phenolics

In this study, we have found a series of phenolics with a molecular mass of 80 a.m.u. extra compared to the common compounds found in ascorbic acid-treated potato juice, which is diagnostic for the attachment of a sulfite group. With ^1H and ^{13}C NMR spectroscopy, it was possible to establish that the SO_3H moiety was attached to the C-2' position on the caffeic acid moiety as well as the position of the ester linkage between caffeic acid moiety and quinic acid moiety. Nevertheless, it could not be established whether the SO_3H group is attached to the aromatic ring through the sulfur or oxygen atom. Others have reported sulfated adducts of caffeic acid, 3-*O*- and 4-*O*-caffeoyl quinic acid isomers in urine and plasma, also with 80 a.m.u. extra (21). Interestingly, the MS^2 fragmentation pattern of those sulfated adducts differs from those of **22** and **23** (Figure 3). This suggests that in that study the sulphur-containing groups are differently attached to the aromatic ring compared to **22** and **23**. The MS^2 fragmentation of **22** and **23** yielded m/z 353 in very low abundance, whereas m/z 259, 241 and 215 were quite abundant. In contrast, 5-*O*-caffeoyl quinic acid-*O*-sulfate yielded the ion $[\text{M}-\text{SO}_3-\text{H}]^-$ with m/z 353 as base peak after MS^2 (21), and further fragmentation followed that of the precursor compound. No m/z 415, 387, 301, 259, 241, and 215 ions were reported in MS^2 , as in that study they were present in very low intensities (22). Hence, it is hypothesized that **22** and **23** are sulfo-adducts, in which the sulfur atom is attached directly to the aromatic ring. This is also consistent with the

proposed mechanism underlying the formation of **22** and **23** (see further). In wine model solutions, double-linked sulfate adducts have been reported (**23**), but these have only 64 a.m.u. extra, instead of 80.

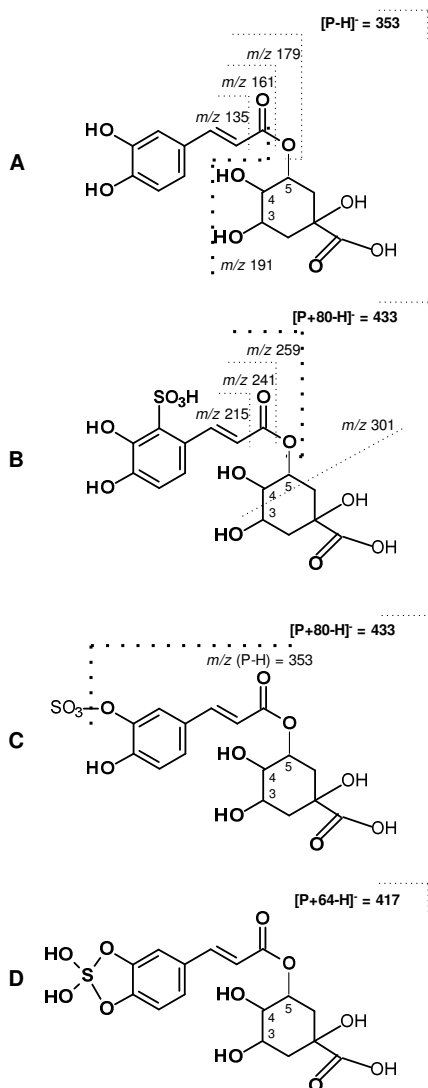


Figure 3. Distinctive MS fragmentation pattern of (A) 5-O-caffeoyl quinic acid (**3**) (B) 2'-sulfo-5-O-caffeoyl quinic acid (**23**) (C) 5-O-caffeoyl quinic acid sulfate, and (D) 5-O-caffeoyl quinic acid-double linked-O-sulfate. Part C was based on published results for 3-O- and 4-O-caffeoyl quinic acid-O-sulfate (**21**). Part D was based on results for adducts between catechin and sulfite (**23**). In part C, the hydroxyl group to which SO_3 is attached is arbitrary. P denotes the molecular mass of the precursor compound, 354 a.m.u. In each case, the thickest dotted line represents the most abundant fragment in MS^2 .

Following the MS fragmentation data, as presented in **Figure 3**, **14-18**, **20** and **21** are, analogous to **22** and **23**, annotated as sulfo-phenolics. More specifically, **15-18** and **20** as sulfo-caffeoyl quinic acid isomers and **14** and **21** as sulfo-caffeic acid isomers. Isomer **13**, with parent ion of m/z 433, gave the ion m/z 353 with relatively high intensity (80%) after MS fragmentation, which indicated that **13** might be a sulfated compound. Nevertheless, the presence of ions m/z 259, 241, and 215 in lower intensity suggested that it cannot be excluded that **13** is a sulfo-compound. MS² fragmentation of **19**, identified as sulfo-caffeoyl putrescine, gave the ion m/z 249 [caffeoyl putrescine-H]⁻ as base peak and m/z 241 [sulfocaffeic acid-H₂O-H]⁻ in high abundance.

Similar to sulfo-caffeoyl adducts, two modified flavonols were found and assigned as sulfo-quercetin glycosides. Fragmentation of the two modified quercetin glycosides (**24** and **25**) yielded the ion m/z 381 [sulfoquercetin-H]⁻ as base peak (**Table 2**). Its further fragmentation produced the aglycone m/z 301 [quercetin-H]⁻. In contrast, MS fragmentation of a glycosylated sulfate-flavonol has been shown to result in the glycosylated flavonol ion [M-80-H]⁻ (**24**), and its further fragmentation yielded the aglycone as base peak. It seems that the glycosidic linkage in quercetin glycoside sulfates is stronger than the bond attaching the sulfates, whereas in sulfo-quercetin glycosides this is the opposite.

Mechanism and position of sulfonation

With the commercial PPO it was shown that PPO is involved in the reaction between 5-*O*-caffeoyl quinic acid and NaHSO₃ to produce the sulfo-derivative. PPO catalyzes the oxidation of the *o*-diphenol in 5-*O*-caffeoyl quinic acid to its respective *o*-quinone (**Figure 4A**), which is prone to nucleophilic attack by HSO₃⁻. After this attack, the resulting ketone tautomerizes to the thermodynamically more stable enol form, which can exist in equilibrium with 2'-sulfo-5-*O*-caffeoyl quinic acid depending on the pH. This final compound is less reactive than the *o*-quinone and, therefore, the browning process is stopped.

For caffeic acid-containing compounds the addition might occur at positions C-2', C-5' and C-6'. As shown in **Figure 4B**, the C-2' position is preferred due to the conjugative delocalization of an electron to the side chain carbonyl, as well as to an oxygen on the aromatic ring (17). For the C-5' or C-6' position, only a single activation by electron migration to the oxygens attached to the aromatic ring is possible (17). On the other hand, from a steric perspective, the preferred substitution should follow the order C-5' > C-6' > C-2', with C-2' as the least accessible carbon (18). We postulate that the double activation overrules the steric hindrance effect. Our data are in agreement with the PPO catalyzed reaction between glutathione or cysteine and different caffeic acid derivatives, resulting in C-2' reaction products as the most abundant ones (17, 18, 25). The importance of the double activation is evident if compared to the reactivity of dihydrocaffeic acid *o*-quinone (18). In the latter case, no conjugative delocalization of an electron to the side

chain carbonyl is possible. Hence, the C-5' position is the most reactive, followed by C-6' and C-2', with the steric hindrance effect playing a major role.

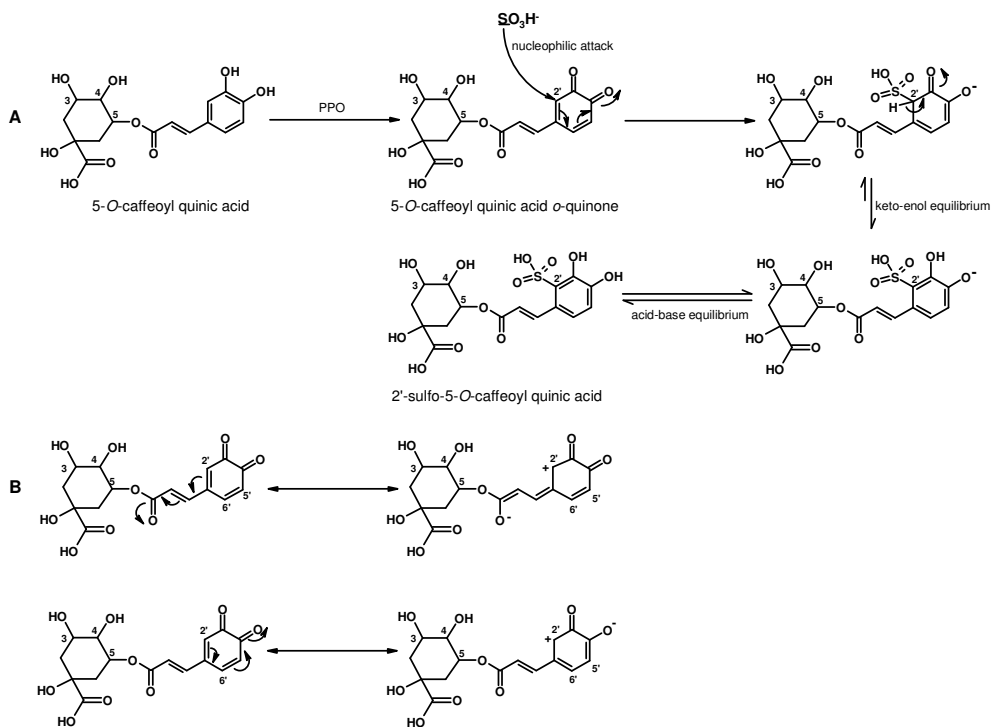


Figure 4. (A) Reaction between 5-*O*-caffeoyl quinic acid and HSO_3^- , after enzymatic activation of the aromatic ring to produce 2'-sulfo-5-*O*-caffeoyl quinic acid. **(B)** Double activation of the C-2' position of caffeic acid in 5-*O*-caffeoyl quinic acid.

Reaction of other phenolics with NaHSO_3

The lack of reactivity of ferulic acid- and sinapic acid-containing compounds with NaHSO_3 supports that PPO is involved in the reaction, as ferulic acid cannot be oxidized by PPO extracted from potato (26). In the case of sinapic acid no *o*-hydroxylation by PPO, and thus no further *o*-quinone formation, is possible.

The C-5' preferred nucleophilic attack has been shown for adducts of epicatechin/catechin and cysteine (25), and for adducts of catechin and glutathione (18). In these reactions, the initial enzymatic oxidation is crucial for the activation of the B ring. With no enzyme present, no adduct formation was observed. The C-5' is the most electrophilic and the least sterically hindered position and; therefore, a nucleophilic attack is more probable at this position (18). Hence, we postulate that **24** and **25** correspond to 5'-sulfo-quercetin-3-*O*-diglucoside and 5'-sulfo-rutin, respectively.

ACKNOWLEDGEMENTS

The authors are grateful to COLCIENCIAS and Universidad Nacional de Colombia for providing a fellowship to Carlos-Eduardo Narváez-Cuenca supporting this work. Part of this work was supported by the Commission of the European Communities within the Seventh Framework Programme for research and technological development (FP7), Grant Agreement No. 226930, title “Replacement of sulphur dioxide (SO₂) in food keeping the same quality and shelf-life of the products”, acronym SO2SAY. We thank Prof. Ricaurte Rodríguez-Angulo from Universidad Nacional de Colombia for his advice on the reactivity of *o*-quinones with HSO₃⁻ (**Figure 4**). Information about fragmentation of sulfated hydroxycinnamic acids by Dr. Angélique Stalmach, Prof. Alan Crozier (both University of Glasgow), and Prof. Gary Williamson (University of Leeds) is greatly appreciated by the authors.

REFERENCES

1. Andre, C. M.; Oufir, M.; Guignard, C.; Hoffmann, L.; Hausman, J. F.; Evers, D.; Larondelle, Y., Antioxidant profiling of native Andean potato tubers (*Solanum tuberosum* L.) reveals cultivars with high levels of β-carotene, α-tocopherol, chlorogenic acid, and petanin. *J. Agric. Food Chem.* **2007**, *55*, 10839-10849.
2. Shakya, R.; Navarre, D. A., Rapid screening of ascorbic acid, glycoalkaloids, and phenolics in potato using high-performance liquid chromatography. *J. Agric. Food Chem.* **2006**, *54*, 5253-5260.
3. Tudela, J. A.; Cantos, E.; Espin, J. C.; Tomas-Barberan, F. A.; Gil, M. I., Induction of antioxidant flavonol biosynthesis in fresh-cut potatoes. Effect of domestic cooking. *J. Agric. Food Chem.* **2002**, *50*, 5925-5931.
4. Gómez-López, V. M., Some biochemical properties of polyphenol oxidase from two varieties of avocado. *Food Chem.* **2002**, *77*, 163-169.
5. Makris, D. P.; Rossiter, J. T., An investigation on structural aspects influencing product formation in enzymic and chemical oxidation of quercetin and related flavonols. *Food Chem.* **2002**, *77*, 177-185.
6. Timbo, B.; Koehler, K. M.; Wolyniak, C.; Klontz, K. C., Sulfites - A food and drug administration review of recalls and reported adverse events. *J. Food Prot.* **2004**, *67*, 1806-1811.
7. Brunt, K.; Drost, W. C., Design, construction, and testing of an automated NIR in-line analysis system for potatoes. Part I: Off-line NIR feasibility study for the characterization of potato composition. *Potato Res.* **2010**, *53*, 25-39.
8. Guerrero-Beltrán, J. A.; Swanson, B. G.; Barbosa-Cánovas, G. V., Inhibition of polyphenoloxidase in mango puree with 4-hexylresorcinol, cysteine and ascorbic acid. *LWT - Food Sci. Tech.* **2005**, *38*, 625-630.
9. Sayavedra-Soto, L. A.; Montgomery, M. W., Inhibition of polyphenoloxidase by sulfite. *J. Food Sci.* **1986**, *51*, 1531-1536.
10. Ferrer, J. O.; Otwell, W. S.; Marshall, M. R., Effect of bisulfite on lobster shell phenoloxidase. *J. Food Sci.* **1989**, *54*, 478-480.

11. Narváez-Cuenca, C. E.; Vincken, J.-P.; Gruppen, H., Identification and quantification of (dihydro) hydroxycinnamic acids and their conjugates in potato by UHPLC-DAD-ESI-MSⁿ. *Food Chem.* **2012**, *130*, 467-475.
12. Ferreres, F.; Llorach, R.; Gil-Izquierdo, A., Characterization of the interglycosidic linkage in di-, tri-, tetra- and pentaglycosylated flavonoids and differentiation of positional isomers by liquid chromatography/electrospray ionization tandem mass spectrometry. *J. Mass Spectrom.* **2004**, *39*, 312-321.
13. Balcerzak, M.; Kopacz, M.; Kosiorek, A.; Swiecicka, E.; Kus, S., Spectrophotometric studies of the interaction of noble metals with quercetin and quercetin-5'-sulfonic acid. *Anal. Sci.* **2004**, *20*, 1333-1337.
14. Justino, G. C.; Santos, M. R.; Canário, S.; Borges, C.; Florêncio, M. H.; Mira, L., Plasma quercetin metabolites: Structure-antioxidant activity relationships. *Arch. Biochem. Biophys.* **2004**, *432*, 109-121.
15. Scholz-Bottcher B.M., E. L., Maier HG, New stereoisomers of quinic acid and their lactones. *Liebigs Ann. Chem.* **1991**, 1029-1036.
16. Clifford, M. N.; Johnston, K. L.; Knight, S.; Kuhnert, N., Hierarchical scheme for LC-MSⁿ identification of chlorogenic acids. *J. Agric. Food Chem.* **2003**, *51*, 2900-2911.
17. Cheynier, V. F.; Trousdale, E. K.; Singleton, V. L.; Salgues, M. J.; Wylde, R., Characterization of 2-S-glutathionylcaftaric acid and its hydrolysis in relation to grape wines. *J. Agric. Food Chem.* **1986**, *34*, 217-221.
18. Moridani, M. Y.; Scobie, H.; Jamshidzadeh, A.; Salehi, P.; O'Brien, P. J., Caffeic acid, chlorogenic acid, and dihydrocaffeic acid metabolism: Glutathione conjugate formation. *Drug Metab. Dispos.* **2001**, *29*, 1432-1439.
19. Chen, M.; Song, F.; Guo, M.; Liu, Z.; Liu, S., Analysis of flavonoid constituents from leaves of *Acanthopanax senticosus* Harms by electrospray tandem mass spectrometry. *Rapid Commun. Mass Spec.* **2002**, *16*, 264-271.
20. Dao L., F. M., Chlorogenic acid content of fresh and processed potatoes determined by ultraviolet spectrophotometry. *J. Agric. Food Chem.* **1992**, *40*, 2152-2156.
21. Stalmach, A.; Mullen, W.; Barron, D.; Uchida, K.; Yokota, T.; Cavin, C.; Steiling, H.; Williamson, G.; Crozier, A., Metabolite profiling of hydroxycinnamate derivatives in plasma and urine after the ingestion of coffee by humans: Identification of biomarkers of coffee consumption. *Drug Metab. Dispos.* **2009**, *37*, 1749-1758.
22. Stalmach, A. W., G.; Crozier, A., Personal communication. In **2011**.
23. Nonier, M. F.; Vivas, N.; Gaulejac, N. V. d.; Absalon, C.; Vitry, C., Study by LC/ESI/MSⁿ and ESI/HR/MS of SO₂ interactions in flavanols-aldehydes nucleophilic reactions. *Food Chem.* **2010**, *122*, 488-494.
24. Ferreres, F.; Fernandes, F.; Oliveira, J. M. A.; Valentão, P.; Pereira, J. A.; Andrade, P. B., Metabolic profiling and biological capacity of *Pieris brassicae* fed with kale (*Brassica oleracea* L. var. *acephala*). *Food Chem. Toxicol.* **2009**, *47*, 1209-1220.
25. Richard, F. C.; Goupy, P. M.; Nicolas, J. J.; Lacombe, J. M.; Pavia, A. A., Cysteine as an inhibitor of enzymatic browning. 1. Isolation and characterization of addition compounds formed during oxidation of phenolics by apple polyphenol oxidase. *J. Agric. Food Chem.* **1991**, *39*, 841-847.
26. Ni Eidhin, D.; Degn, P.; O'Beirne, D., Characterization of polyphenol oxidase from rooster potato (*Solanum tuberosum* cv Rooster). *J. Food Biochem.* **2010**, *34*, 13-30.

Chapter 3

Inhibition of enzymatic browning of chlorogenic acid by sulfur-containing compounds

The anti-browning activity of sodium hydrogen sulfite (NaHSO_3) was compared to that of other sulfur-containing compounds. Inhibition of enzymatic browning was investigated using a model browning system consisting of mushroom tyrosinase and chlorogenic acid (ChA). Development of brown color (spectral analysis), oxygen consumption, and reaction product formation (RP-UHPLC-DAD-MS) were monitored in time. It was found that the compounds showing anti-browning activity either prevented browning by forming colorless addition products with *o*-quinones of ChA (NaHSO_3 , cysteine, glutathione) or by inhibiting the enzymatic activity of tyrosinase (NaHSO_3 , dithiothreitol). NaHSO_3 was different from the other sulfur-containing compounds investigated, as it showed a dual inhibitory effect on browning. Initial browning was prevented by trapping the *o*-quinones formed in colorless addition products (sulfo-ChA), while at the same time tyrosinase activity was inhibited in a time-dependent way, as was shown by pre-incubation experiments of tyrosinase with NaHSO_3 . Furthermore, it was demonstrated that sulfo-ChA and cysteinyl-ChA were not inhibitors of mushroom tyrosinase.

Based on: Kuijpers, T.F.M.; Narváez-Cuenca, C.-E.; Vincken, J.-P.; Verloop, A.J.W.; van Berkel, W.J.H.; Gruppen, H. *J. Agric. Food Chem.* **2012**, *60*, 3507-3514.

INTRODUCTION

Enzymatic browning is a major quality problem in the processing of fruits and vegetables. The enzymes responsible for enzymatic browning are polyphenol oxidases (PPOs), which, depending on their source, can either catalyze the *o*-hydroxylation and subsequent oxidation of a wide range of phenolic substrates (tyrosinase, cresolase or monophenolase activity), or only the oxidation of *o*-diphenols (catecholase or diphenolase activity) (1,2). The oxidation of *o*-diphenols results in *o*-quinones, which in turn react with each other and other compounds present, resulting in dark colored pigments (3). Additives widely used to inhibit enzymatic browning include sulfites and ascorbic acid (2,4).

Different sulfites used as food additives are sodium sulfite (Na_2SO_3), sodium metabisulfite ($\text{Na}_2\text{S}_2\text{O}_5$), and sodium hydrogen sulfite (NaHSO_3 , also referred to as sodium bisulfite). When dissolved, these salts yield a mixture of SO_3^{2-} and HSO_3^- (5). Three possible mechanisms for browning inhibition by sulfite have been suggested: (i) irreversible inhibition of PPO (6), (ii) reduction of *o*-quinones, thereby reversing the enzymatic reaction (4), and (iii) formation of addition products between sulfite and *o*-quinones, preventing them to react further into brown pigments (7).

Using sulfites in food products is controversial because of related health risks (8). An alternative anti-browning agent is ascorbic acid. The mechanism by which ascorbic acid inhibits browning is well known: *o*-quinones formed by PPO are reduced to their precursors, *o*-diphenols, which subsequently can be oxidized again (9). This redox cycling continues until all ascorbic acid is consumed, after which the brown colored pigments are still formed. Therefore, ascorbic acid can delay browning, but it does not inhibit enzymatic activity. Hence, much effort has been put in finding natural sulfite alternatives. Many PPO inhibitors have been identified and often their mode of inhibition has been determined (10). Surprisingly, the mechanism by which sulfite inhibits browning is still unclear, despite its common use for a long time.

Recently, it was found that, when extracting phenolic compounds from potato in the presence of sulfite, the expected phenolic compounds, mainly chlorogenic acid, were absent in the extracted material (11). Sulfonated derivatives were found instead. It was proposed that PPO-catalyzed *o*-quinone formation was a prerequisite for the formation of these sulfophenolics, and that formation of these compounds might be responsible for inhibition of browning.

In the present study, the effect of sulfite on PPO-catalyzed browning was further investigated. In contrast to the previous research (11), a model browning system was used, consisting of chlorogenic acid (**Figure 1**) and a commercially available mushroom PPO (tyrosinase; EC 1.14.18.1). The mechanism of action of NaHSO_3 is compared to that of other sulfur-containing compounds (**Figure 1**). Cysteine and glutathione (GSH) were selected, as these compounds are known to form adducts with *o*-quinones (12-15). Besides

formation of adducts with *o*-quinones, the anti-browning activity of cysteine has also been proposed to be due to irreversible inhibition of PPO (16). Dithiothreitol (DTT) was chosen because it was reported to be an inhibitor of tyrosinase-catalyzed browning. However, different explanations have been given: DTT was found to form addition products with *o*-quinones, it was found to reversibly inhibit tyrosinase, and it was found to reduce the copper in the active site of tyrosinase (17, 18). It should be noted that the results for the sulfur-containing compounds mentioned above were obtained in different studies, under a variety of conditions. For example, type of substrate, substrate concentration, inhibitor concentration, and enzyme source varied over the different studies.

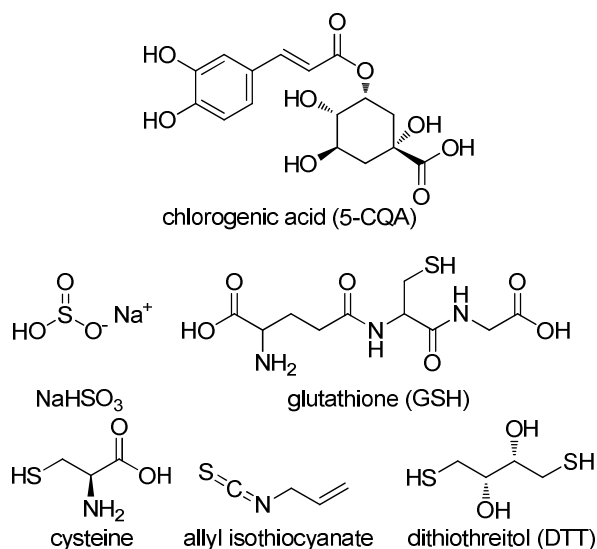


Figure 1. Structures of substrate and different sulfur-containing compounds used in this study.

Here, we compared the anti-browning properties of the different sulfur-containing compounds under similar conditions. To investigate whether other natural sulfur-containing compounds might have the potential to function as a sulfite alternative, allyl isothiocyanate was selected. Isothiocyanates result from the hydrolysis and subsequent rearrangements of their precursors, glucosinolates, which widely occur in for instance the Brassicaceae plant family (19).

MATERIALS AND METHODS

Materials

Mushroom tyrosinase, chlorogenic acid (5-*O*-caffeoylquinic acid, ChA), sodium hydrogen sulphite (NaHSO₃), L-ascorbic acid, L-cysteine, L-glutathione (GSH), dithiothreitol (DTT) and allyl isothiocyanate were purchased from Sigma Aldrich (St. Louis, MO, USA). Ultra-high-performance liquid chromatography/mass spectrometry (UHPLC/MS) grade acetonitrile (ACN) was obtained from Biosolve BV (Valkenswaard, The Netherlands). Water was prepared using a Milli-Q water purification system (Millipore, Billerica, MA, USA).

Purification of mushroom tyrosinase

Commercial mushroom tyrosinase was purified by a single gel filtration step (20). A HiLoad 26/60 Superdex 200 column connected to an Akta Explorer system (GE Healthcare, Uppsala, Sweden) was used. A total of 50 mg of the commercial enzyme [dissolved in 50 mM *N*-2-hydroxyethylpiperazine-*N'*-2-ethanesulfonic acid (HEPES) buffer pH 6.8] was loaded and eluted with 50 mM HEPES buffer at pH 6.8 at 4 mL/min. Fractions (5 mL) were collected, and activity was assayed by a spectrophotometric assay: 50 μ L of each fraction was combined with 100 μ L 0.8 mM tyrosine in a 96-well plate, and absorbance at 520 nm was monitored in time. Active fractions were pooled and stored at -20 °C until use. Tyrosinase activity was expressed in units, according to the suppliers definition (1 unit increases the A₂₈₀ by 0.001 min⁻¹ with L-tyrosine as substrate, at pH 6.5 and 25 °C).

Incubation of ChA and tyrosinase with browning inhibitors

ChA (0.1 mM), sulfur-containing compounds (0.2 mM) or ascorbic acid (0.2 mM), and tyrosinase (7 units/mL) were mixed in 10 mM HEPES buffer pH 6.5. Samples were incubated at room temperature for 1 h, centrifuged (10,000 \times g; 5 min; room temperature), and analyzed by RP-UHPLC. For spectrophotometric analysis, the same reaction mixtures were incubated in quartz cuvettes in a UV-1601 spectrophotometer (Shimadzu, Kyoto, Japan). Wavelength scans were made from 200 to 600 nm. A scan was made every min, for a total of 60 min.

RP-UHPLC analysis

Samples were analysed on an Accela UHPLC system (Thermo Scientific, San Jose, CA, USA) equipped with a pump, an autosampler and a diode array detector (DAD). Samples (5 μ L) were injected onto a Hypersil Gold column (2.1 \times 150 mm, particle size 1.9 μ m; Thermo Scientific). Water acidified with 0.1% (v/v) acetic acid, eluent A, and ACN acidified with 0.1% (v/v) acetic acid, eluent B, were used as eluents. The flow rate was 400

$\mu\text{L}/\text{min}$, and the column oven temperature was controlled at 30 °C. The DAD was set to measure the range 200-600 nm. The following elution profile was used: 0-1 min, isocratic on 0% (v/v) B; 1-6 min, linear gradient from 0% to 35% (v/v) B; 6-7 min, linear gradient from 35% to 100% (v/v) B; 7-9 min, isocratic on 100% (v/v) B; 9-10 min, linear gradient from 100% to 0% (v/v) B; and 10-12 min, isocratic on 0% (v/v) B.

Electrospray ionization-mass spectrometry (ESI-MS)

Mass spectrometric data were obtained by analyzing samples on a LTQ-XL (Thermo Scientific) equipped with an ESI probe coupled to the RP-UHPLC system. Nitrogen was used as sheath gas and auxiliary gas. Data were collected over the m/z range 150-1,500. Data-dependent MSⁿ analysis was performed with a normalized collision energy of 35%. The MSⁿ fragmentation was performed on the most intense product ion in the MSⁿ⁻¹ spectrum. Most settings were optimized via automatic tuning using 'Tune Plus' (Xcalibur 2.07, Thermo Scientific). The system was auto-tuned with ChA in negative ionization (NI) mode. The transfer tube temperature was 350 °C, and the source voltage 3.5 kV. Data acquisition and reprocessing were done with Xcalibur 2.07 (Thermo Scientific).

Preparative HPLC purification of sulfoChA

Samples of ChA (1 mM) incubated with NaHSO₃ (2 mM) and tyrosinase (70 units/mL) were fractionated on a preparative HPLC system (Waters, Milford, MA, USA), using a semi-preparative Hypersil Gold column (20 × 150 mm, particle size 5 μm ; Thermo Scientific) with a Hypersil guard column (20 × 20 mm, particle size 5 μm ; Thermo Scientific). Water acidified with 0.2% (v/v) acetic acid (eluent A) and ACN acidified with 0.2% (v/v) acetic acid (eluent B) were used as eluents. The flow rate was 30 mL/min. The following elution profile was used: 0-2 min, isocratic on 2% (v/v) B; 2-17 min, linear gradient from 2 to 10% (v/v) B; 17-20 min, linear gradient from 10 to 100% (v/v) B; 20-25 min, isocratic on 100% (v/v) B; 25-27 min, linear gradient from 100 to 2% (v/v) B; and 27-37 min, isocratic on 2% (v/v) B. Fractions (14 mL) were collected and pooled based on UV response at 320 nm. The major reaction product was found to be 2'-SO₃H-ChA (11), with a purity of 94% (based on peak integration at 320 nm), which was in accordance with the MS base peak chromatogram.

Preparative purification of cysteinyl-ChA using flash chromatography

Samples of ChA (1 mM) incubated with cysteine (2 mM) and tyrosinase (70 units/mL) were fractionated on a flash chromatography system (Grace, Deerfield, IL, USA) using a Reveleris C18 flash cartridge (Grace). Water acidified with 0.1% (v/v) acetic acid (eluent A) and ACN acidified with 0.1% (v/v) acetic acid (eluent B) were used as eluents. The cartridge was equilibrated with 5 column volumes of B, followed by 5 column volumes of A. The following elution profile was used: 0-10 min, linear gradient from 0 to 40% (v/v) B;

10-14 min, linear gradient from 40 to 100% (v/v) B; and 14-16 min, isocratic on 100% (v/v) B. Fractions (25 mL) were collected and pooled based on UV response at 320 nm. The major reaction product was found to be 2'-S-cysteiny-ChA (12), with a purity of 95% (on the basis of peak integration at 320 nm), which was in accordance with the MS base peak chromatogram.

Oxygen consumption measurements

Oxygen consumption of tyrosinase was measured using an Oxytherm System (Hansatech, Kings Lynn, UK). Incubations with ChA (0.5 mM) and tyrosinase (35 U/mL) with or without sulfur-containing compound (1 mM) or ascorbic acid (1 mM) were done in a total volume of 1 mL 10 mM HEPES buffer at pH 6.5 and 25 °C. Data acquisition and analysis were performed using Oxygraph Plus software (Hansatech).

In case of pre-incubation experiments, tyrosinase (35 units/mL) and sulfur-containing compounds (1 mM) were incubated for different times (specified in the text) at 25 °C, after which concentrated ChA (50 mM) was added to reach a final concentration of 0.5 mM.

RESULTS AND DISCUSSION

In vitro browning of ChA by tyrosinase

To investigate the effect of different sulfur-containing compounds on ChA conversion by tyrosinase, the reaction products of the *in vitro* browning of ChA by tyrosinase were analyzed. The formation of reaction products was monitored by both RP-UHPLC-DAD-MS analysis and recording absorption spectra of the reaction mixture at different time intervals (**Figure 2**). Results were compared to those obtained in the presence of ascorbic acid, which was used as a reference anti-browning agent.

After incubation the absorption spectra of a mixture of ChA and tyrosinase (**Figure 2A**) showed a clear decrease in absorbance at the typical maximum for ChA, 326 nm. New maxima at 250 nm and around 400 nm appeared, the latter being responsible for the brown color observed after the reaction. The corresponding RP-UHPLC-DAD trace (**Figure 2F**) showed that different reaction products were formed. Based on the rise of the baseline, it seemed that a multitude of compounds eluted between 4.5 and 6.5 min, with three clear peaks standing out (peaks **1**, **2** and **3**). Peak **1** was identified as ChA, both based on MS analysis (**Table 1**) and by comparing to RP-UHPLC analysis of the authentic standard. MS analysis of peak **2** revealed an m/z of 351, corresponding to a mass of 352, which might represent the mass of the *o*-quinone of ChA, an expected reaction product of ChA and tyrosinase (21). MS² analysis yielded m/z 215 as the most abundant product ion, which could not be explained. Two less abundant product ions were m/z 177 and m/z 133, which might correspond to the fragments m/z 179 and m/z 135, respectively, found in MS² of

ChA, taking into account the loss of two protons upon oxidation of ChA. Peak **3** had m/z 705, and MS² resulted in a predominant fragment with m/z 513, the MS³ fragmentation of which resulted in a major product ion of m/z 339. Dimers of ChA, resulting from oxidation by tyrosinase, showing the same MS fragmentation have been described before (22), and were also found in oxidized apple extracts (23). Based on these data, compounds **2** and **3** (Table 1) were tentatively identified as the *o*-quinone and dimer of ChA, respectively.

Table 1. Identification of reaction products of ChA, NaHSO₃, cysteine, GSH and tyrosinase.

No	RT (min)	[M-H] (m/z)	MS ⁿ fragments (% relative abundance) (m/z)	UV λ_{\max} (nm)	Tentative identification
1	5.11	353	MS ² [353]: 191 (100), 179 (4), 135 (1)	326	5-O-Caffeoylquinic acid (ChA)
2	4.75	351	MS ² [351]: 215 (100), 177 (15), 195 (8), 133 (6), 307 (6), 173 (5), 123 (5), 261 (2), 155 (2), 149 (2), 191 (1)	251, 300	ChA quinone
3	5.61	705	MS ² [705]: 513 (100) MS ³ [705 → 513]: 339 (100), 321 (10), 496 (7), 295 (2)	323	ChA dimer
4	4.45	433	MS ² [433]: 259 (100), 415 (47), 215 (38), 241 (23), 387 (17), 161 (16) 301 (7)	240, 328	2'-Sulfo-5-O-caffeoylquinic acid (2'-SO ₃ H-ChA)
5	1.77	433	MS ² [433]: 353 (100), 191 (30), 241 (24), 161 (13), 415 (7), 271 (4), 179 (1) MS ³ [433 → 353]: 191 (100), 179 (6), 135 (1)	244, 302	Sulfo-caffeoylquinic acid isomer
6	3.16	433	MS ² [433]: 241 (100), 415 (93), 387 (11), 259 (9), 213 (7), 416 (4), 433 (3), 242 (3), 161 (1), 133 (1) MS ³ [433 → 241]: 213 (100), 241 (56), 161 (5), 133 (3)	296, 324	Sulfo-caffeoylquinic acid isomer
7	4.09	433	MS ² [433]: 259 (100), 415 (37), 215 (33), 241 (20), 387 (18), 161 (12), 301 (11)	315	Sulfo-caffeoylquinic acid isomer
8	4.49	472	MS ² [472]: 385 (100), 193 (18), 191 (17), 236 (12), 280 (3), 351 (2), 298 (2), 167 (2) MS ³ [472 → 385]: 191 (100), 193 (89), 211 (1)	250, 326	2'-S-Cysteinyl-5-O-caffeoylquinic acid
9	4.57	658	MS ² [658]: 385 (100), 466 (55), 272 (24), 193 (13), 529 (12), 191 (11), 448 (4), 379 (4), 254 (4), 337 (2), 211 (2), 340 (1), 306 (1), 293 (1), 210 (1) MS ³ [658 → 385]: 191 (100), 193 (94), 211 (1)	252, 325	2'-S-Glutathionyl-5-O-caffeoylquinic acid

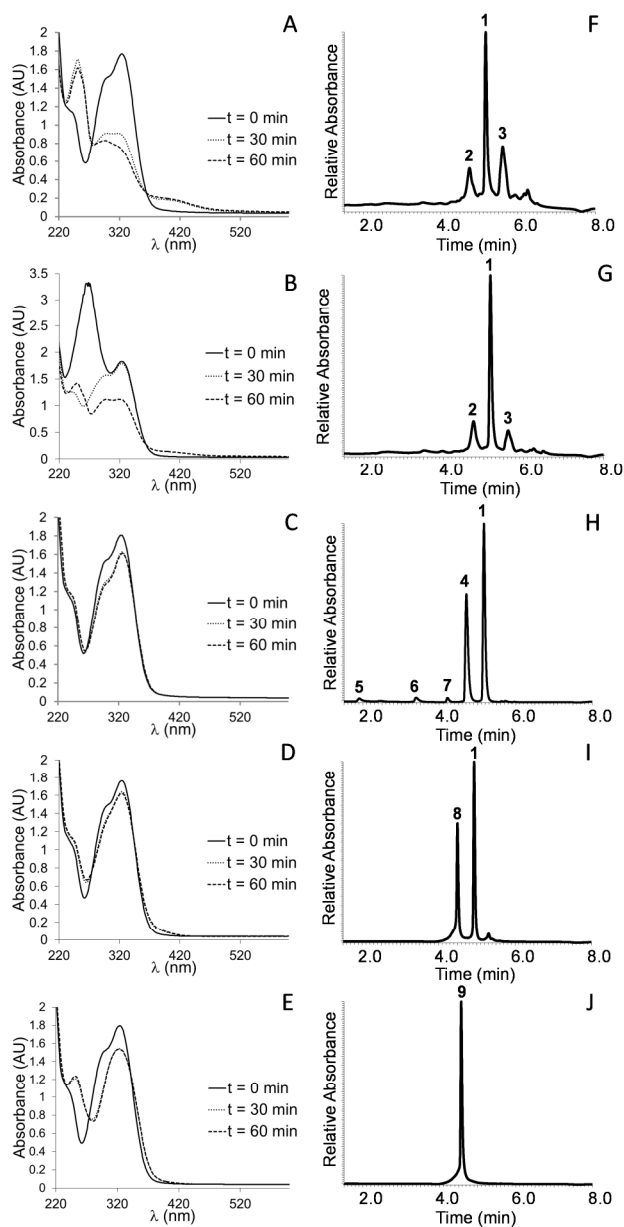


Figure 2. Absorption spectra of ChA (0.1 mM) incubated with tyrosinase (7 units/mL) with and without potential browning inhibitors (**A** to **E**) at different incubation times and RP-UHPLC-DAD traces (320 nm) of the reaction mixtures after incubation (**F** to **J**): (**A** and **F**), ChA with tyrosinase alone; (**B** and **G**), ChA with tyrosinase and ascorbic acid (0.2 mM); (**C** and **H**), ChA with tyrosinase and NaHSO₃ (0.2 mM); (**D** and **I**), ChA with tyrosinase and cysteine (0.2 mM); and (**E** and **J**), ChA with tyrosinase and GSH (0.2 mM).

The absorption spectra of ChA and tyrosinase incubated in the presence of ascorbic acid (**Figure 2B**) showed that ascorbic acid delays enzymatic browning. At time zero, besides the typical 326 nm maximum for ChA, also a maximum at 265 nm was observed, caused by the ascorbic acid present. After 30 min of incubation, this maximum disappeared, whereas the ChA maximum remained. After 60 min of incubation, the spectrum was similar to the spectrum of ChA incubated with tyrosinase after 30 and 60 min: a decrease in absorbance at 326 nm, and new maxima formed at 250 nm and around 400 nm. The RP-UHPLC-DAD trace (**Figure 2G**) was similar to that of ChA incubated with tyrosinase alone (**Figure 2F**). The same compounds were present, only the ratio between them differing. These results confirmed that ascorbic acid delays browning.

Effect of different sulfur-containing compounds on ChA conversion by tyrosinase

To investigate the influence of different sulfur-containing compounds on tyrosinase-catalyzed browning of ChA, combinations of ChA, tyrosinase, and NaHSO₃, cysteine, GSH, DTT, or allyl isothiocyanate were incubated. Formation of reaction products was monitored as described above.

The absorption spectra of ChA did not change substantially upon incubation with tyrosinase and NaHSO₃ (**Figure 2C**). After 30 and 60 min a small decrease in absorption at 326 nm was observed, with no new maxima formed. RP-UHPLC-DAD analysis resulted in five peaks (**Figure 2F**). Besides ChA (compound **1**), four reaction products were present, which were identified by MS analysis (**Table 1**). Comparing the product ions found for compounds **4-7** with published MS fragmentation data for ChA (24-26), the fragments diagnostic for ChA were observed, only with an increase of 80 a.m.u.. The product ions with m/z 259, 241 and 215 corresponded to product ions with m/z 179, 161 and 135, respectively. According to the fragmentation pattern of ChA, these three product ions all contained the phenolic ring of the caffeic acid moiety of ChA, indicating that the addition of HSO₃⁻ occurred on this phenolic ring. Compounds **4-7** were tentatively identified as different sulfo-caffeoyl quinic acid isomers, with the main reaction product being 2'-sulfo-5-*O*-caffeoylquinic acid (2'-SO₃H-ChA) (**11**).

For the incubation of ChA with tyrosinase and cysteine, the absorption spectra also did not change substantially (**Figure 2D**). After incubation, a small decrease in absorption at 326 nm and a small increase in absorption at 260 nm were observed. RP-UHPLC-DAD analysis revealed two major peaks (**Figure 2I**). Besides ChA, a new peak was observed (compound **8**). MS analysis of compound **8** revealed a mass of 473, equal to the combined masses of ChA (354) and cysteine (121), minus 2 for the two hydrogen atoms lost due to the formation of a covalent bond between cysteine and ChA. Upon fragmentation of compound **8**, a product ion with m/z 385 was predominantly formed. The occurrence of this product can be explained by the loss of part of the cysteine moiety, with the sulfur of

cysteine remaining bound to ChA. MS³ analysis of this fragment resulted in fragments with m/z 191 and 193, which could be explained as the quinic acid and dehydrated caffeoyl moiety with sulfur attached, respectively. Similar fragmentation has been observed for addition products of ChA and *N*-acetyl-cysteine (22). An addition product of cysteine and ChA has been identified as 2'-*S*-cysteinyl-5-*O*-caffeoylquinic acid (12). Based on these data, compound **8** was tentatively identified as 2'-*S*-cysteinyl-5-*O*-caffeoylquinic acid.

When incubated with tyrosinase and GSH, the absorption spectra of ChA showed a small decrease in absorption at 326 nm and a bathochromic shift for the minimum observed at 260 nm before incubation to 275 nm after incubation (**Figure 2E**). RP-UHPLC-DAD analysis revealed total depletion of ChA with formation of a single reaction product, compound **9** (**Figure 2J**). MS analysis of compound **9** resulted in a mass of 659, corresponding to a covalent addition product of ChA and GSH (354 + 307 - 2). MS² and MS³ analysis resulted in the same fragments as described above for the fragmentation of 2'-*S*-cysteinyl-5-*O*-caffeoylquinic acid. On the basis of this and previous data (15, 27), compound **9** was tentatively identified as 2'-*S*-glutathionyl-5-*O*-caffeoylquinic acid.

Incubation of ChA with tyrosinase and DTT resulted in total inhibition of ChA conversion: The absorption spectra after 30 and 60 min were the same as at 0 min, and RP-UHPLC analysis showed that only ChA was present after incubation (See panels **A** and **C** of **Figure S1** of the **Supporting Information**). Complete inhibition of tyrosinase by DTT was found before (18), while also adduct formation between *o*-quinones and DTT was observed (17). Interestingly, our results did not indicate such adduct formation. Possibly, adduct formation is concentration dependent: at relative high concentrations of DTT tyrosinase is strongly inhibited, while at lower concentrations tyrosinase remains (partly) active, making *o*-quinones available for addition of DTT.

Allyl isothiocyanate seemed to have little influence on ChA conversion, both absorption spectra and UHPLC-DAD trace (See panels **B** and **D** of **Figure S1** of the **Supporting Information**) were similar to the ones obtained with the control experiment of only ChA and tyrosinase (Panels **A** and **F** of **Figure 2**).

Influence of sulfur-containing compounds on brown color formation and oxygen consumption

The rate of color formation and oxygen consumption during incubations of ChA with tyrosinase and different potential anti-browning agents was determined by monitoring the absorbance at 400 nm and the oxygen consumption in time (**Figure 3**). It can be seen that there is not always a correlation between these parameters. While incubations with cysteine and GSH showed oxygen consumption rates comparable to the control experiment of only ChA and tyrosinase, they showed much less color development. The reduced color formation corresponded to the formation of 2'-*S*-cysteinyl-5-*O*-caffeoylquinic acid and 2'-*S*-glutathionyl-5-*O*-caffeoylquinic acid, respectively (Panels **I** and **J** of **Figure 2**).

Ascorbic acid showed a higher oxygen consumption compared to the control experiment, while the onset of color formation in the presence of ascorbic acid was delayed. This confirmed the mechanism of browning inhibition by ascorbic acid, as described before. Incubation with allyl isothiocyanate resulted in both slightly reduced oxygen consumption and slightly reduced brown coloration. DTT seemed to prevent browning by inhibiting tyrosinase activity: both oxygen consumption and brown color formation were totally inhibited at the concentration used. This corresponds well with the absorption spectra and UHPLC-MS analysis of the incubation of ChA with tyrosinase and DTT (See panels A and C of **Figure S1** of the **Supporting Information**), where no conversion of ChA was observed. When ChA was incubated with tyrosinase and NaHSO₃, it was observed that oxygen consumption leveled off during the experiment, to a plateau value of around 75% of the starting concentration of oxygen. This indicated that tyrosinase activity was somehow lost during the course of the incubation. In the presence of NaHSO₃, no color development was observed, consistent with the spectra in **Figure 2C**.

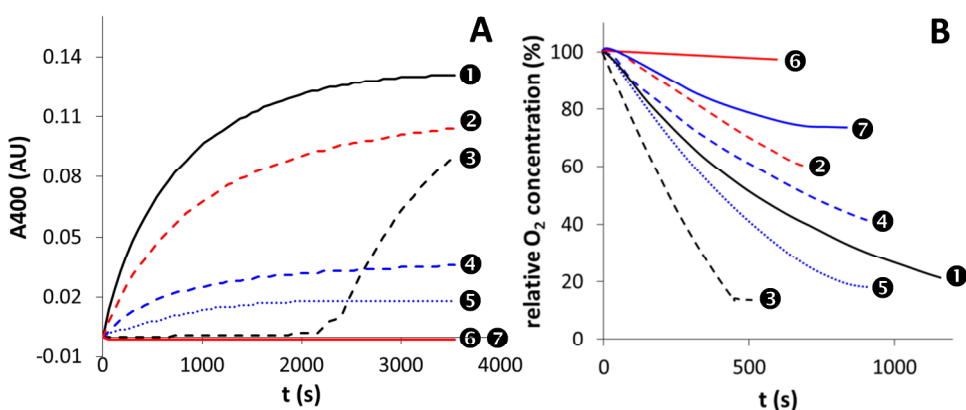


Figure 3. Development of brown color measured by (A) monitoring absorbance at 400 nm and (B) monitoring of oxygen consumption in time during incubations of ChA (A, 0.1 mM; B, 0.5 mM) with tyrosinase (A, 7 units/mL; B, 35 units/mL), in the presence of different sulfur-containing compounds and ascorbic acid (A, 0.2 mM; B, 1 mM). ①, control; ②, allyl isothiocyanate; ③, ascorbic acid; ④, cysteine; ⑤, GSH; ⑥, DTT; ⑦, NaHSO₃.

In contrast to incubations of ChA and tyrosinase with NaHSO₃, those with cysteine and GSH resulted in some browning. Comparing the UHPLC-DAD absorption spectra of the different addition products and ChA, it was found that 2'-S-cysteinyl-5-O-caffeoylquinic acid and 2'-S-glutathionyl-5-O-caffeoylquinic acid had a higher absorbance around 400 nm compared to ChA, while that for 2'-SO₃H-ChA was comparable to that of ChA (**Figure 4**). Although the absorbance at 400 nm of 2'-S-glutathionyl-5-O-caffeoylquinic acid is higher than that of 2'-S-cysteinyl-5-O-caffeoylquinic acid, for

the total reaction mixtures with these compounds one observes the opposite (**Figure 3A**). This suggests that the absorbance of the cysteine addition product only partially explains the observed browning. A possible explanation might be that some of the *o*-quinones formed reacted further into brown pigments prior to reaction with cysteine.

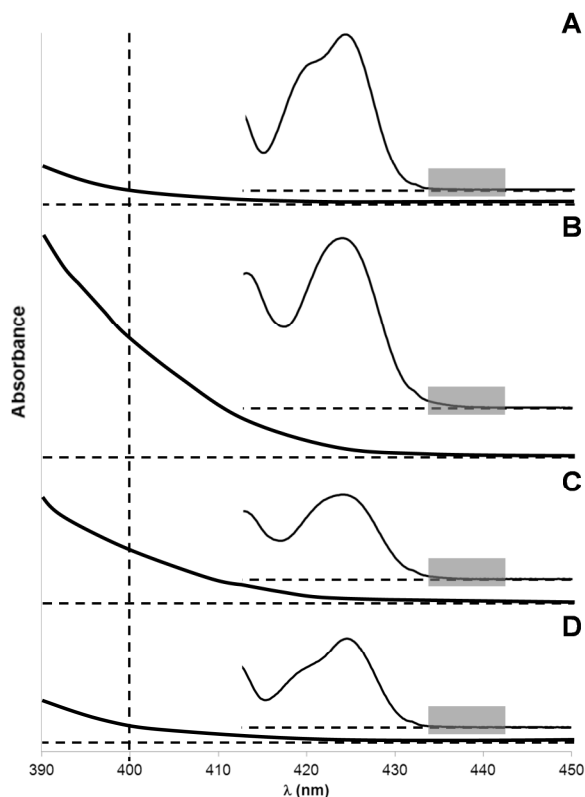


Figure 4. UHPLC-DAD absorption spectra of (A) ChA, (B) 2'-S-glutathionyl-5-O-caffeoylquinic acid, (C) 2'-S-cysteinyl-5-O-caffeoylquinic acid, and (D) 2'-SO₃H-5-O-caffeoylquinic acid. Absorption spectra were derived from peaks 1, 9, 8 and 4 (**Figure 2**), respectively. Insets show spectra of 250-500 nm, and the grey windows indicate the wavelength range (390-450 nm) of the zoom.

Reduction of tyrosinase activity during formation of sulfoChA

NaHSO₃ showed a distinctly different effect compared to the other inhibitors investigated: no brown color formation was observed and oxygen consumption leveled off during incubation with ChA and tyrosinase. This observation was investigated further by monitoring the amount of ChA converted by tyrosinase in time with or without NaHSO₃ using RP-UHPLC (See **Figure S2** of the **Supporting Information**). It was found that, with NaHSO₃ present, not all ChA was converted, consistent with the observation that less

oxygen was consumed when ChA was incubated in combination with NaHSO_3 and tyrosinase, compared to an incubation of ChA and tyrosinase alone. The addition of a second dose of tyrosinase restored oxygen consumption and ChA conversion (**Figure 5A**). Markakis and Embs (28) found a similar effect of NaHSO_3 when following the activity of mushroom tyrosinase in a reaction mixture containing tyrosine and NaHSO_3 .

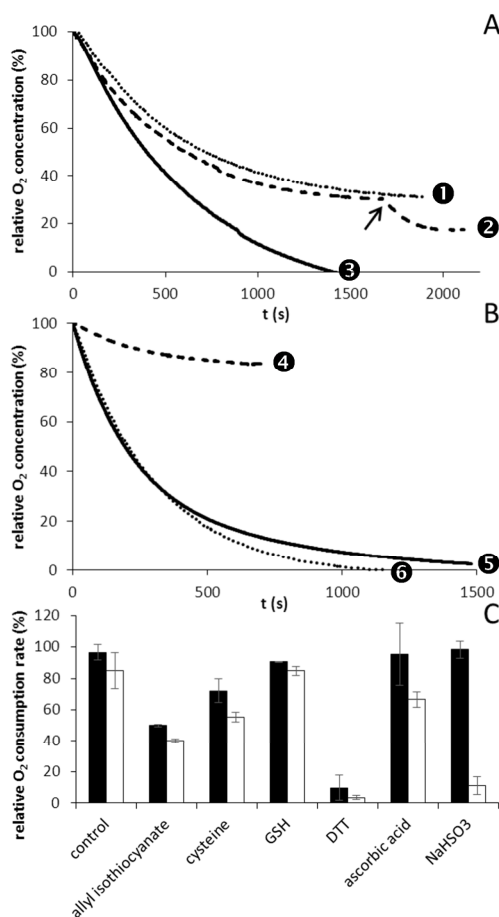


Figure 5. Oxygen consumption in time upon (A) incubation of ChA (0.5 mM) and tyrosinase (35 units/mL) with and without NaHSO_3 (1 mM), (B) incubation of ChA (0.5 mM) with 2'- SO_3H -ChA (0.5 mM) and ChA (0.5 mM) with tyrosinase pre-incubated with NaHSO_3 (1 mM, 1 h, 25 °C), and (C) relative O_2 consumption rate obtained when incubating ChA (0.5 mM) with different potential browning inhibitors (1 mM) and tyrosinase (35 units/mL), which was either pre-incubated with the potential browning inhibitor (15 min, 25 °C; white bars) or not pre-incubated (black bars). ①, ChA + NaHSO_3 + tyrosinase (single addition); ②, ChA + NaHSO_3 + tyrosinase (double addition); ③, ChA + tyrosinase; ④, ChA + pre-incubated tyrosinase with NaHSO_3 ; ⑤, ChA + tyrosinase; ⑥, ChA + 2'- SO_3H -ChA + tyrosinase. The arrow indicates the second tyrosinase addition.

The fact that a second addition of tyrosinase was necessary to convert all ChA in the presence of NaHSO₃ indicated that tyrosinase was somehow inhibited in the course of the reaction. Two explanations for the observed enzyme inhibition might be: (i) NaHSO₃ inhibited tyrosinase directly in a rather slow, time-dependent manner or (ii) the 2'-SO₃H-ChA formed inhibited the enzyme. To investigate these possible scenarios of inhibition, 2'-SO₃H-ChA was purified from a reaction mixture in order to test its influence on tyrosinase activity.

The addition of 0.5 mM 2'-SO₃H-ChA to an incubation of ChA with tyrosinase did not influence the rate of oxygen consumption (**Figure 5B**), showing that 2'-SO₃H-ChA was not a tyrosinase inhibitor. This is in contrast with addition products of cysteine and ChA, which were found to be competitive inhibitors for PPO from apple (13). Based on the observations with apple PPO, 2'-S-cysteinyl-5-O-caffeoylquinic acid was purified from a reaction mixture containing ChA, cysteine and mushroom tyrosinase. Addition of 0.5 mM purified 2'-S-cysteinyl-5-O-caffeoylquinic acid to an incubation of ChA and tyrosinase did not result in tyrosinase inhibition (results not shown). Thus, 2'-S-cysteinyl-5-O-caffeoylquinic acid does not inhibit mushroom tyrosinase, similar to 2'-SO₃H-ChA. The fact that 2'-S-cysteinyl-5-O-caffeoylquinic acid was found before to inhibit apple PPO (13) might be explained by the different origin of the two enzymes.

To investigate whether NaHSO₃ inhibits the enzymatic activity of tyrosinase in time, tyrosinase was pre-incubated with NaHSO₃ (1 h). Oxygen consumption measurements with this pre-incubated tyrosinase showed a decreased activity compared to its control without prior pre-incubation with NaHSO₃ (**Figure 5B**). This experiment indicated that scenario (i) is most likely. To establish the time dependency of tyrosinase inhibition by NaHSO₃, tyrosinase was pre-incubated with NaHSO₃ for different times, after which a concentrated substrate solution was added. The initial reaction rate was determined by measuring the oxygen consumption rate (See **Figure S3** of the **Supporting Information**). It was found that the reaction rate rapidly decreased with an increasing pre-incubation time: already after 1 min, approximately 50% of activity was lost. After 15 min of pre-incubation, activity decreased further to approximately 10% of the initial activity. Sayavedra-Soto and Montgomery (6) found that pre-incubation of pear PPO with sulfite resulted in irreversible inhibition of the enzyme: indications for modification of the protein structure were found, although the nature of the modifications was not established.

The effects of pre-incubation of tyrosinase with the other sulfur-containing compounds tested in this study were also investigated. Oxygen consumption with and without pre-incubation of tyrosinase was determined and expressed relative to a control experiment using untreated tyrosinase. Pre-incubation of tyrosinase with other sulfur-containing compounds had little effect on tyrosinase activity (**Figure 5C**).

NaHSO₃ has a dual inhibitory effect on tyrosinase-catalyzed browning

In conclusion, our results show that different sulfur-containing compounds can inhibit *in vitro* browning of ChA by mushroom tyrosinase in two different ways: by inhibition of enzymatic activity (NaHSO₃, DTT) or by formation of colorless adducts with enzymatically formed *o*-quinones (NaHSO₃, cysteine, GSH). A schematic representation of enzymatic browning of ChA and possible inhibitory routes is shown in **Figure 6**. It is evident that NaHSO₃ has a unique position within the group of sulfur-containing compounds investigated: it has a dual inhibitory effect on tyrosinase-catalyzed browning of ChA. Initially, the formation of brown pigments is inhibited by formation of sulfo-ChA, while at the same time tyrosinase is inhibited in a time-dependent way. The exact mechanism of the time-dependent inhibition of tyrosinase by NaHSO₃ remains unclear. It is possibly due to covalent interactions between NaHSO₃ and tyrosinase. This will be subject of further investigation.

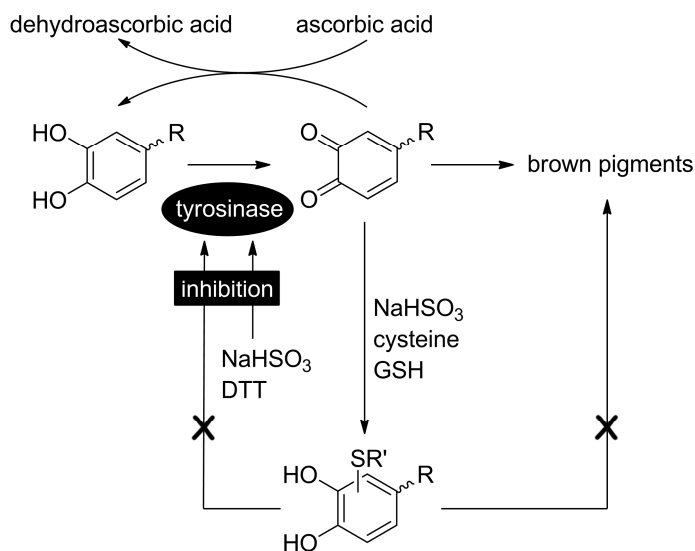


Figure 6. Schematic representation of the action of tyrosinase on ChA, together with possible mechanisms of inhibition of ChA browning.

ACKNOWLEDGEMENTS

This study has been carried out with financial support from the Commission of the European Communities within the Seventh Framework Programme for research and technological development (FP7), Grant Agreement No. 226930, title “Replacement of sulphur dioxide (SO₂) in food keeping the same quality and shelf-life of the products”,

acronym SO2SAY. This work was partly supported by COLCIENCIAS and Universidad Nacional de Colombia by providing a fellowship for Carlos-Eduardo Narváez-Cuenca.

REFERENCES

1. Sánchez-Ferrer, Á.; Neptuno Rodríguez-López, J.; García-Cánovas, F.; García-Carmona, F., Tyrosinase: a comprehensive review of its mechanism. *Biochim. Biophys. Acta* **1995**, *1247*, 1-11.
2. Yoruk, R.; Marshall, M. R., Physicochemical properties and function of plant polyphenol oxidase: a review. *J. Food Biochem.* **2003**, *27*, 361-422.
3. Friedman, M., Food browning and its prevention: an overview. *J. Agric. Food Chem.* **1996**, *44*, 631-653.
4. Iyengar, R.; McEvily, A. J., Anti-browning agents: alternatives to the use of sulfites in foods. *Trends Food Sci. Technol.* **1992**, *3*, 60-64.
5. Green, L. F., Sulphur dioxide and food preservation--A review. *Food Chem.* **1976**, *1*, 103-124.
6. Sayavedra-Soto, L. A.; Montgomery, M. W., Inhibition of polyphenoloxidase by sulfite. *J. Food Sci.* **1986**, *51*, 1531-1536.
7. Ferrer, O. J.; Otwell, W. S.; Marshall, M. R., Effect of bisulfite on lobster shell phenoloxidase. *J. Food Sci.* **1989**, *54*, 478-480.
8. Wilson, B. G.; Bahna, S. L., Adverse reactions to food additives. *Ann. Allergy, Asthma, Immunol.* **2005**, *95*, 499-507.
9. Ros, J. R.; Rodríguez-Lopez, J. N.; García-Cánovas, F., Effect of L-ascorbic acid on the monophenolase activity of tyrosinase. *Biochem. J.* **1993**, *295*, 309-312.
10. Chang, T.-S., An updated review of tyrosinase inhibitors. *Int. J. Mol. Sci.* **2009**, *10*, 2440-2475.
11. Narváez-Cuenca, C.-E.; Kuijpers, T. F. M.; Vincken, J.-P.; de Waard, P.; Gruppen, H., New insights into an ancient antibrowning agent: formation of sulfophenolics in sodium hydrogen sulfite-treated potato extracts. *J. Agric. Food Chem.* **2011**, *59*, 10247-10255.
12. Richard, F. C.; Goupy, P. M.; Nicolas, J. J.; Lacombe, J. M.; Pavia, A. A., Cysteine as an inhibitor of enzymic browning. 1. Isolation and characterization of addition compounds formed during oxidation of phenolics by apple polyphenol oxidase. *J. Agric. Food Chem.* **1991**, *39*, 841-847.
13. Richard-Forget, F. C.; Goupy, P. M.; Nicolas, J. J., Cysteine as an inhibitor of enzymic browning. 2. Kinetic studies. *J. Agric. Food Chem.* **1992**, *40*, 2108-2113.
14. Moridani, M. Y.; Scobie, H.; Jamshidzadeh, A.; Salehi, P.; O'Brien, P. J., Caffeic acid, chlorogenic acid, and dihydrocaffeic acid metabolism: Glutathione conjugate formation. *Drug Metabol. Dispos.* **2001**, *29*, 1432-1439.
15. Panzella, L.; Napolitano, A.; d'Ischia, M., Oxidative conjugation of chlorogenic acid with glutathione: Structural characterization of addition products and a new nitrite-promoted pathway. *Bioorg. Med. Chem.* **2003**, *11*, 4797-4805.
16. Valero, E.; Varón, R.; García-Carmona, F., A kinetic study of irreversible enzyme inhibition by an inhibitor that is rendered unstable by enzymic catalysis. The inhibition of polyphenol oxidase by L-cysteine. *Biochemical Journal* **1991**, *277*, 869-874.
17. Naish-Byfield, S.; Cooksey, C. J.; Riley, P. A., Oxidation of monohydric phenol substrates by tyrosinase: effect of dithiothreitol on kinetics. *Biochem. J.* **1994**, *304*, 155-162.
18. Park, Y.-D.; Lee, S.-J.; Park, K.-H.; Kim, S.-y.; Hahn, M.-J.; Yang, J.-M., Effect of thiohydroxyl compounds on tyrosinase: Inactivation and reactivation study. *J. Protein Chem.* **2003**, *22*, 613-623.
19. Fahey, J. W.; Zalcman, A. T.; Talalay, P., The chemical diversity and distribution of glucosinolates and isothiocyanates among plants. *Phytochemistry* **2001**, *56*, 5-51.

20. Schurink, M.; van Berkel, W. J. H.; Wichers, H. J.; Boeriu, C. G., Novel peptides with tyrosinase inhibitory activity. *Peptides* **2007**, *28*, 485-495.
21. Murata, M.; Sugiura, M.; Sonokawa, Y.; Shimamura, T.; Homma, S., Properties of chlorogenic acid quinone: Relationship between browning and the formation of hydrogen peroxide from a quinone solution. *Biosci., Biotechnol., Biochem.* **2002**, *66*, 2525-2530.
22. Schilling, S.; Sigolotto, C.-I.; Carle, R.; Schieber, A., Characterization of covalent addition products of chlorogenic acid quinone with amino acid derivatives in model systems and apple juice by high-performance liquid chromatography/electrospray ionization tandem mass spectrometry. *Rapid Commun. Mass Spectrom.* **2008**, *22*, 441-448.
23. Bernillon, S.; Guyot, S.; Renard, C. M. G. C., Detection of phenolic oxidation products in cider apple juice by high-performance liquid chromatography electrospray ionisation ion trap mass spectrometry. *Rapid Commun. Mass Spectrom.* **2004**, *18*, 939-943.
24. Clifford, M. N.; Johnston, K. L.; Knight, S.; Kuhnert, N., Hierarchical scheme for LC-MSⁿ identification of chlorogenic acids. *J. Agric. Food Chem.* **2003**, *51*, 2900-2911.
25. Clifford, M. N.; Knight, S.; Kuhnert, N., Discriminating between the six isomers of dicaffeoylquinic acid by LC-MSⁿ. *J. Agric. Food Chem.* **2005**, *53*, 3821-3832.
26. Shakya, R.; Navarre, D. A., Rapid screening of ascorbic acid, glycoalkaloids, and phenolics in potato using high-performance liquid chromatography. *J. Agric. Food Chem.* **2006**, *54*, 5253-5260.
27. De Lucia, M.; Panzella, L.; Pezzella, A.; Napolitano, A.; d'Ischia, M., Plant catechols and their S-glutathionyl conjugates as antinitrosating agents: expedient synthesis and remarkable potency of 5-S-glutathionylpiceatannol. *Chem. Res. Toxicol.* **2008**, *21*, 2407-2413.
28. Markakis, P.; Embs, R. J., Effect of sulfite and ascorbic acid on mushroom phenol oxidase. *J. Food Sci.* **1966**, *31*, 807-811.

SUPPORTING INFORMATION

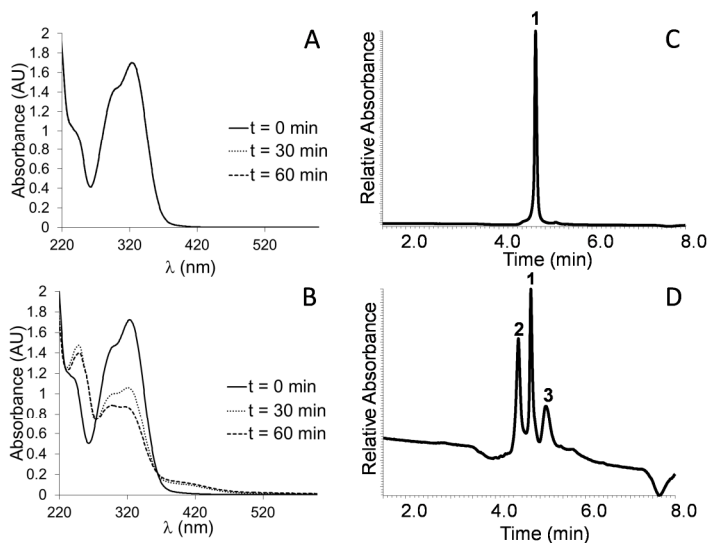


Figure S1. Absorption spectra of ChA (0.1 mM) incubated with tyrosinase (7 units/mL) with different sulfur-containing compounds (**A** and **B**) at different incubation times and RP-UHPLC-DAD traces (320 nm) of the reaction mixtures after incubation (**C** and **D**). (**A** and **C**) ChA with tyrosinase and DTT (0.2 mM); (**B** and **D**) ChA with tyrosinase and allyl isothiocyanate (0.2 mM).

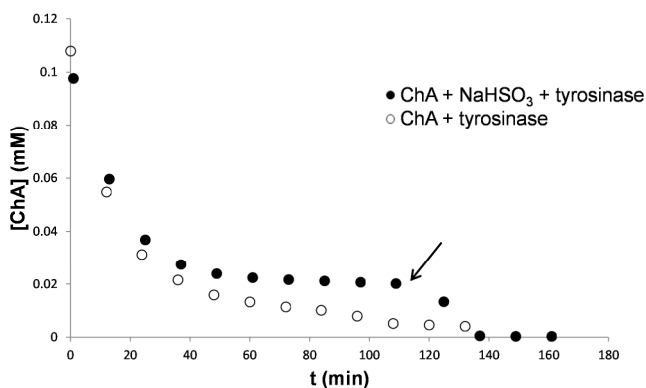


Figure S2. Decrease in concentration of ChA in time when incubated with tyrosinase with or without NaHSO_3 , determined by RP-UHPLC-DAD analysis. The arrow indicates the second addition of tyrosinase.

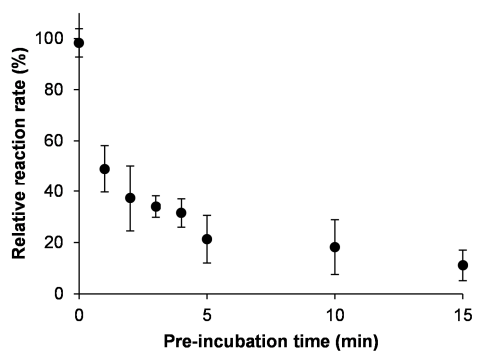


Figure S3. Relative oxygen consumption rate of incubations of ChA (0.5 mM) with tyrosinase (35 U/mL) pre-incubated with NaHSO₃ (1 mM) for different times. Data points represent duplicate measurements, error bars indicate standard deviations.

The anti-browning agent sulfite inactivates mushroom tyrosinase through covalent modification of the copper-B site

Sulfite salts are widely used as anti-browning agents in food processing. Nevertheless, the exact mechanism by which sulfite prevents enzymatic browning has remained unknown. Here, we show that sodium hydrogen sulfite (NaHSO_3) irreversibly blocks the active site of mushroom tyrosinase, and that the competitive inhibitors tropolone and kojic acid protect the enzyme from NaHSO_3 inactivation. LC-MS analysis of pepsin digests of NaHSO_3 -treated tyrosinase revealed two peptides showing a neutral loss corresponding to the mass of SO_3 upon MS^2 fragmentation. These peptides were found to be homologous peptides containing two of the three histidine residues that form the copper-B binding site of mushroom tyrosinase isoforms PPO3 and PPO4, which were both present in the tyrosinase preparation used. Peptides showing this neutral loss behavior were not found in the untreated control. Comparing the effect of NaHSO_3 on apo and holo-tyrosinase indicated that inactivation is facilitated by the active site copper ions. These data provide compelling evidence that inactivation of mushroom tyrosinase by NaHSO_3 occurs through covalent modification of a single amino acid residue, likely via addition of HSO_3^- to one of the copper-coordinating histidines in the copper-B site of the enzyme.

INTRODUCTION

Tyrosinase is a polyphenol oxidase (PPO) that catalyzes either the *o*-hydroxylation and subsequent oxidation of phenolic compounds, or the oxidation of *o*-diphenolic compounds. The resulting *o*-quinones in turn polymerize into brown pigments (1). In foods this reaction is often unwanted, and accounts for major losses in fruit and vegetable processing. Among the possible ways to inhibit enzymatic browning during food processing, sulfite salts are widely used as additives. These sulfite salts yield a mixture of SO_3^{2-} and HSO_3^- when dissolved, the ratio of which depends on the pH. Despite the importance of sulfite as anti-browning agent, the exact mechanism by which it prevents enzymatic browning has remained unknown.

Recently, we demonstrated that sulfite inhibits browning by trapping enzymatically formed *o*-quinones in colorless addition products, referred to as sulfo-phenolics. This was demonstrated both when extracting phenolics from potato in the presence of sodium hydrogen sulfite (also denoted as sodium bisulfite, NaHSO_3) (2), as well as in model systems consisting of commercially available mushroom tyrosinase and chlorogenic acid (3). Furthermore, it was found (3) that the catalytic activity of mushroom tyrosinase was inhibited by NaHSO_3 in a relatively slow, time-dependent way.

Here, we further investigate the time-dependent inhibition of mushroom tyrosinase by sulfite. We hypothesized that covalent modification of the enzyme by HSO_3^- might be responsible for the observed time-dependent inhibition, and that the active site would be the obvious target for such a modification.

The catalytic center of mushroom tyrosinase, a type-3 copper protein, contains two copper ions, each of which is coordinated by three histidine residues. The two copper binding sites, Cu-A and Cu-B, are highly conserved among different species (4). The copper center can be in different states, depending on the oxidation state of the copper ions and their interaction with oxygen (5). In the met state the copper ions are in the Cu(II) oxidation state, with hydroxyl ligands bridging the two copper ions. In this state, an *o*-diphenol can bind to the copper ions, after which oxidation takes place and an *o*-quinone is released, reducing Cu(II) to Cu(I). The resulting deoxy state is subsequently oxidized to the Cu(II) oxy state by binding oxygen. Oxy-tyrosinase can bind either an *o*-diphenol that is oxidized, or a monophenol, which is *o*-hydroxylated and subsequently oxidized, after which the cycle described can take place again. In the resting state, tyrosinase is considered to be predominantly in the met state, causing a lag phase to be observed when assaying the activity of tyrosinase with monophenolic substrates.

One of the histidines (His85) coordinating the Cu-A ion in mushroom tyrosinase is covalently linked via a thioether to Cys83, which fixes the orientation of this histidine side chain (6). This thioether is also found in PPOs from other species, for instance grape (*Vitis vinifera*) (7), sweet potato (*Ipomoea batatas*) (8) and the fungus *Neurospora crassa* (9). It has been proposed that thioether formation is catalyzed by presence of copper in the active

site (7). The copper-catalyzed formation of the thioether might indicate that the other histidine residues in the active site of mushroom tyrosinase are also reactive with sulfur-containing nucleophiles, such as HSO_3^- .

To elucidate its mechanism, the time-dependent inhibition of mushroom tyrosinase by NaHSO_3 was investigated in more detail. First, the effect of sulfite on the monophenolase and diphenolase activity of tyrosinase was compared. Next, to further characterize the molecular basis of tyrosinase inhibition by sulfite, we investigated the reversibility of inhibition and the possible covalent modification of amino acid residues in the active site.

MATERIALS AND METHODS

Materials

Mushroom tyrosinase, L-tyrosine, L-3,4-dihydroxyphenylalanine (L-DOPA), sodium hydrogen sulfite (NaHSO_3), dithiothreitol (DTT), tropolone (2-hydroxy-2,4,6-cycloheptatrien-1-one), copper chloride (CuCl_2) and ethylenediaminetetraacetic acid (EDTA) were purchased from Sigma Aldrich (St. Louis, MO, USA). Kojic acid (5-hydroxy-2-(hydroxymethyl-4H-pyran-4-one) was purchased from Acros Organics (Geel, Belgium), sequencing grade pepsin was from Promega (Madison, WI, USA), sequencing grade chymotrypsin was from Roche (Basel, Switzerland), glu-1-fibrinopeptide was from Waters (Milford, MA, USA). Ultra-high-performance liquid chromatography/mass spectrometry (UHPLC/MS) grade acetonitrile (ACN) and water were obtained from Biosolve BV (Valkenswaard, The Netherlands). Water was prepared using a Milli-Q water purification system (Millipore, Billerica, MA, USA).

Purification of mushroom tyrosinase

The mushroom tyrosinase was purified by a single gel filtration step (10). A HiLoad 26/60 Superdex 200 column connected to an Akta Explorer system (GE Healthcare, Uppsala, Sweden) was used. Fifty mg of the enzyme, dissolved in 50 mM HEPES buffer pH 6.8, was loaded and eluted with the same buffer at 4 mL/min. Fractions (5 mL) were collected and activity was determined by a spectrophotometric assay: 50 μL of each fraction was combined with 100 μL 0.8 mM tyrosine in a 96 well plate and absorbance at 520 nm was monitored in time. Active fractions were pooled and stored at -20°C until further use. One unit of tyrosinase activity was expressed as the increase of A280 by 0.001 per min with L-tyrosine as substrate, at pH 6.5 and 25°C .

RP-UHPLC analysis

Samples were analysed on an Accela UHPLC system (Thermo Scientific, San Jose, CA, USA) equipped with pump, autosampler and photodiode array detector.

Enzyme reaction products - Samples (5 μL) were injected onto a Hypersil Gold aQ column (2.1 \times 150 mm, particle size 1.9 μm ; Thermo Scientific). Water acidified with 0.1% (v/v) acetic acid, eluent A, and ACN acidified with 0.1% (v/v) acetic acid, eluent B, were used as eluents. The flow rate was 400 $\mu\text{L}/\text{min}$, the temperature was controlled at 5 $^{\circ}\text{C}$. The photodiode array detector was set to measure the range 200-600 nm. The following elution profile was used: 0-5 min, isocratic on 0% (v/v) B; 5-10 min, linear gradient from 0%-35% (v/v) B; 10-10.1 min, linear gradient from 35%-100% (v/v) B; 10.1-13 min, isocratic on 100% (v/v) B; 13-14 min, linear gradient from 100%-0% (v/v) B; 14-19 min, isocratic on 0% (v/v) B.

Peptides from protease digests - Samples (5 μL) were injected onto an Acquity UPLC BEH Shield RP18 column (2.1 \times 150 mm, particle size 1.7 μm ; Waters). Water acidified with 0.1% (v/v) formic acid, eluent A, and ACN acidified with 0.1% (v/v) formic acid, eluent B, were used as eluents. The flow rate was 300 $\mu\text{L}/\text{min}$, the temperature was controlled at 25 $^{\circ}\text{C}$. The photodiode array detector was set to measure the range 200-600 nm. The following elution profile was used: 0-2 min, isocratic on 5% (v/v) B; 2-27 min, linear gradient from 5%-50% (v/v) B; 27-27.1 min, linear gradient from 50%-100% (v/v) B; 27.1-30 min, isocratic on 100% (v/v) B; 30-30.1 min, linear gradient from 100%-5% (v/v) B; 30.1-35 min, isocratic on 5% (v/v) B.

Electrospray ionization mass spectrometry (ESI-MS)

Enzyme reaction products - Mass spectrometric data were obtained by analyzing samples on a LTQ-Velos (Thermo Scientific) equipped with an heated ESI probe coupled to the RP-UHPLC system. Nitrogen was used as sheath gas and auxiliary gas. Data were collected over the m/z range 150-500. Data-dependent MS^n analysis was performed with a normalized collision energy of 35%. The MS^n fragmentation was performed on the most intense product ion in the MS^{n-1} spectrum. Most settings were optimized via automatic tuning using 'Tune Plus' (Xcalibur 2.1, Thermo Scientific). The system was tuned with L-DOPA in negative ionization (NI) mode. The source heater temperature was 100 $^{\circ}\text{C}$, the transfer tube temperature was 300 $^{\circ}\text{C}$ and the source voltage was 4 kV. Data acquisition and reprocessing were done with Xcalibur 2.1 (Thermo Scientific).

Peptides from protease digests - Mass spectrometric data were obtained by analyzing samples on a LTQ-VelosPro (Thermo Scientific) equipped with an heated ESI probe coupled to the RP-UHPLC system. Nitrogen was used as sheath gas and auxiliary gas. Data were collected over the m/z range 200-2000. Data-dependent MS^2 analysis was performed with a normalized collision energy of 35%. The MS^2 fragmentation was performed on the most intense ion in the preceding MS spectrum. A neutral loss of 40 in MS^2 triggered subsequent MS^3 fragmentation of the fragment ion showing the neutral loss of 40. Most settings were optimized via automatic tuning using 'Tune Plus' (Xcalibur 2.1, Thermo Scientific). The system was tuned with the peptide glu-1-fibrinopeptide in positive ionization (PI) mode. The source heater temperature was 100 $^{\circ}\text{C}$, the transfer tube

temperature was 350 °C and the source voltage was 4 kV. Data acquisition and reprocessing were done with Xcalibur 2.1 (Thermo Scientific). *De novo* sequencing of peptide fragmentation spectra was done with PEAKS Studio 6.0 (Bioinformatics Solutions, Waterloo, Canada).

Oxygen consumption measurements

Oxygen consumption during the incubation of substrate with tyrosinase was measured using an Oxytherm System (Hansatech, Kings Lynn, UK). Incubations with L-DOPA (1 mM) or L-tyrosine (1 mM) and tyrosinase (35 U/mL), with or without NaHSO₃ (1 mM) were done in a total volume of 1 mL 50 mM HEPES buffer, pH 6.5 at 25 °C. Data acquisition and analysis were performed using Oxygraph Plus software (Hansatech).

Pre-treatment of tyrosinase with different inhibitors

Tyrosinase was pre-incubated with different inhibitors, as specified below. After incubation, inhibitors were removed by diafiltration, using centrifugal filters (Amicon Ultra, 0.5 mL, 10 kDa molecular mass cut-off (Millipore)). Filters were centrifuged (15 min, 14000g, 4 °C), after which the filtrate was discarded. The retentate (40 µL) was re-suspended in 400 µL 50 mM HEPES pH 6.5, after which filters were centrifuged again. A total of 6 cycles of centrifugation and re-suspension was performed. After the final centrifugation, the retentate was re-suspended in the initial sample volume, using 50 mM HEPES pH 6.5.

Pre-treatment of tyrosinase with NaHSO₃/DTT/EDTA - Tyrosinase (3000 U/mL) was incubated with NaHSO₃ (1 mM) or DTT (1 mM) in 50 mM HEPES pH 6.5 (1 h, 25 °C). Subsequently, NaHSO₃ or DTT was removed by diafiltration, after which CuCl₂ (1 mM) was added. After incubation (1 h, 25 °C), CuCl₂ was removed by diafiltration.

Pre-treatment of tyrosinase with NaHSO₃ in the presence of competitive tyrosinase inhibitors - Tyrosinase (3000 U/mL) was incubated with NaHSO₃, tropolone and kojic acid (each 1 or 10 mM), alone or in combinations of NaHSO₃ with tropolone or kojic acid. After incubation (1 h, 25 °C) the inhibitors were removed by diafiltration.

Pre-treatment of apo-tyrosinase with NaHSO₃ - Tyrosinase (3000 U/mL) was incubated with DTT (10 mM) or EDTA (10 mM) in 50 mM HEPES pH 6.5. After incubation (1 h, 25 °C) DTT or EDTA was removed by diafiltration, after which NaHSO₃ (1 mM) was added. After incubation (1 h, 25 °C) NaHSO₃ was removed by diafiltration, and CuCl₂ (1 mM) was added. After incubation (1 h, 25 °C) CuCl₂ was removed by diafiltration.

Protease digestion of NaHSO₃-treated tyrosinase

Crude tyrosinase (2 mg/mL) was incubated with 100 mM NaHSO₃ (1 h, 25 °C) in 50 mM HEPES pH 6.5. After incubation, NaHSO₃ was removed by diafiltration, as described above. After the last cycle of diafiltration the samples were in 50 mM HEPES pH 6.5, which was exchanged for the solution used for protease digestion (100 mM HCl (pH 1) in

case pepsin was used; 50 mM ammonium bicarbonate (pH 7.8) in case chymotrypsin was used) by an additional two cycles of diafiltration. Pepsin or chymotrypsin was added in a ratio of 1:20 (w/w) to the NaHSO₃-treated tyrosinase and to an untreated control. Samples were digested overnight at 37 °C.

RESULTS

Inhibition of monophenolase vs. diphenolase reaction

In order to determine whether NaHSO₃ selectively inhibits either the monophenolase or the diphenolase reaction catalyzed by tyrosinase, oxygen consumption measurements were performed with combinations of L-tyrosine, L-DOPA, NaHSO₃ and tyrosinase (**Figure 1**). When L-DOPA was incubated with tyrosinase in the presence of NaHSO₃, oxygen consumption initially was similar to a control incubation of L-DOPA and tyrosinase. However, in time a leveling off of oxygen consumption occurred, until a plateau was reached before all oxygen was consumed. This observation is in accordance with our previous observations on the time-dependent inhibition of tyrosinase-catalyzed oxidation of chlorogenic acid by NaHSO₃ (3). With tyrosinase and tyrosine, an initial lag-phase (approx. 200 s) before a linear decrease in oxygen concentration was observed. The lag-phase is typical for activity of tyrosinase on monophenolic substrates (11). When incubating the combination of tyrosine, NaHSO₃ and tyrosinase, no oxygen consumption was observed, also not after a time corresponding to the previously described lag-phase. Based on this observation, one might conclude that NaHSO₃ inhibited the monophenolase reaction stronger than the diphenolase reaction. Alternatively, the total inhibition of oxygen consumption might also be explained by the typical lag-phase for the oxidation of monophenols combined with the time-dependent inhibition of tyrosinase by NaHSO₃: if the time required to inhibit tyrosinase by NaHSO₃ coincides with the lag-phase of tyrosinase activity on tyrosine, no oxygen consumption will be observed. To investigate whether this was indeed the case, an experiment was carried out in which NaHSO₃ was added to an incubation of tyrosine and tyrosinase 300 s after the incubation started, when the oxidation of tyrosine was at its linear rate. It was observed that NaHSO₃ showed a similar time-dependent effect as it did with the oxidation of L-DOPA: initially the reaction rate was similar to the control without NaHSO₃, but in time it leveled off until a plateau was reached. Based on this experiment it was concluded that the time-dependent inhibition of tyrosinase by NaHSO₃ is independent of the type of reaction, monophenolase or diphenolase, that it catalyzes.

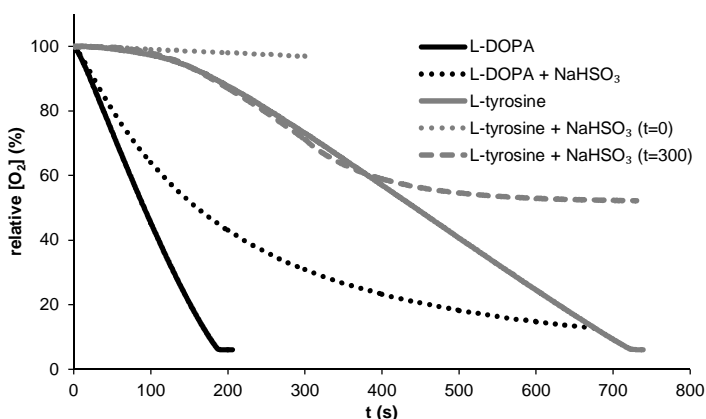


Figure 1. Oxygen consumption in time for incubations of tyrosinase (35 U/mL) with L-tyrosine (1 mM) or L-DOPA (1 mM), with and without NaHSO₃ (1 mM), and for L-tyrosine with NaHSO₃ addition after 300 s of incubation.

Tyrosinase-mediated sulfo-DOPA formation

During the time-dependent inhibition of tyrosinase-catalyzed oxidation of L-DOPA with NaHSO₃ no color formation was observed (data not shown). Although tyrosinase is active, as indicated by oxygen consumption (**Figure 1**), no dopachrome was formed from the resulting DOPA-quinone. This might be explained by formation of sulfonated derivatives of L-DOPA, in this way trapping the *o*-quinones, rendering them unavailable for further reactions. To investigate whether the sulfonation of DOPA-quinone indeed occurred, reaction products of incubations of L-DOPA with tyrosinase, with and without NaHSO₃, were analyzed using RP-UHPLC-PDA-MS (**Figure 2**, **Table 1**). After incubation of L-DOPA with tyrosinase, two peaks were observed. Peak **1** was identified as residual L-DOPA, both by MS and by comparison with the untreated L-DOPA sample. Peak **2** showed a molecular mass of 193, corresponding to the mass of dopachrome. Furthermore, it also had an absorption maximum at 475 nm, corresponding to the characteristic red color of dopachrome (12).

When L-DOPA was incubated with tyrosinase in the presence of NaHSO₃, three new peaks were observed in the UV280 trace, besides residual L-DOPA. Compounds **3**, **4** and **5** all had a mass of 277, which corresponds to the mass of L-DOPA with an additional 80 Da. This mass can be explained by the addition of HSO₃⁻ to L-DOPA. Assuming a similar reaction as observed earlier for the sulfonation of chlorogenic acid (2), we suggest that these three reaction products represent L-DOPA substituted with HSO₃⁻ at the three free positions of the phenyl ring. Considering steric influences of the phenyl ring substituents, and based on data on the substitution of dihydrocaffeic acid and catechin with glutathione (13, 14), the most abundant sulfo-DOPA isomer probably represents L-DOPA substituted at the 5-position on the phenyl, followed in abundance by substitution at the 6 and the 2-position (corresponding to peaks **4**, **3** and **5**, respectively).

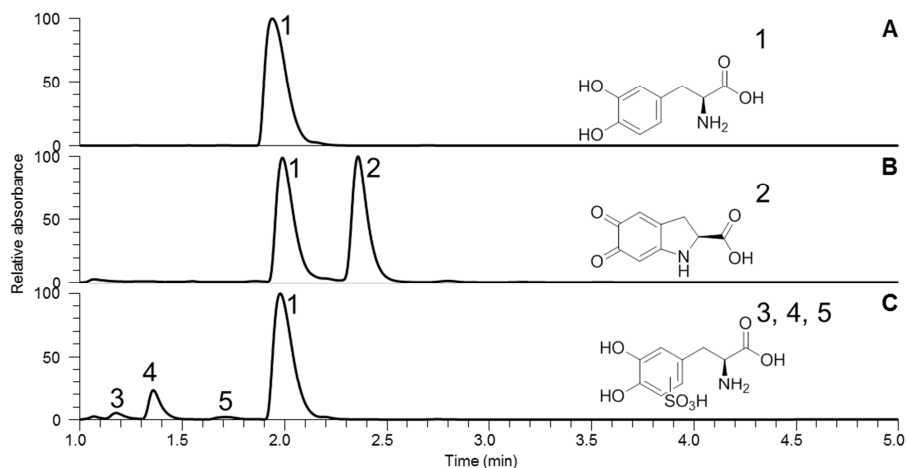


Figure 2. UV trace (280 nm) of RP-UHPLC of L-DOPA (A), L-DOPA incubated with tyrosinase (B) and L-DOPA incubated with tyrosinase and NaHSO₃ (C). Peaks were annotated based on MS analysis (Table 1). Chemical structures of L-DOPA (1), dopachrome (2) and sulfo-L-DOPA (3,4,5) are indicated.

Table 1. Peak annotation of RP-UHPLC-PDA-MS analysis of the reaction products of L-DOPA with NaHSO₃ and tyrosinase.

Peak	Retention time (min)	[M-H] ⁻	MS ² fragments [M-H] ⁻ (relative abundance)	λ _{max} (nm)	Tentative identification
1	1.94	196	135 (100), 152 (50), 196 (41), 134 (9), 107 (6), 72 (4), 91 (3), 109 (3), 122 (2), 123 (2), 124 (1)	232, 280	L-DOPA
2	2.36	192	148 (100), 192 (2)	292, 475	dopachrome
3	1.18	276	196 (100), 215 (89), 231 (43), 150 (30), 276 (14), 179 (9), 194 (9), 135 (8), 202 (3), 152 (1)	217, 238, 284	6-sulfo-L-DOPA
4	1.36	276	215 (100), 276 (27), 231 (37), 202 (3)	229, 392	5-sulfo-L-DOPA
5	1.72	276	215 (100), 276 (21), 179 (2), 231 (2), 135 (1), 259 (1)	212, 232, 293	2-sulfo-L-DOPA

Tyrosinase is irreversibly inactivated by NaHSO₃

To establish whether the observed time-dependent inhibition of tyrosinase by NaHSO₃ is reversible, a pre-incubation and re-activation experiment was done. When tyrosinase was incubated with NaHSO₃, which was subsequently removed, the enzyme, upon incubation with L-DOPA, showed decreased oxygen consumption compared to a diafiltered, CuCl₂-treated control (Figure 3). To investigate whether the inactivation of tyrosinase by NaHSO₃ involves loss of copper ions, reactivation was attempted by supplementing pretreated tyrosinase with CuCl₂. As a control, an experiment with DTT, which is known to reversibly inhibit tyrosinase (15), was performed. When comparing the activities of these pretreated tyrosinase samples (Figure 3), it was found that copper supplementation could

not reactivate NaHSO_3 -inactivated tyrosinase, while it could reactivate DTT-inactivated tyrosinase. Based on these results it was concluded that NaHSO_3 irreversibly inactivates tyrosinase, and that inactivation was not caused by chelation of copper ions.

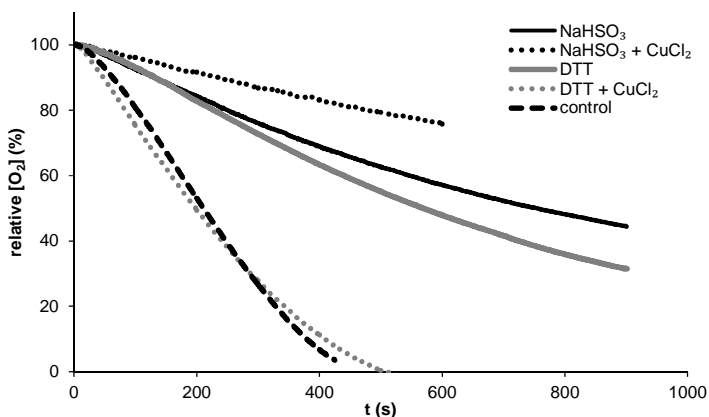


Figure 3. Oxygen consumption in time of incubations of L-DOPA (1 mM) with differently pretreated tyrosinase samples (35 U/mL), as indicated in the legend. The control sample of tyrosinase was incubated without inhibitor, and underwent the same diafiltration and CuCl_2 -treatment as the other samples.

Competitive inhibitors hinder NaHSO_3 -mediated inactivation of tyrosinase

To investigate the possible location of action of NaHSO_3 in its inactivation of tyrosinase, tyrosinase pre-treatment with NaHSO_3 was done in the presence of competitive tyrosinase inhibitors. If NaHSO_3 cannot inactivate tyrosinase when its active site is occupied by an inhibitor, it would be an indication that NaHSO_3 needs access to the active site to exert its action. The competitive inhibitors kojic acid and tropolone (16, 17) were used for this experiment.

Pre-treatment with NaHSO_3 led to partial or complete inactivation of tyrosinase, depending on the concentration NaHSO_3 used (Figure 4). Pre-treatment of tyrosinase with tropolone and kojic acid did not lead to inactivation after their removal by diafiltration, confirming that inhibition by these compounds is indeed reversible. When tyrosinase was incubated with equimolar amounts of NaHSO_3 and tropolone, no inactivation of tyrosinase was observed. When the molar ratio of NaHSO_3 to tropolone was increased to 10:1, a partial inactivation of tyrosinase compared to the control was observed (Figure 4A).

Combined pre-treatment with equimolar amounts of NaHSO_3 and kojic acid resulted in similar effects as with tropolone: the enzyme activity was not affected. In contrast to the findings with tropolone, tyrosinase was completely inactivated when the ratio NaHSO_3 to kojic acid was increased to 10:1, (Figure 4B).

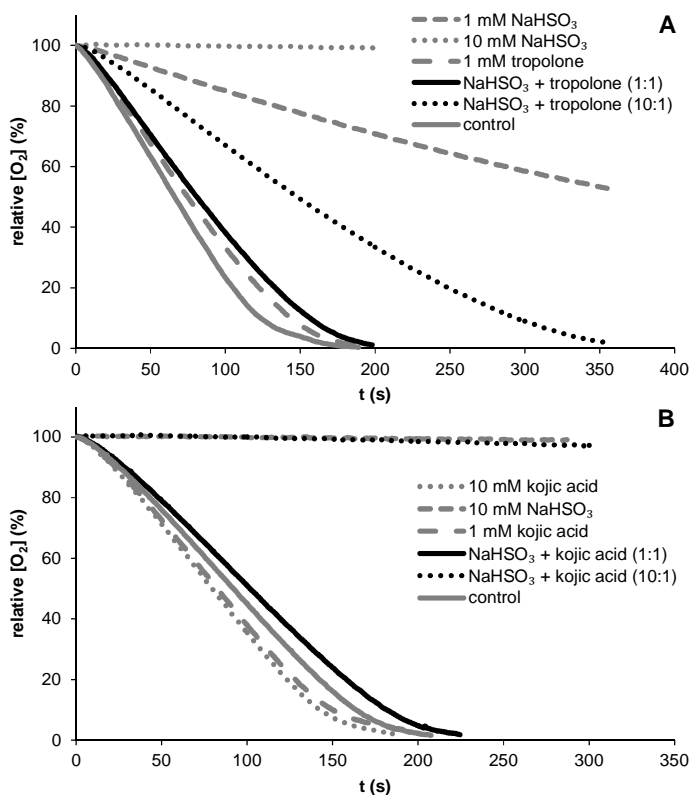


Figure 4. Oxygen consumption in time of incubations of L-DOPA (1 mM) with pre-treated and subsequently dialyzed tyrosinase (35 U/mL). The competitive tyrosinase inhibitors tropolone (A) and kojic acid (B) were used in the pretreatments.

These observations show that the presence of competitive inhibitors in the active site of tyrosinase prevents inactivation by NaHSO₃, which suggests that the NaHSO₃-mediated inactivation of tyrosinase occurs in the active site. The observation that tropolone prevents inactivation at a higher NaHSO₃ to inhibitor ratio than kojic acid is probably due to the higher affinity of tropolone for the active site compared to kojic acid (16, 17).

The copper-B site of mushroom tyrosinase is covalently modified by NaHSO₃

Considering the irreversibility of tyrosinase inactivation by NaHSO₃ and the fact that inactivation seems to take place in the active site, it was hypothesized that a covalent modification of active site amino acid residues was responsible for the inactivation.

A NaHSO₃-pretreated and an untreated tyrosinase sample were digested with pepsin and the resulting peptides were analyzed by RP-UHPLC-MSⁿ. If a sulfonic acid group would be covalently linked to a peptide, a mass increase of 80 Da compared to an untreated

control is expected. When screening the MS² data for a neutral loss of 80 Da, two peaks (m/z 536.8 and m/z 532.8) clearly stood out in the NaHSO₃-treated tyrosinase, which were not found in the untreated control (**Figure 5B**). The MS² spectra for these two peaks were atypical for peptide fragmentation, showing only one major peak, representing the parent ion minus the neutral loss of 80 Da. Fragmentation of product ions that showed a neutral loss of 80 Da was achieved by MS³ experiments performed on these product ions.

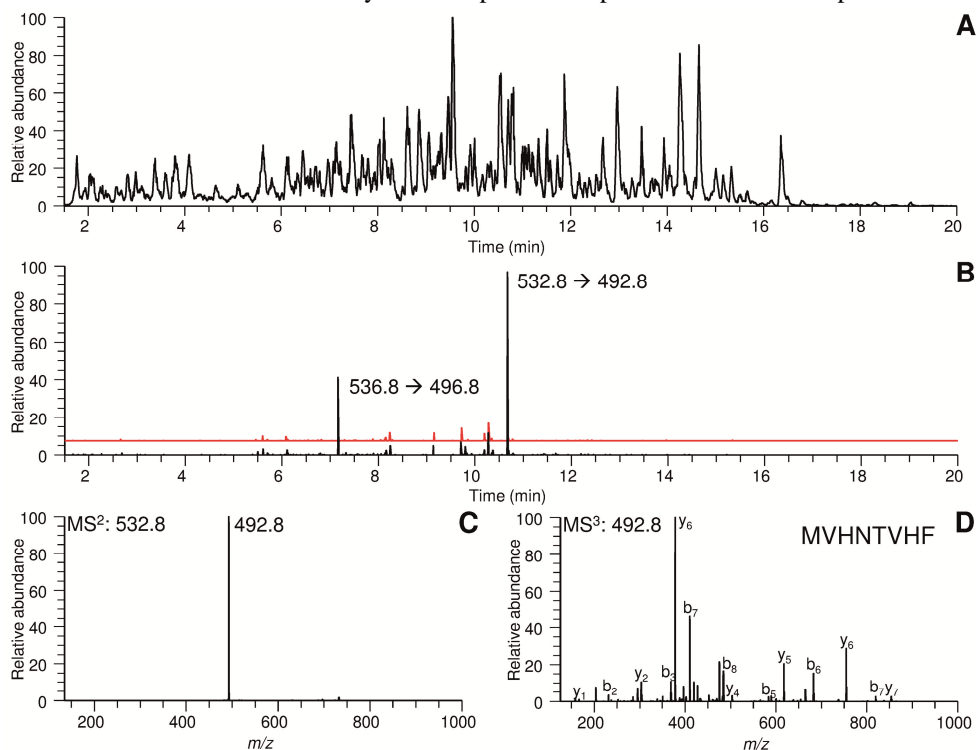


Figure 5. Basepeak MS trace (**A**) and MS trace of a scan for a neutral loss of 40 (**B**) of the NaHSO₃-treated, pepsin digested tyrosinase sample. MS² scan of the ion with m/z 532.8 (**C**) and subsequent MS³ scan of the resulting ion with m/z 492.8 (**D**). The red trace in **B** represents the neutral loss scan of the untreated, pepsin digested tyrosinase sample. The spectrum in **D** is annotated with the y and b ions used to identify the peptide MVHNTVHF.

As an example the MS² spectrum of the peak with a m/z of 532.8 is shown (**Figure 5C**), the fragmentation of which yielded only one fragment, with a m/z of 492.8. Both precursor ion and fragment ion were doubly charged, as was clearly shown by the isotope pattern. So, the difference of 40 in m/z values corresponds to a mass loss of 80 Da. Fragmentation of the ion with a m/z of 492.8 resulted in a typical peptide fragmentation spectrum (**Figure 5D**). *De novo* sequencing of the spectrum resulted in the amino acid sequence MVHNTVHF (theoretically doubly charged ion m/z 492.7), which corresponds to a region of the copper-B site of mushroom tyrosinase isoform PPO3 (amino acid residues 257-264) (**Figure 6**).

Similarly, MS³ on the fragment ion 496.8 resulted in annotation of the amino acid sequence EAVHDDIHG (theoretically doubly charged ion m/z 496.7), which corresponds to a region of the copper-B site of mushroom tyrosinase isoform PPO4 (amino acid residues 248-256) (**Figure 6**). The peptides MVHNTVHF and EAVHDDIHG, without an extra mass of 80 Da, were also found in the MS trace of the control digest, at different retention times. The protease digestion and UHPLC-MSⁿ analysis was repeated with chymotrypsin (LC-MS data not shown), resulting in four peptides (EMVHNTVHF and VHNTVHF of PPO3, SLEAVHDDIHGF and EAVHDDIHGF of PPO4) showing the same neutral loss behavior as the peptides found in the peptic digest, and corresponding to the same region of the copper-B site of tyrosinase (**Figure 6**).

Copper-A site

PPO3	55	<u>F</u> <u>OLGGI</u> <u>H</u> <u>GLPYTEWAKAQPQ</u> . <u>LHLYKANY</u> <u>CT</u> <u>HGT</u> <u>VLFP</u> <u>TWH</u> <u>RAYESTW</u>	101
PPO4	51	<u>F</u> <u>OLSGI</u> <u>H</u> <u>GLPTFPWAKPKDPTVPY</u> <u>ESGY</u> <u>CT</u> <u>HSQ</u> <u>VLFP</u> <u>TWH</u> <u>RVVYSIY</u>	98

Copper-B site

PPO3	253	<u>NS</u> <u>LEMV</u> <u>H</u> <u>NTV</u> <u>H</u> <u>FLIGRDP</u> <u>TL</u> <u>DPLV</u> <u>PGH</u> <u>MG</u> <u>SV</u> <u>PHAA</u> <u>FDP</u> <u>IF</u> <u>W</u> <u>M</u> <u>H</u> <u>C</u> <u>N</u> <u>V</u> <u>D</u> <u>R</u> <u>L</u> <u>L</u>	303
PPO4	245	<u>NS</u> <u>LEAV</u> <u>H</u> <u>DDI</u> <u>H</u> <u>GFVGRG</u> <u>AIRGH</u> <u>M</u> <u>THAL</u> <u>F</u> <u>AA</u> <u>FDP</u> <u>IF</u> <u>W</u> <u>L</u> <u>H</u> <u>H</u> <u>S</u> <u>N</u> <u>V</u> <u>D</u> <u>R</u> <u>H</u> <u>L</u>	290

Figure 6. Sequence alignments of the Cu-A and Cu-B sites of PPO3 and PPO4. Copper coordinating histidines and thioether forming cysteine are indicated in red, relevant peptides found in LC-MS of protease digests are underlined. Solid lines indicate peptic peptides, dashed lines indicate chymotryptic peptides. Sequences were aligned using Clustal W (26).

Peptides showing a neutral loss corresponding to the addition of two sulfonic acid groups were not found. These results indicated that covalent addition of a single HSO_3^- to an active site amino acid in the copper-B site occurs in mushroom tyrosinase. Because sulfite is a nucleophile it would need an electrophilic reaction site for attachment to an amino acid residue. Considering the reactivities of the amino acid residues of the modified peptides, valine, isoleucine and alanine have alkyl side chains deprived of any functional group. Methionine and threonine are nucleophilic, making reaction with HSO_3^- unlikely. Likewise, the aromatic ring of phenylalanine is electron rich, making it more reactive towards electrophiles than to nucleophiles. The carbamoyl moiety of asparagine, being an amide, and the deprotonated carboxyl moieties of aspartic acid and glutamic acid are very weak electrophiles and reaction with sulphite ions of these groups is unprecedented in the literature. The imidazole group of histidine is electron rich, making it prone to electrophilic attack. On the other hand, nucleophilic addition on imidazole has also been reported (18), as well as nucleophilic addition of the sulfite ion to heteroaromatic rings (19). Moreover, the coordination with copper makes the imidazole side chains of histidine more electron poor, thus more prone to nucleophilic attack. Looking at similarities between the

sulfite-modified peptides found, the only amino acid residues they have in common are valine and histidine (**Figure 6**). This finding, combined with the reactivity of the constituent amino acids of the sulfite-modified peptides, strongly suggests that sulfite is attached to one of the copper-B coordinating histidine residues (His259 or His263 in PPO3; His251 or His255 in PPO4). To confirm that modification only happened on one of these positions and not on the third copper-B coordinating histidine residue, peptides containing this third histidine residue (His296 for PPO3 and His283 for PPO4) were searched for. Peptides containing His296 from PPO3 were not found for both the NaHSO₃-treated and control samples, whereas peptides from PPO4 containing His283 were found, in unmodified form (**Figure 6**).

The copper-A site thioether of mushroom tyrosinase is not modified by sulfite

Considering the fact that a histidine residue in the copper-B site of tyrosinase appeared to be covalently modified by NaHSO₃, it was investigated whether the three copper-A coordinating histidine residues in NaHSO₃-treated tyrosinase were also affected by NaHSO₃. Peptides containing the residues His61 and His94 of PPO3, and peptides containing the residues His57 and His91 of PPO4, were found in protease digests of both NaHSO₃-treated and untreated tyrosinase (**Figure 6**). The third copper-A coordinating histidine residue in PPO3, His85, is engaged in a thioether bond with Cys83 (6), which will affect the molecular mass of peptides containing this thioether bond. Depending on its specificity, pepsin digestion of PPO3 would theoretically result in the peptides CTHGTVL or YKANYCTHGTVL. The theoretical molecular masses of these peptides are 729.3 and 1368.6 Da, respectively, which would be 727.3 and 1366.6 Da in case the thioether is present. The latter masses were found in the LC-MS data, for both the untreated and the sulfite-treated tyrosinase samples (**Figure 7B**). The identity of the peptides was confirmed by MS/MS spectra. The masses of the b and y ions representing fragments of the peptide including the thioether matched the theoretical masses minus two, whereas the masses of the ions not including the thioether corresponded to their theoretical masses (**Figures 7C and 7D**). The thioether containing peptide CTHSQVL from PPO4 was found in the same way. Similar mass spectrometric evidence of a Cys-His thioether in molluscan hemocyanin, a type-3 copper protein functioning as a dioxygen carrier, has been provided before (20). Taken together, these results demonstrate that the copper-A site of mushroom tyrosinase is not affected by sulfite treatment.

Copper ions facilitate NaHSO₃-modification of the copper-B site of tyrosinase

To investigate whether the copper ions play a role in the covalent modification of the copper-B site of tyrosinase, apo and holo-tyrosinase were incubated with NaHSO₃. EDTA, a well-known metal chelator, has been reported before to inhibit tyrosinase (21). Under our

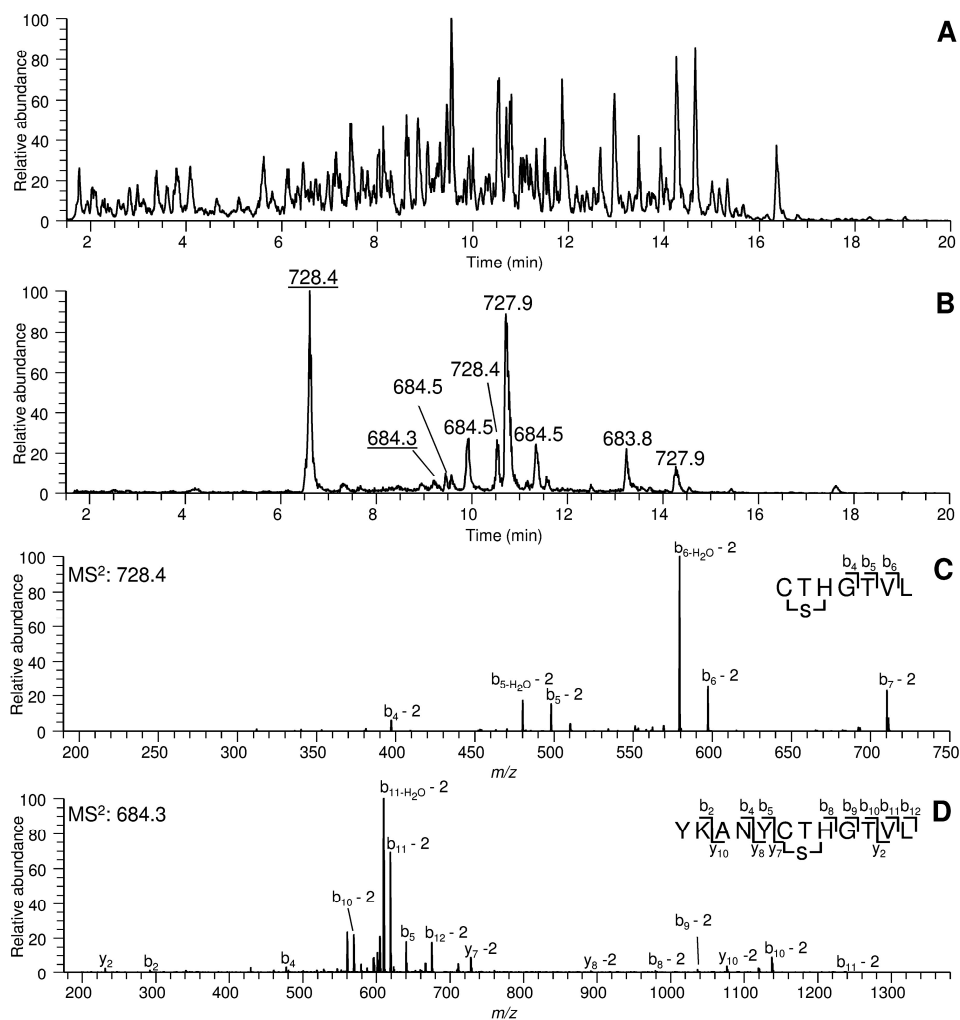


Figure 7. Basepeak MS trace (**A**) and extracted ion chromatogram for m/z 683.8-684.8 and m/z 727.9-728.9 (**B**) of a $NaHSO_3$ -treated, pepsin digested tyrosinase sample. MS² scan of the ions with m/z 728.4 (**C**) and m/z 683.3 (**D**). Spectra in **C** and **D** are annotated with the b and y ions used to identify the thioether containing peptide.

experimental conditions, however, no inactivation of tyrosinase by EDTA occurred (data not shown). As we found that DTT treatment resulted in reversible inactivation of tyrosinase (**Figure 3**), probably caused by copper chelation (22), DTT was used to remove the copper ions from tyrosinase prior to $NaHSO_3$ treatment.

When comparing the activity of $NaHSO_3$ -pretreated holo-tyrosinase to that of $NaHSO_3$ -pretreated apo-tyrosinase, it can be seen that the $NaHSO_3$ treatment had a larger effect on active tyrosinase than on the DTT-inactivated enzyme (**Figure 8**). Tyrosinase

pretreated with DTT and subsequently re-activated with CuCl_2 showed full recovery of activity, compared to a control sample that underwent three cycles of diafiltration and CuCl_2 -treatment. These results suggest that the presence of copper is not essential for NaHSO_3 -mediated inactivation of mushroom tyrosinase, but the presence of copper facilitates the inactivation.

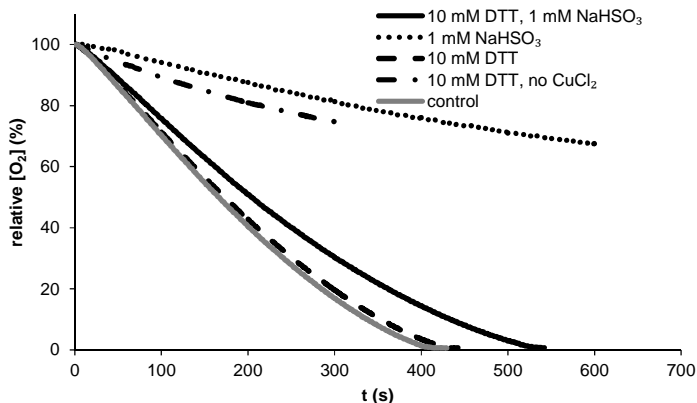


Figure 8. Oxygen consumption in time of incubations of L-DOPA (1 mM) with pretreated and subsequently diafiltered tyrosinase (35 U/mL). The control sample was pre-incubated without inhibitors and subsequently diafiltered and CuCl_2 -treated.

DISCUSSION

Although sulfite is widely used to inhibit enzymatic browning, the exact mechanism of this inhibition has remained unknown. Previously, we found that sulfite prevents formation of brown pigments by converting *o*-quinones into colorless sulfo-phenolics, and by time-dependent inhibition of tyrosinase activity (3). Here, using different pretreatments, we demonstrated that this time-dependent inhibition is caused by irreversible inactivation of mushroom tyrosinase. The inactivation was likely to be the result of covalent modification of one of the copper-B coordinating histidine residues, which is probably catalyzed by the presence of copper in the active site.

A possible explanation for the covalent reaction of sulfite with a histidine residue might be a nucleophilic addition of the sulfur of HSO_3^- to C ϵ 1 of histidine, followed by hydride removal upon oxidation to restore aromaticity. As it was found that the presence of copper facilitated inactivation by NaHSO_3 , probably the interaction of N ϵ 2 with Cu(II) results in reduced electron density of C ϵ 1, in this way making it more prone to nucleophilic addition. Moreover, Cu(II) possibly promotes the oxidative step through reduction to Cu(I) (**Figure 9B**). A similar mechanism has been suggested for the formation of the thioether bond in grape PPO (7) (**Figure 9A**). Alternatively, addition of HSO_3^- to one of the nitrogens in the histidine side chain might occur. Reactions of sulfite with the N5 atom of flavin in different

flavoproteins are known to occur, depending on the amino acid residues surrounding the flavin binding site (23,24). A possible mechanism of HSO_3^- addition to $\text{N}\epsilon 2$ is proposed in **Figure 9C**. In this mechanism, restoration of aromaticity through hydride removal upon oxidation would lead to loss of the copper coordinating ability of $\text{N}\epsilon 2$. MS^2 of the

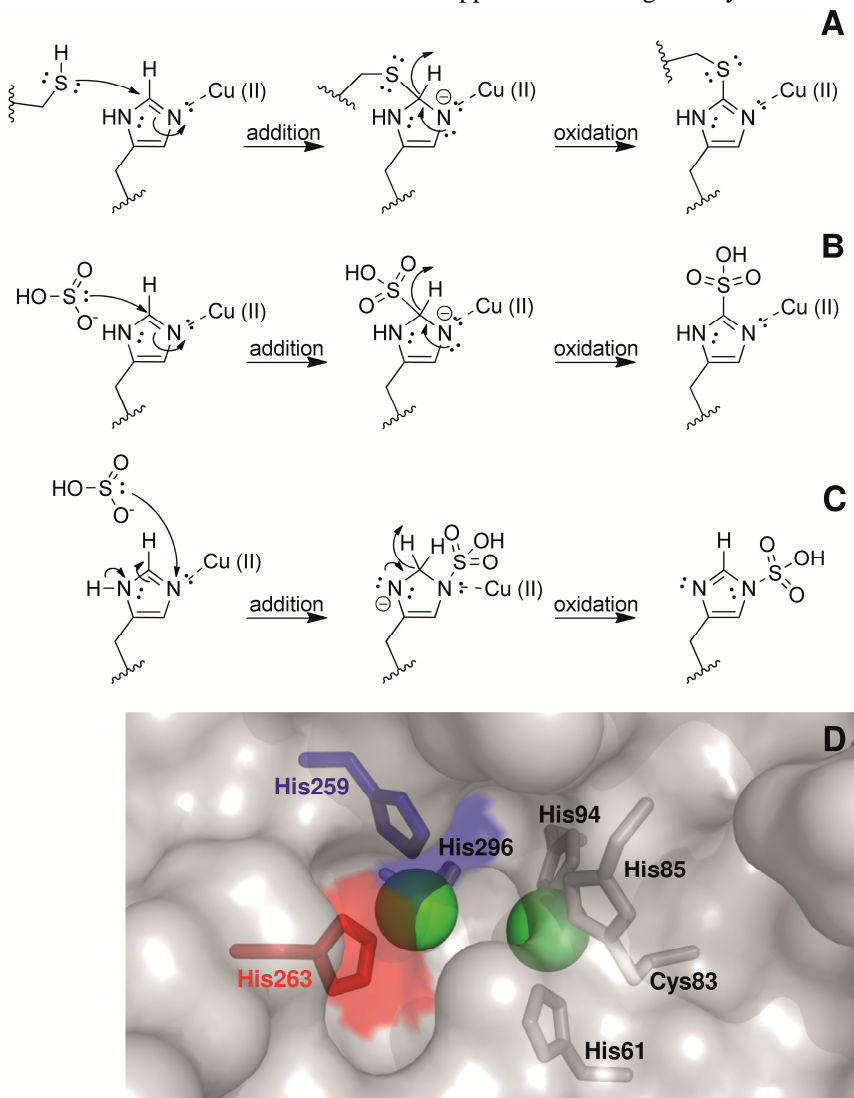


Figure 9. Formation of thioether in the active site of tyrosinase, as proposed by Virador et al (7) **(A)**, proposed addition of HSO_3^- to $\text{C}\epsilon 1$ of Cu-B coordinating histidine **(B)**, proposed addition of HSO_3^- to $\text{N}\epsilon 2$ of Cu-B coordinating histidine **(C)**. Surface representation of the active site of mushroom tyrosinase (6) **(D)**. The six copper coordinating histidines and Cys83 are drawn in stick representation, the copper ions are represented by green spheres. His259 is colored blue, His263 is colored red.

sulfite-substituted peptides resulted in only a single fragment with a neutral loss corresponding to the mass of SO_3 . The relative ease with which this fragmentation occurred, might be an indication that substitution on N ϵ 2 is more likely than on C ϵ 1, as a C-S bond is likely to be more stable than a N-S bond.

Looking at the active site cavity (6), it seems that His263 is more exposed than His259 (**Figure 9D**). Being better accessible, we speculate that it is more likely that sulfite addition takes place on His263. In order to identify which of the two histidine residues is modified, MS fragmentation applying electron transfer dissociation (ETD) instead of collision induced dissociation (CID) might be used. While CID is known to break the most labile bond, ETD is known to preferentially break peptide bonds, while leaving post-translational modifications on amino acid side chains intact (25).

We demonstrated that modification of a single amino acid residue in the copper-B site irreversibly inactivated tyrosinase, probably by addition to a copper-coordinating histidine residue. The question why sulfite-modified tyrosinase is inactivated remains to be answered. If sulfonation would occur on C ϵ 1, a possible explanation might be that the sulfite occupies too much space in the active site for substrates to bind efficiently. Another explanation might be that the modified histidine residue is not able to coordinate Cu-B in the proper position relative to Cu-A for catalysis to occur. If sulfite would add to N ϵ 2, N ϵ 2 would lose its ability to coordinate copper, because its lone pair of electrons will be engaged in the aromatic system of the imidazole ring. Based on this argument, and on the relative ease with which the sulfite moiety is lost upon MS fragmentation, we speculate that sulfite addition occurs on N ϵ 2. Crystallography of sulfite treated tyrosinase would give more insight in the exact location of sulfite addition to histidine.

ACKNOWLEDGMENTS

We thank Adrie Westphal for technical support. This study has been carried out with financial support from the Commission of the European Communities within the Seventh Framework Programme for research and technological development (FP7), Grant Agreement No. 226930, title "Replacement of sulphur dioxide (SO_2) in food keeping the same quality and shelf-life of the products", acronym SO2SAY.

REFERENCES

1. Friedman, M., Food browning and its prevention: an overview. *J. Agric. Food Chem.* **1996**, *44*, 631-653.
2. Narváez-Cuenca, C.-E.; Kuijpers, T. F. M.; Vincken, J.-P.; de Waard, P.; Gruppen, H., New insights into an ancient antibrowning agent: formation of sulfophenolics in sodium hydrogen sulfite-treated potato extracts. *J. Agric. Food Chem.* **2011**, *59*, 10247-10255.

3. Kuijpers, T. F. M.; Narváez-Cuenca, C.-E.; Vincken, J.-P.; Verloop, A. J. W.; van Berkel, W. J. H.; Gruppen, H., Inhibition of enzymatic browning of chlorogenic acid by sulfur-containing compounds. *J. Agric. Food Chem.* **2012**, *60*, 3507-3514.
4. van Gelder, C. W. G.; Flurkey, W. H.; Wichers, H. J., Sequence and structural features of plant and fungal tyrosinases. *Phytochemistry* **1997**, *45*, 1309-1323.
5. Yoruk, R.; Marshall, M. R., Physicochemical properties and function of plant polyphenol oxidase: a review. *J. Food Biochem.* **2003**, *27*, 361-422.
6. Ismaya, W. T.; Rozeboom, H. J.; Weijn, A.; Mes, J. J.; Fusetti, F.; Wichers, H. J.; Dijkstra, B. W., Crystal structure of *Agaricus bisporus* mushroom tyrosinase: Identity of the tetramer subunits and interaction with tropolone. *Biochemistry* **2011**, *50*, 5477-5486.
7. Virador, V. M.; Reyes Grajeda, J. P.; Blanco-Labra, A.; Mendiola-Olaya, E.; Smith, G. M.; Moreno, A.; Whitaker, J. R., Cloning, sequencing, purification, and crystal structure of grenache (*Vitis vinifera*) polyphenol oxidase. *J. Agric. Food Chem.* **2010**, *58*, 1189-1201.
8. Klabunde, T.; Eicken, C.; Sacchettini, J. C.; Krebs, B., Crystal structure of a plant catechol oxidase containing a dicopper center. *Nat. Struct. Biol.* **1998**, *5*, 1084-1090.
9. Lerch, K., Primary structure of tyrosinase from *Neurospora crassa*. II. Complete amino acid sequence and chemical structure of a tripeptide containing an unusual thioether. *J. Biol. Chem.* **1982**, *257*, 6414-9.
10. Schurink, M.; van Berkel, W. J. H.; Wichers, H. J.; Boeriu, C. G., Novel peptides with tyrosinase inhibitory activity. *Peptides* **2007**, *28*, 485-495.
11. Sánchez-Ferrer, Á.; Neptuno Rodríguez-López, J.; García-Cánovas, F.; García-Carmona, F., Tyrosinase: a comprehensive review of its mechanism. *Biochim. Biophys. Acta* **1995**, *1247*, 1-11.
12. Winder, A. J.; Harris, H., New assays for the tyrosine hydroxylase and dopa oxidase activities of tyrosinase. *Eur. J. Biochem.* **1991**, *198*, 317-326.
13. Moridani, M. Y.; Scobie, H.; Jamshidzadeh, A.; Salehi, P.; O'Brien, P. J., Caffeic acid, chlorogenic acid, and dihydrocaffeic acid metabolism: Glutathione conjugate formation. *Drug Metab. Dispos.* **2001**, *29*, 1432-1439.
14. Moridani, M. Y.; Scobie, H.; Salehi, P.; O'Brien, P. J., Catechin metabolism: Glutathione conjugate formation catalyzed by tyrosinase, peroxidase, and cytochrome P450. *Chem. Res. Toxicol.* **2001**, *14*, 841-848.
15. Park, Y.-D.; Lee, S.-J.; Park, K.-H.; Kim, S.-y.; Hahn, M.-J.; Yang, J.-M., Effect of thiohydroxyl compounds on tyrosinase: Inactivation and reactivation study. *J. Protein Chem.* **2003**, *22*, 613-623.
16. Flurkey, A.; Cooksey, J.; Reddy, A.; Spoonmore, K.; Rescigno, A.; Inlow, J.; Flurkey, W. H., Enzyme, protein, carbohydrate, and phenolic contaminants in commercial tyrosinase preparations: potential problems affecting tyrosinase activity and inhibition studies. *J. Agric. Food Chem.* **2008**, *56*, 4760-4768.
17. Neeley, E.; Fritch, G.; Fuller, A.; Wolfe, J.; Wright, J.; Flurkey, W., Variations in IC50 values with purity of mushroom tyrosinase. *Int. J. Mol. Sci.* **2009**, *10*, 3811-3823.
18. Ohta, S.; Osaki, T.; Nishio, S.; Furusawa, A.; Yamashita, M.; Kawasaki, I., Serial double nucleophilic addition of amines to the imidazole nucleus. *Tetrahedron Lett.* **2000**, *41*, 7503-7506.
19. Zoltewicz, J. A.; Kauffman, G. M.; Uray, G., A mechanism for sulphite ion reacting with vitamin B1 and its analogues. *Food Chem.* **1984**, *15*, 75-91.
20. Gielens, C.; Idakieva, K.; De Maeyer, M.; Van den Bergh, V.; Siddiqui, N. I.; Compernelle, F., Conformational stabilization at the active site of molluscan (*Rapana thomasiana*) hemocyanin by a cysteine-histidine thioether bridge: A study by mass spectrometry and molecular modeling. *Peptides* **2007**, *28*, 790-797.
21. Friedman, M.; Grosjean, O. K.; Zahnley, J. C., Inactivation of metalloenzymes by lysinoalanine, phenylethylaminoalanine, alkali-treated food proteins, and sulfur amino acids. *Adv. Exp. Med. Biol.* **1986**, *199*, 531-560.

22. Krężel, A.; Leśniak, W.; Jeżowska-Bojczuk, M.; Młynarz, P.; Brasuń, J.; Kozłowski, H.; Bal, W., Coordination of heavy metals by dithiothreitol, a commonly used thiol group protectant. *J. Inorg. Biochem.* **2001**, *84*, 77-88.
23. Meyer, T. E.; Bartsch, R. G.; Cusanovich, M. A., Adduct formation between sulfite and the flavin of phototrophic bacterial flavocytochromes c. Kinetics of sequential bleach, recolor, and rebleach of flavin as a function of pH. *Biochemistry* **1991**, *30*, 8840-8845.
24. Massey, V.; Müller, F.; Feldberg, R.; Schuman, M.; Sullivan, P. A.; Howell, L. G.; Mayhew, S. G.; Matthews, R. G.; Foust, G. P., The reactivity of flavoproteins with sulfite: possible relevance to the problem of oxygen reactivity. *J. Biol. Chem.* **1969**, *244*, 3999-4006.
25. Mikesch, L. M.; Ueberheide, B.; Chi, A.; Coon, J. J.; Syka, J. E. P.; Shabanowitz, J.; Hunt, D. F., The utility of ETD mass spectrometry in proteomic analysis. *BBA-Proteins Proteom.* **2006**, *1764*, 1811-1822.
26. Larkin, M. A.; Blackshields, G.; Brown, N. P.; Chenna, R.; McGettigan, P. A.; McWilliam, H.; Valentin, F.; Wallace, I. M.; Wilm, A.; Lopez, R.; Thompson, J. D.; Gibson, T. J.; Higgins, D. G., Clustal W and Clustal X version 2.0. *Bioinformatics* **2007**, *23*, 2947-2948.

Potato and mushroom polyphenol oxidase activities are differently modulated by natural plant extracts

Sulfite is widely used to counteract enzymatic browning, which causes major losses in food processing. Due to its presumed health risks, plant extracts are screened for natural inhibitors of enzymatic browning, which can potentially replace sulfite. In this study, polyphenol oxidases (PPOs) from mushroom (*Agaricus bisporus*, AbPPO) and potato (*Solanum tuberosum*, StPPO) were used to screen a collection of 60 plant extracts for potential inhibitors of enzymatic browning. Some plant extracts had different effects on the two PPOs: an extract that inhibited one PPO could be an activator for the other. As an example of this, the mate (*Ilex paraguariensis*) extract was investigated in more detail. In the presence of mate, oxygen consumption by AbPPO was found to be reduced more than 5-fold compared to a control reaction, whereas that of StPPO was increased more than 9-fold. RP-UHPLC-MS analysis showed that mate contained a mixture of phenolic compounds and saponins. Upon incubation of mate with StPPO, phenolic compounds disappeared completely and saponins remained. Flash chromatography was used to separate saponins and phenolic compounds. It was found that the phenolic fraction was mainly responsible for inhibition of AbPPO and activation of StPPO. Activation of StPPO was probably caused by activation of latent StPPO by chlorogenic acid quinones.

Based on: Kuijpers, T.F.M.; van Herk, T.; Vincken, J.-P.; Janssen, R.H.; Narh, D.L.; van Berkel, W.J.H.; Gruppen, H. *Submitted*.

INTRODUCTION

Polyphenol oxidases (PPOs) catalyze enzymatic browning by oxidizing phenolic compounds to their respective *o*-quinones, which subsequently undergo non-enzymatic reactions with each other and other compounds present, resulting in the formation of dark-colored pigments, also referred to as melanins (1). This phenomenon is a major quality problem in fruit and vegetable processing (e.g. apple, potato, mushroom), while it is also associated with discoloration of shrimps (2) and formation of hyperpigmentation in human skin (3).

In order to inhibit the undesired browning, several food additives have been used, of which different sulfites are best known. The use of sulfites in food, however, is controversial, due to presumed health risks (4). In order to avoid using sulfites, much research is dedicated to finding natural alternatives (5-8). In such research, it is important to distinguish between (i) actual PPO inhibitors that prevent the formation of *o*-quinones, (ii) compounds that reduce the *o*-quinones to their *o*-diphenolic precursors (e.g. ascorbic acid (9)), and (iii) compounds that form colorless addition products with *o*-quinones (e.g. cysteine (10)).

Inhibition studies have been conducted on PPOs from a range of different sources. Because of its commercial availability, mushroom tyrosinase is often used as a model system, both for browning of food products, as well as for skin pigmentation (11). Little is known on whether results of inhibition studies with one PPO can be extrapolated to another PPO, as most of such studies were conducted with a single PPO. To address this issue, we compared the PPO inhibitory activities of a selection of plant extracts on two different PPOs: a commercially available mushroom (*Agaricus bisporus*) tyrosinase (AbPPO) and PPO isolated from potato tubers (*Solanum tuberosum*) (StPPO).

MATERIALS AND METHODS

Materials

Potato (*Solanum tuberosum* cv Celino) tubers were obtained from Gemüse Meyer (Twistringen, Germany). Plant extracts (**Table 1**) were obtained from Frutarom (Wädenswil, Switzerland). Mushroom (*Agaricus bisporus*) tyrosinase, L-3,4-dihydroxyphenylalanine (L-DOPA), chlorogenic acid and theobromine were obtained from Sigma Aldrich (St. Louis, MO, USA). Ultra-high-performance liquid chromatography-mass spectrometry (UHPLC-MS) grade acetonitrile (ACN) was obtained from Biosolve BV (Valkenswaard, The Netherlands), and caffeine was from Boom (Meppel, The Netherlands). Water was prepared using a Milli-Q water purification system (Millipore, Billerica, MA, USA).

Purification of mushroom tyrosinase

The mushroom tyrosinase was purified by a single gel filtration step (12). A HiLoad 26/60 Superdex 200 column connected to an Akta Explorer system (GE Healthcare, Uppsala, Sweden) was used. Fifty mg of the commercial enzyme (dissolved in 50 mM HEPES buffer pH 6.8) was loaded and eluted with 50 mM HEPES buffer pH 6.8 at 4 mL/min. Fractions (5 mL) were collected and activity was assayed by a spectrophotometric assay: 50 μ L of each fraction was combined with 100 μ L 0.8 mM tyrosine in a 96 well plate and absorbance at 520 nm was monitored in time. Active fractions were pooled and stored at -20 °C until use. Tyrosinase activity was expressed in U, according to the suppliers definition (1 U increases the A280 by 0.001 per min with L-tyrosine as substrate, at pH 6.5 and 25 °C). Purified mushroom tyrosinase is further referred to as AbPPO.

Purification of potato PPO

One kg of potatoes was cooled to 4 °C, washed and homogenized in 1 L ice-cold 50 mM HEPES buffer pH 6.9 containing 1 % ascorbic acid and 2 tablets of protease inhibitor (Complete - EDTA free, Roche Diagnostics GmbH) using a commercial blender. The homogenate was filtered through 4 layers of cheesecloth and the filtrate was centrifuged at 13600 x g at 4 °C for 1 h (Crude extract, CE). Ammonium sulfate was added to 40 % saturation and the resulting solution was stirred overnight at 4 °C. The precipitate was collected by centrifugation at 13600 x g at 4 °C for 1.5 h, and dissolved in a minimal amount of 50 mM HEPES buffer pH 6.9 containing 1 % ascorbic acid. The obtained protein solution obtained was three times dialyzed against 2 L of 50 mM HEPES buffer pH 6.9 containing 0.1 % ascorbic acid and 2 tablets of the protease inhibitor, after which it was centrifuged at 13600 x g at 4 °C for 30 min.

All subsequent chromatographic steps were performed using an Akta Explorer system (GE Healthcare) at room temperature. The dialyzed protein solution (268 mL) was applied onto a Fast Flow Q-sepharose column (2.6 x 10 cm), pre-equilibrated with 50 mM HEPES buffer pH 6.9. After washing with 400 mL starting buffer, bound protein was eluted using a 800 mL linear gradient of 0 – 1 M NaCl in the same buffer. The flow rate was 4 mL/min, and 15 mL fractions were collected. Fractions showing maximal PPO activity were pooled and concentrated using a 10 kDa Amicon membrane filter (Millipore) under air pressure. The concentrated enzyme solution (5 mL) was applied onto a Superdex S-200 column (2.6 x 100 cm), and eluted with 50 mM HEPES buffer pH 6.9 at a flow rate of 1.5 mL/min. Fractions (5 mL) showing maximal PPO activity were concentrated as described above. This purification procedure gave an activity yield of 10.6 % and resulted in a 11-fold purified enzyme preparation with a specific activity of 5.9 U/mg (**Table S1**).

Fractionation of mate extract

Mate extract was fractionated using a 12 g Reveleris C18 column on a Reveleris flash chromatography system (Grace, Deerfield, IL, USA) operated at 30 mL/min. Twenty mL of

a 30 g/L solution of mate extract in MQ was applied onto the column. Water acidified with 0.1% (v/v) acetic acid, eluent A, and ACN acidified with 0.1% (v/v) acetic acid, eluent B, were used as eluents. The following elution profile was used: 0-2 min, isocratic on 0% (v/v) B; 2-3 min, linear gradient from 0%-30% (v/v) B; 3-8 min, isocratic at 30% (v/v) B; 8-13 min, linear gradient from 30%-100% (v/v) B; 13-15 min, isocratic at 100% (v/v) B. Fractions of 10 mL were collected, and pooled based on RP-UHPLC-MS analysis.

Screening of plant extracts

Inhibitory activity of plant extracts was assayed using a spectrophotometric assay. Plant extracts (5 g/L) dissolved in either water or dimethyl sulfoxide were diluted (0.16 g/L) into 0.2 mM L-DOPA and 6.5 U/mL AbPPO or 0.4 mM L-DOPA and 0.19 U/mL StPPO in 50 mM HEPES buffer pH 6.9 in a total volume of 155 μ L in a 96 well plate. The absorbance at 520 nm was measured every 20 s for 20 min at 25 °C. The initial rate of color formation (100-240 s) was compared to the appropriate water or dimethyl sulfoxide controls, and expressed as relative activity. To ensure that potential competitive inhibition could be observed, substrate concentrations were chosen below the K_m of the two PPOs for L-DOPA.

Oxygen consumption measurements

Oxygen consumption of AbPPO or StPPO with selected extracts was measured using an Oxytherm System (Hansatech, Kings Lynn, UK). Incubations with plant extracts or fractionated mate extracts (0.16 g/L) were done with 0.4 mM L-DOPA and 0.19 U/mL StPPO or 0.2 mM L-DOPA and 65 U/mL AbPPO in a total volume of 1 mL 50 mM HEPES buffer pH 6.9 at 25 °C. Data acquisition and analysis were performed using Oxygraph Plus software (Hansatech).

RP-UHPLC analysis

Samples were analysed on an Accela UHPLC system (Thermo Scientific, San Jose, CA, USA) equipped with pump, autosampler and PDA detector. Samples (1 μ L) were injected onto a Hypersil Gold column (2.1 \times 150 mm, particle size 1.9 μ m; Thermo Scientific). Water acidified with 0.1% (v/v) acetic acid, eluent A, and ACN acidified with 0.1% (v/v) acetic acid, eluent B, were used as eluents. The flow rate was 400 μ L/min, the column oven temperature was controlled at 30 °C. The PDA detector was set to measure the range 200-600 nm. The following elution profile was used: 0-1 min, isocratic on 5% (v/v) B; 1-21 min, linear gradient from 5%-75% (v/v) B; 21-21.1 min, linear gradient from 75%-100% (v/v) B; 21.1-24 min, isocratic on 100% (v/v) B; 24-24.1 min, linear gradient from 100%-5% (v/v) B; 24.1-27 min, isocratic on 5% (v/v) B.

Electrospray ionization mass spectrometry (ESI-MS)

Mass spectrometric data were obtained by analyzing samples on a LTQ-Velos (Thermo Scientific) equipped with a heated ESI probe coupled to the RP-UHPLC system. Nitrogen was used as sheath gas and auxiliary gas. Data were collected over the m/z range 150-1500. Data-dependent MS^n analysis was performed with a normalized collision energy of 35%. The MS^n fragmentation was performed on the most intense product ion in the MS^{n-1} spectrum. Most settings were optimized via automatic tuning using 'Tune Plus' (Xcalibur 2.1, Thermo Scientific). The system was tuned with a mate extract in negative ionization (NI) mode. The source heater temperature was 45 °C, the transfer tube temperature was 350 °C and the source voltage was 3.5 kV. Data acquisition and analysis were done with Xcalibur 2.1 (Thermo Scientific).

RESULTS

Screening of plant extracts for PPO inhibitory activity

The effect of 60 different plant extracts on dopachrome formation by AbPPO and StPPO was compared by expressing the rate of dopachrome formation as activity relative to the appropriate control (L-DOPA with AbPPO or StPPO and the solvent used to dissolve the plant extract) (**Table 1**). To facilitate this comparison, the relative activities were plotted against each other (**Figure 1**).

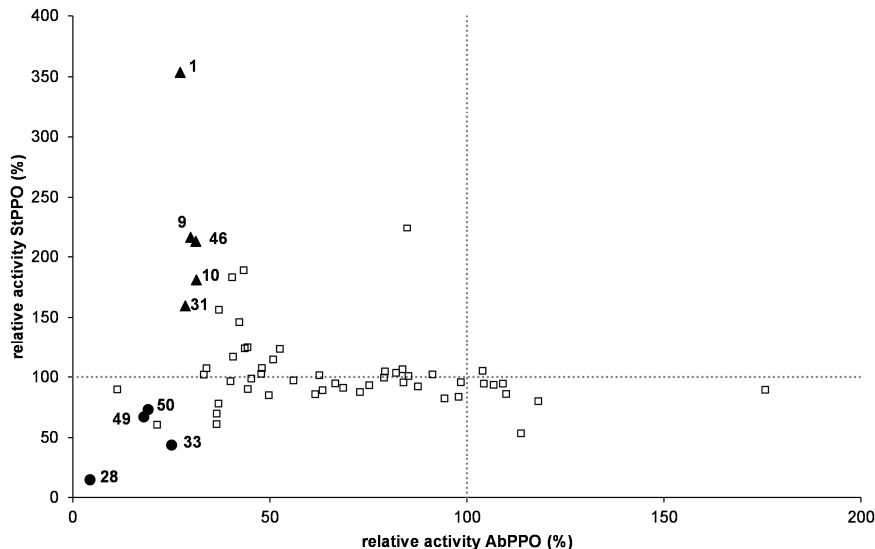


Figure 1. Comparison of the influence of different plant extracts on the conversion of L-DOPA to dopachrome by AbPPO and StPPO. Filled circles indicate extracts that were relatively good inhibitors for both reactions, filled triangles indicate extracts that showed a large difference in inhibition, open squares indicate all other plant extracts. The numbers refer to **Table 1**.

Table 1. The effect of plant extracts on the rate of dopachrome formation by AbPPO and StPPO.

Extract	Plant species	Relative activity AbPPO (%)*	Relative activity StPPO (%)*
1 Green mate leaf	<i>Ilex paraguariensis</i>	27 ± 1.0	354 ± 41.5
2 Oats herb	<i>Avena sativa</i>	73 ± 1.8	88 ± 10.6
3 Olive leaf	<i>Olea europaea</i>	85 ± 3.2	224 ± 2.3
4 Echinacea dry pressed juice	<i>Echinaceae purpurea</i>	104 ± 3.7	105 ± 6.7
5 Echinacea purpurea root	<i>Echinaceae purpurea</i>	91 ± 2.2	102 ± 7.3
6 Pumpkin seed	<i>Curcubita pepo</i>	85 ± 1.6	101 ± 3.7
7 Green tea leaf	<i>Camillia sinensis</i>	22 ± 1.1	61 ± 1.9
8 Nettle leaf	<i>Urtica dioica</i> , <i>Urtica urens</i>	84 ± 2.7	106 ± 3.8
9 Balm herb	<i>Melissa officinalis</i>	30 ± 2.9	216 ± 9.9
10 Sage leaf	<i>Salvia officinalis</i>	31 ± 2.6	181 ± 4.1
11 Rhubarb	<i>Rheum rhabarbarum</i>	50 ± 1.1	85 ± 3.4
12 Red vine leaf	<i>Vitis vinifera</i>	63 ± 7.2	89 ± 0.8
13 Peppermint leaf	<i>Mentha piperita</i>	44 ± 3.3	124 ± 13.8
14 Dandelion herb and root	<i>Taraxum officinale</i>	79 ± 8.6	100 ± 8.4
15 Thyme herb	<i>Thymus vulgaris</i>	37 ± 1.8	156 ± 0.2
16 Pink rockrose herb	<i>Cistus incanus</i>	37 ± 2.1	70 ± 1.5
17 Passion flower herb	<i>Passiflora incarnata</i>	67 ± 3.5	95 ± 4.3
18 Damiana leaf	<i>Turnera diffusa</i>	75 ± 3.3	93 ± 10.7
19 Goldenrod herb	<i>Solidago sp.</i>	43 ± 0.2	189 ± 11.2
20 Artichoke leaf	<i>Cynara scolymus</i>	63 ± 2.2	102 ± 25.4
21 Java tea	<i>Orthosiphon stamineus</i>	34 ± 0.2	107 ± 0.13
22 Eyebright herb	<i>Euphrasia sp.</i>	42 ± 2.7	146 ± 3.9
23 Ivy leaf	<i>Hedera helix</i>	53 ± 3.8	123 ± 1.4
24 Marshmallow root	<i>Althea officinalis</i>	99 ± 2.7	96 ± 1.4
25 Bearberry leaf	<i>Arctostaphylos uva-ursi</i>	36 ± 6.6	61 ± 0.9
26 Schisandra fruit	<i>Schisandra chinensis</i>	88 ± 5.7	92 ± 2.2
27 Licorice root	<i>Glycyrrhiza glabra</i>	4 ± 1.8	15 ± 1.1
28 Chaste berry	<i>Vitex agnus-castus</i>	51 ± 12.8	115 ± 0.4
29 Juniper fruit	<i>Juniperus sp.</i>	84 ± 3.2	96 ± 1.3
30 Rosemary leaf	<i>Rosmarinus officinalis</i>	29 ± 3.4	160 ± 0.0
31 Devil's claw root	<i>Harpagophytum procumbens</i> and/or <i>H. Zeyheri</i>	41 ± 1.5	117 ± 1.6
32 Pelargonium root	<i>Pelargonium sidoides</i>	25 ± 1.0	44 ± 9.6

Table 1. (Continued)

33	Chamomile flower	<i>Chamomilla recutita</i>	33 ± 0.2	102 ± 1.9
34	Caraway seed	<i>Carum carvu</i>	56 ± 1.0	97 ± 2.4
35	Puslane herb	<i>Potulaca oleracea</i>	62 ± 3.3	86 ± 8.7
36	Rosehip	<i>Rosa canina</i>	98 ± 0.5	84 ± 13.0
37	SoyLife 40	<i>Glycine max</i>	48 ± 0.5	103 ± 17.0
38	LinumLife EXTRA	<i>Linum usitatissimum</i>	82 ± 2.9	103 ± 9.4
39	Brocoraphanin 10% glucoraphanin	<i>Brassica oleracea</i> var. <i>italica</i>	118 ± 11.5	80 ± 12.7
40	Biocurcumin	<i>Curcuma longa</i>	-\$	-\$
41	Pomactiv AGE	<i>Malus</i> sp.	44 ± 2.7	90 ± 5.8
42	SuperBerry 6000	blend of 7 berries	37 ± 8.0	78 ± 3.7
43	Acai	<i>Euterpe oleracea</i>	94 ± 5.5	82 ± 10.2
44	Blackcurrant 25% anthocyanins	<i>Ribes nigrum</i>	11 ± 10.3	90 ± 18.1
45	Origanox WS-LB	<i>Origanum vulgare</i> and/ or <i>Melissa officinalis</i>	31 ± 2.4	213 ± 3.0
46	Origanox WS	<i>Origanum vulgare</i>	44 ± 2.1	125 ± 3.0
47	Cranberry High PAC 25:1	<i>Vaccinum macrocarpon</i>	176 ± 4.5	90 ± 1.6
48	OPC Grape Seed ActiVin	<i>Vitis vinifera</i>	18 ± 0.4	67 ± 0.7
49	Neohesperidine dihydrochalcone (NHDC)	extracted from citrus and chemically modified	19 ± 0.8	73 ± 2.3
50	Neohesperidine	extracted from citrus	40 ± 4.9	97 ± 4.0
51	Hesperidine	extracted from citrus	45 ± 5.1	99 ± 1.3
52	Black garlic	<i>Allium sativum</i>	109 ± 3.0	95 ± 0.6
53	Horse radish	<i>Armoracia rusticana</i>	110 ± 1.2	86 ± 12.9
54	Hibiscus	<i>Hibiscus</i> sp.	114 ± 12.3	54 ± 15.0
55	Baobab	<i>Adansonia digitata</i>	107 ± 0.1	94 ± 1.5
56	Coriander	<i>Coriandrum sativum</i>	79 ± 4.5	105 ± 2.4
57	Cinnamon	<i>Cinnamomum</i> sp.	69 ± 5.6	91 ± 4.3
58	Cinnamon 2	<i>Cinnamomum</i> sp.	104 ± 40.4	95 ± 4.0
69	Pomactiv HFV	<i>Malus</i> sp.	48 ± 1.8	107 ± 13.7
60	Pomactiv Shape	<i>Malus</i> sp.	40 ± 2.4	183 ± 4.6

*The rate of dopachrome formation relative to the appropriate control (L-DOPA with AbPPO or StPPO and the solvent used to dissolve the plant extract).

§ Biocurcumin was not included in the spectrophotometric assay due to interfering color of the extract.

From this plot it can be observed that, in general, the StPPO-mediated color formation seemed to be less inhibited than color formation caused by AbPPO. Interestingly, some extracts seemed to inhibit AbPPO, while they stimulated StPPO. It should be taken into account that the observed effect on color formation is not necessarily caused by influencing the enzymatic activity. An alternative explanation for an observed inhibition of color formation could be the presence of reducing compounds in the plant extracts, which can either reduce the enzymatically formed *o*-quinone back to the corresponding *o*-diphenol (e.g. ascorbic acid (13)), or combine with the *o*-quinone in an addition product (e.g. cysteine (10) or sulfite (14)). An explanation for enhanced color formation could be the presence of substrates for enzymatic browning in the plant extract itself. To investigate whether enzymatic activity was truly affected, five extracts that showed a large difference in effect on AbPPO and StPPO, and four extracts that appeared to be relatively good inhibitors for both the AbPPO and StPPO-mediated color formation were selected for oxygen consumption measurements.

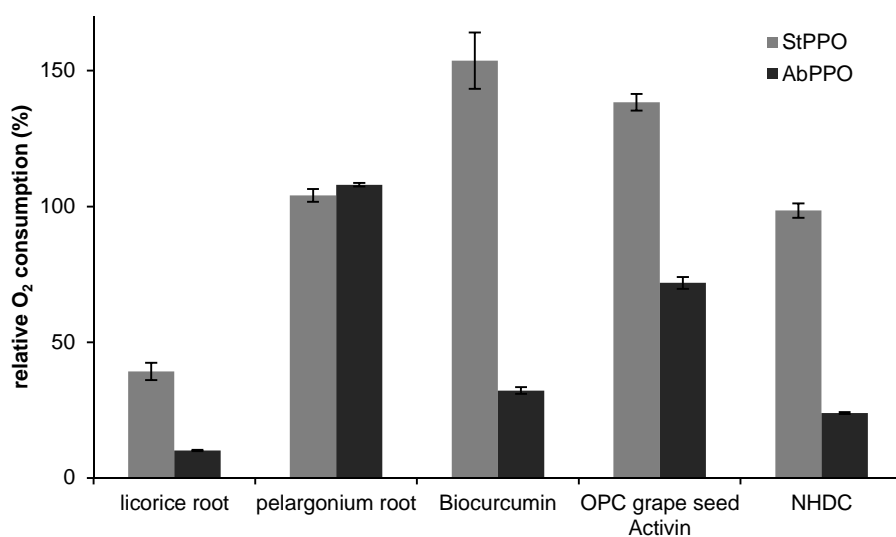


Figure 2. Relative oxygen consumption rates of StPPO and AbPPO with combinations of plant extracts and L-DOPA. Averages of duplicate determinations, error bars indicate standard deviation.

Oxygen consumption measurements discriminate between inhibition of color formation and enzyme activity

The four extracts indicated with a circle in **Figure 1** (licorice root, pelargonium root, OPC grape seed ActiVin and NHDC) were used in oxygen consumption measurements to determine whether the observed inhibitory effect on dopachrome formation for both enzymes was caused by inhibition of PPO activity. Biocurcumin was also used in this

assay, as the color of this extract was found to interfere with the spectrophotometric assay. The trend of color formation with StPPO being less inhibited than that with AbPPO (**Figure 1**) was confirmed by oxygen consumption of the two enzymes (**Figure 2**). Remarkably, the relative oxygen consumption of StPPO in the presence of biocurcumin, grape seed, pelargonium root and NHDC was 100 % or more, while the relative color formation with StPPO and these extracts was below 100 %. Possibly, the extract contained substrates for StPPO, the oxidation of which did not result in products with an absorption at 520 nm, the wavelength used for the screening assay. If these substrates are preferentially used by StPPO, no color development at 520 nm would be observed, while oxygen consumption occurs. It is unlikely that this effect could be attributed to the presence of reducing compounds in the extracts, as no differences between StPPO and AbPPO would then be expected.

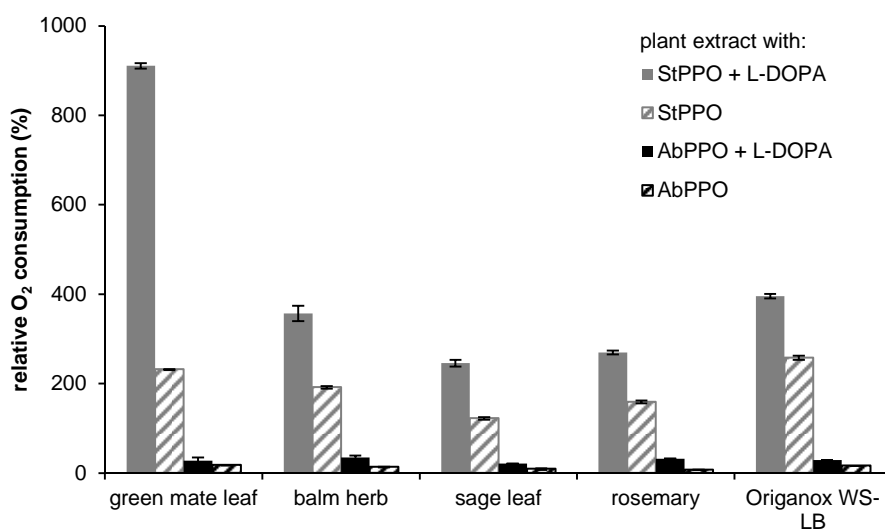


Figure 3. Relative oxygen consumption rates of StPPO and AbPPO in the presence of plant extracts alone, or combinations of plant extracts and L-DOPA. Oxygen consumption was expressed relative to the control reaction of either StPPO or AbPPO with L-DOPA. Averages of duplicate determinations, error bars indicate standard deviation.

The influence on oxygen consumption of StPPO and AbPPO of five extracts that showed a large difference in their effect on StPPO and AbPPO-mediated color formation (mate leaf, balm herb, sage leaf, rosemary and oregano, indicated with triangles in **Figure 1**) was investigated. Because compounds present in the extracts could potentially be substrates for either one of the PPOs, in this way possibly enhancing enzyme activity, incubations of PPO with only plant extract were compared to incubations of PPO, plant extracts and L-DOPA (**Figure 3**). The oxygen consumption of StPPO with all of the plant

extracts alone was higher than that of the control reaction (StPPO with L-DOPA) used for standardization, indicating that these plant extracts either contained substrates that had a higher affinity for StPPO than L-DOPA, or substrates in a considerably higher concentration than the L-DOPA used (0.4 mM). Assuming a molecular weight of 150-300 g/mol for possible substrates in the plant extracts, and assuming that these extracts consisted only of substrate, it can be calculated that the maximum theoretical substrate concentration is approximately 0.5-1 mM, with the concentration of plant extracts used in the assay. Balm herb, sage, rosemary and oregano are all members of the Lamiaceae plant family, which are known to contain a variety of phenolics, including phenolic acids, flavonoids and phenolic terpenes (15,16). LC-MS analysis of the extracts used confirmed the presence of a range of compounds, with the most abundant compounds being rosmarinic acid and derivatives of rosmarinic acid (data not shown). The fact that the extracts consisted of multiple components, indicated that substrates present in the extracts had higher affinities for StPPO than L-DOPA. The relative activity of AbPPO on the plant extracts alone was lower than the activity on combinations of plant extract and L-DOPA, and activity of both reactions was lower than that of the control reaction (AbPPO with L-DOPA). This indicated that the selected plant extracts effectively reduced the rate of AbPPO-mediated color formation by inhibiting the enzyme. The observation that AbPPO showed some activity on the plant extracts alone indicated that besides inhibitors for AbPPO, the extracts also contained substrates for AbPPO. Furthermore, comparing the activity of StPPO and AbPPO on the plant extracts alone, it can be concluded that the substrates present in the extracts are probably better substrates for StPPO than for AbPPO.

Comparing the effect of the plant extracts in combination with L-DOPA on StPPO to the activity of StPPO on the plant extracts alone, the effect of the mate extract stands out. While activity of StPPO on the mate extract alone was approximately double that of StPPO on L-DOPA, the activity of StPPO on a combination of L-DOPA and mate was more than nine times that of StPPO on L-DOPA alone. It seems unlikely that this effect can only be attributed to the presence of substrates in the mate extract. The effect of mate on StPPO and AbPPO was further investigated.

Mate extract accelerates oxygen consumption of StPPO, while it inhibits that of AbPPO

The effect of sequential addition of mate extract and L-DOPA to StPPO was compared to a control incubation of StPPO with L-DOPA alone and an incubation of StPPO with L-DOPA and mate extract added simultaneously (**Figure 4A**). The initial activity of StPPO on mate extract is comparable to that on the combination of mate and L-DOPA, both of which are higher than the activity on L-DOPA alone. The activity of StPPO on mate alone started to decrease shortly after the beginning of the reaction and eventually leveled off, indicating that the substrates present in mate were all converted. When L-DOPA was added after complete conversion of the substrates present in the mate extract, enhanced StPPO

activity was still observed. This is an indication that the enhanced oxygen consumption of StPPO with combinations of L-DOPA and mate extract is not only due to supplementation of L-DOPA with additional substrates present in the extract, but rather points towards activation of StPPO.

Activity of AbPPO on mate was much lower than that of StPPO, and the L-DOPA oxidation rate of AbPPO was lower in the presence of mate than without mate (**Figure 4B**). AbPPO was also inhibited upon sequential addition of mate and L-DOPA.

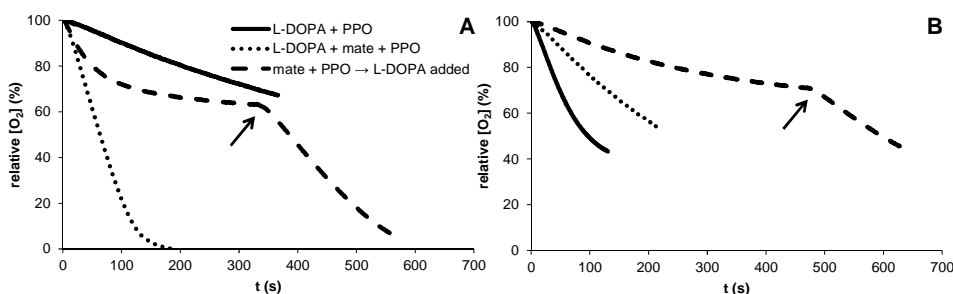


Figure 4. Oxygen consumption in time of incubations of StPPO (**A**) and AbPPO (**B**) with L-DOPA and mate extract. Arrows indicate the time point at which L-DOPA was added.

These results seemed to indicate that the mate extract used contained one or more activators for StPPO and one or more inhibitors for AbPPO. It is not known whether the same compounds are responsible for activation of StPPO and inhibition of AbPPO, or whether activators for StPPO are present alongside inhibitors for AbPPO.

Characterization of mate extract

To identify the compound(s) responsible for activation of StPPO and inhibition of AbPPO, the composition of the mate extract was characterized based on RP-UHPLC-MS analysis (**Figure 5A**). Peaks were annotated based on comparison of MS/MS fragmentation with published data (**Table 2**) (17-19). Two distinct groups of compounds were found, hydroxycinnamic acid conjugates and saponins. Furthermore, quercetin-3-*O*-rutinoside, a glycosylated flavonol, caffeine and theobromine were found. The hydroxycinnamic acid conjugates were, besides a small amount of feruloyl quinic acid, all chlorogenic acid-like compounds, i.e. different caffeoyl and dicaffeoyl quinic acid isomers. Chlorogenic acid is a well-known substrate for PPO (20,21), so the presence of these compounds explains the observed activity of StPPO and AbPPO when incubated with mate extract as substrate. Chlorogenic acids are the most abundant phenolic compounds in potato (22), which might explain the much higher activity of StPPO than AbPPO on the mate extract, considering that chlorogenic acid is likely to be the natural substrate for StPPO. To investigate whether indeed the different chlorogenic acid isomers were used as substrate by PPO,

RP-UHPLC-MS analysis of incubations of mate with StPPO and AbPPO were done. The MS traces of these samples revealed that the different chlorogenic acids and quercetin-3-*O*-rutinoside were converted, while the saponins remained (data not shown). No reaction products of the oxidation of the different substrates were found, while the mate sample after incubation with PPO visibly turned brown. This might be explained by formation of a wide variety of reaction products from the *o*-quinones resulting from PPO oxidation, which individually fall below the detection limit of the RP-UHPLC analysis.

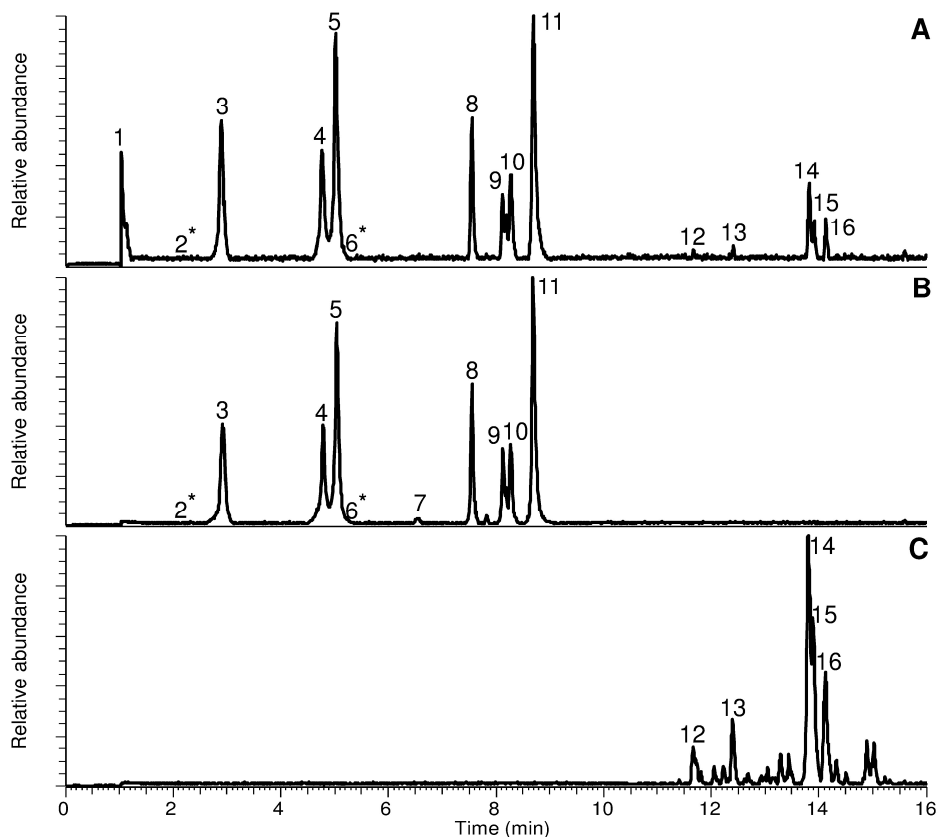


Figure 5. RP-UHPLC-MS traces of mate extract (A), polar fraction of mate (B) and apolar fraction of mate (C). Peak numbers refer to annotation in **Table 2**. * indicates the retention time of theobromine and caffeine, which were observed only in the UV trace, not in negative ionization mode MS.

Polar compounds in mate extract are responsible for activation of StPPO

The fact that the saponins remained after PPO activity, led to the hypothesis that they might be responsible for the observed activation of StPPO and inhibition of AbPPO. Saponins extracted from *Paris polyphylla* have been found to inhibit AbPPO (23). To investigate this, reversed-phase flash chromatography was used to fractionate the mate extract to investigate

the effect of the saponins separately from the chlorogenic acid-like compounds. Fractions from flash chromatography were pooled such that a fraction containing mainly chlorogenic acid-like compounds (polar fraction, **Figure 5B**) and a fraction containing mainly saponins (apolar fraction, **Figure 5C**) were obtained.

Table 2. RP-UHPLC-MS characterization of mate extract. Peaks were annotated based on MS² fragmentation.

Peak	Retention time	[M-H] ⁻	MS ² fragments (relative abundance)	Tentative identification
1	1.04	191	191 (100), 111 (42), 127 (30), 85 (30), 93 (17), 87 (7), 109 (6), 155 (4), 71 (3), 153 (3)	Quinic acid
2	2.15	-	-	Theobromine
3	2.90	353	191 (100), 179 (39), 353 (8), 135 (3), 173 (1)	3-O-caffeoyl quinic acid
4	4.76	353	191 (100), 179 (1)	5-O-caffeoyl quinic acid
5	5.02	353	173 (100), 179 (72), 191 (28), 353 (9), 135 (4), 155 (1)	4-O-caffeoyl quinic acid
6	5.18	-	-	Caffeine
7	6.57	367	191 (100), 173 (73), 193 (15), 285 (7), 307 (3), 367 (2), 203 (2), 325 (1), 155 (1)	Feruloyl quinic acid
8	7.56	609	301 (100), 300 (48), 609 (9), 343 (8), 271 (8), 255 (5), 179 (2), 273 (1)	Quercetin-3-rutinoside
9	8.12	515	353 (100), 335 (11), 173 (1), 515 (8), 179 (8), 191 (6), 203 (3), 255 (2), 299 (2)	Dicaffeoylquinic acid
10	8.28	515	353 (100), 191 (3), 179 (1)	Dicaffeoylquinic acid
11	8.70	515	353 (100), 203 (6), 173 (5), 299 (5), 255 (4), 179 (3), 335 (2), 317 (2), 191 (1)	Dicaffeoylquinic acid
12	11.67	1073	911 (100), 749 (76), 893 (12), 603 (10), 983 (9), 927 (6), 765 (5), 901 (5), 1043 (5)	Matesaponin 3
13	12.42	1219	895 (100), 733 (13), 937 (2)	Matesaponin 4
14	13.82	1057	895 (100), 733 (14), 937 (8), 587 (5)	Matesaponin 2
15	13.91	1057	895 (100), 733 (64), 893 (8), 587 (7)	Matesaponin 2 isomer
16	14.13	911	749 (100), 791 (19)	Matesaponin 1

Oxygen consumption measurements with L-DOPA and StPPO in the presence of the apolar or polar mate fraction (**Figure 6A**) showed that the polar mate fraction seemed to be mainly responsible for activation of StPPO: while StPPO was slightly more active in the

presence of the apolar mate fraction than with only L-DOPA, activity in the presence of the polar mate fraction was much higher than the blank incubation.

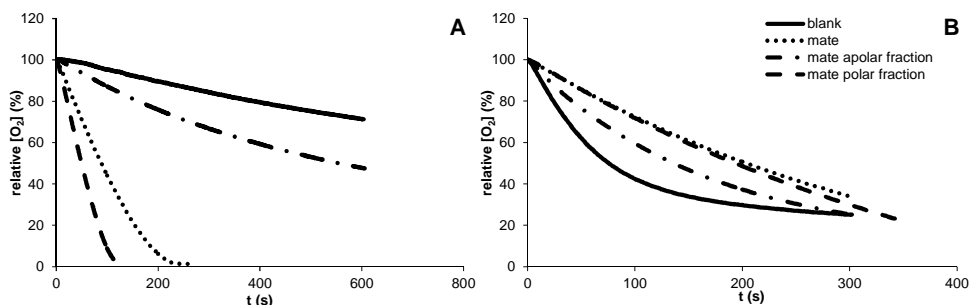


Figure 6. Oxygen consumption in time of incubations of StPPO (A) and AbPPO (B) with L-DOPA (blank), and L-DOPA combined with mate extract, the polar mate fraction and the apolar mate fraction.

Besides chlorogenic acid-like compounds, caffeine and theobromine were also present in the polar fraction. While the chlorogenic acid-like compounds were converted after incubation with PPO, caffeine and theobromine remained. Experiments with pure caffeine and theobromine showed that they were not responsible for activation of StPPO or inhibition of AbPPO (data not shown). Apparently, the substrates present in the mate extract activated StPPO, also after they had reacted (**Figure 4A**). To investigate whether the activation of StPPO was indeed due to the chlorogenic acid-like substrates present in mate, StPPO was incubated with pure chlorogenic acid. When oxygen consumption had leveled off, L-DOPA was added. The results obtained were similar to those obtained with mate: oxygen consumption with sequential chlorogenic acid and L-DOPA addition was accelerated compared to a control of StPPO with only L-DOPA (data not shown). Considering the inhibition of AbPPO by mate, fractionation of the extract learned that the polar fraction was mainly responsible for inhibition (**Figure 6B**). In the presence of the apolar mate fraction, oxygen consumption of AbPPO with L-DOPA was comparable to that in the blank reaction, whereas in the presence of the polar fraction the oxygen consumption was decreased compared to that with the blank.

DISCUSSION

Our results of screening 60 plant extracts for StPPO and AbPPO inhibitory activity demonstrated that the effect that an extract can have on PPO-catalyzed browning is dependent on the source of PPO. Some extracts showed inhibitory activity towards both PPOs, while other extracts inhibited only one PPO, or even inhibited one and activated the other PPO. As an example, a mate extract was investigated in more detail, and it was found to be an activator for StPPO and an inhibitor for AbPPO.

Inhibition of PPOs by plant extracts

Out of 60 plant extracts screened for inhibitory effects on StPPO and AbPPO, four were further investigated by measuring their influence on oxygen consumption. Only the extract of licorice root was found to inhibit the activity of both StPPO and AbPPO (**Figure 2**), indicating that the observed inhibitory effect on color formation of the other extracts was most likely caused by reducing compounds in the extracts. These compounds only prevent formation of color, but do not inhibit enzyme activity.

The inhibitory effect of licorice root on AbPPO has been described before, and several inhibitory (iso)flavonoids and chalcones have been identified (24-26). Licorice extracts were found to inhibit both mushroom tyrosinase *in vitro*, as well as melanin formation in cultured human melanocytes (25). In addition to this, our results demonstrated that licorice also inhibited StPPO. This might indicate that the inhibitors present in licorice are inhibitors with a wide application range.

Activation of StPPO by mate extract

When StPPO was incubated with mate extract, oxygen consumption and conversion of substrates present in the extract was observed. Incubation of StPPO with mate extract had an activating effect on L-DOPA oxidation by the enzyme (**Figure 4A**). Fractionation of the mate extract demonstrated that chlorogenic acid-like compounds were responsible for this activation, which was confirmed by experiments with pure chlorogenic acid. An explanation for the increased StPPO activity observed might be activation of StPPO, which was extracted in a latent state, by *o*-quinones resulting from chlorogenic acid oxidation. Similarly, activation of latent PPO from red clover (*Trifolium pretense*) by *o*-quinones resulting from oxidation of endogenous substrates has been demonstrated (27). It was proposed that a conformational change of clover PPO occurred through interaction of *o*-quinones with the protein. Conformational changes have been implicated before in the activation of latent plant PPOs. Treatment with surfactants such as SDS, addition of fatty acids and pH-induced conformational change have been reported to activate plant PPOs, by making the active site more accessible (28-31). Possibly, interaction of chlorogenic acid quinones with StPPO induced a conformational change, in this way making its active site more accessible.

In conclusion, our results showed that care should be taken when generalizing results of inhibitor studies obtained with one specific PPO to broader food or cosmetic applications. Although screening with a commercially available PPO might be a convenient way to find potential inhibitors, experiments with the target PPO should be done before an inhibitor can be applied in a specific product. Moreover, when using a different PPO for inhibitor screening than for the final application, potentially useful inhibitors might be overlooked.

ACKNOWLEDGMENT

This study has been carried out with financial support from the Commission of the European Communities within the Seventh Framework Programme for research and technological development (FP7), Grant Agreement No. 226930, title “Replacement of sulphur dioxide (SO₂) in food keeping the same quality and shelf-life of the products”, acronym SO2SAY.

REFERENCES

1. Friedman, M., Food browning and its prevention: an overview. *J. Agric. Food Chem.* **1996**, *44*, 631-653.
2. Nirmal, N. P.; Benjakul, S., Effect of ferulic acid on inhibition of polyphenoloxidase and quality changes of Pacific white shrimp (*Litopenaeus vannamei*) during iced storage. *Food Chem.* **2009**, *116*, 323-331.
3. Smit, N.; Vicanova, J.; Pavel, S., The hunt for natural skin whitening agents. *Int. J. Mol. Sci.* **2009**, *10*, 5326-5349.
4. Wilson, B. G.; Bahna, S. L., Adverse reactions to food additives. *Ann. Allergy Asthma Immunol.* **2005**, *95*, 499-507.
5. Chang, T.-S., An updated review of tyrosinase inhibitors. *Int. J. Mol. Sci.* **2009**, *10*, 2440-2475.
6. Loizzo, M. R.; Tundis, R.; Menichini, F., Natural and synthetic tyrosinase inhibitors as antibrowning agents: an update. *Comp. Rev. Food Sci. F* **2012**, *11*, 378-398.
7. Kim, Y. J.; Uyama, H., Tyrosinase inhibitors from natural and synthetic sources: structure, inhibition mechanism and perspective for the future. *Cell. Mol. Life Sci.* **2005**, *62*, 1707-1723.
8. Parvez, S.; Kang, M.; Chung, H.-S.; Bae, H., Naturally occurring tyrosinase inhibitors: mechanism and applications in skin health, cosmetics and agriculture industries. *Phytother. Res.* **2007**, *21*, 805-816.
9. Ros, J. R.; Rodriguez-Lopez, J. N.; Garcia-Canovas, F., Effect of L-ascorbic acid on the monophenolase activity of tyrosinase. *Biochem. J.* **1993**, *295*, 309-312.
10. Richard, F. C.; Goupy, P. M.; Nicolas, J. J.; Lacombe, J. M.; Pavia, A. A., Cysteine as an inhibitor of enzymic browning. I. Isolation and characterization of addition compounds formed during oxidation of phenolics by apple polyphenol oxidase. *J. Agric. Food Chem.* **1991**, *39*, 841-847.
11. Adhikari, A.; Devkota, H. P.; Takano, A.; Masuda, K.; Nakane, T.; Basnet, P.; Skalko-Basnet, N., Screening of Nepalese crude drugs traditionally used to treat hyperpigmentation: *in vitro* tyrosinase inhibition. *Int. J. Cosmetic Sci.* **2008**, *30*, 353-360.
12. Schurink, M.; van Berkel, W. J. H.; Wichers, H. J.; Boeriu, C. G., Novel peptides with tyrosinase inhibitory activity. *Peptides* **2007**, *28*, 485-495.
13. Iyengar, R.; McEvily, A. J., Anti-browning agents: alternatives to the use of sulfites in foods. *Trends Food Sci. Technol.* **1992**, *3*, 60-64.
14. Kuijpers, T. F. M.; Narváez-Cuenca, C.-E.; Vincken, J.-P.; Verloop, A. J. W.; van Berkel, W. J. H.; Gruppen, H., Inhibition of enzymatic browning of chlorogenic acid by sulfur-containing compounds. *J. Agric. Food Chem.* **2012**, *60*, 3507-3514.
15. Hossain, M. B.; Rai, D. K.; Brunton, N. P.; Martin-Diana, A. B.; Barry-Ryan, A. C., Characterization of phenolic composition in lamiaceae spices by LC-ESI-MS/MS. *J. Agric. Food Chem.* **2010**, *58*, 10576-10581.

16. Koukoulitsa, C.; Karioti, A.; Bergonzi, M. C.; Pescitelli, G.; Di Bari, L.; Skaltsa, H., Polar constituents from the aerial parts of *Origanum vulgare* L. ssp. *hirtum* growing wild in Greece. *J. Agric. Food Chem.* **2006**, *54*, 5388-5392.
17. Bravo, L.; Goya, L.; Lecumberri, E., LC/MS characterization of phenolic constituents of mate (*Ilex paraguariensis*, St. Hil.) and its antioxidant activity compared to commonly consumed beverages. *Food Res. Int.* **2007**, *40*, 393-405.
18. Puangraphant, S.; Berhow, M. A.; de Mejia, E. G., Mate (*Ilex paraguariensis* St. Hilaire) saponins induce caspase-3-dependent apoptosis in human colon cancer cells *in vitro*. *Food Chem.* **2011**, *125*, 1171-1178.
19. Martinet, A.; Ndjoko, K.; Terreaux, C.; Marston, A.; Hostettmann, K.; Schutz, Y., NMR and LC-MSⁿ characterisation of two minor saponins from *Ilex paraguariensis*. *Phytochem. Analysis* **2001**, *12*, 48-52.
20. Kermasha, S.; Goetghebeur, M.; Monfette, A.; Metche, M.; Bovel, B., Studies on inhibition of mushroom polyphenol oxidase using chlorogenic acid as substrate. *J. Agric. Food Chem.* **1993**, *41*, 526-531.
21. Oszmianski, J.; Lee, C. Y., Enzymic oxidative reaction of catechin and chlorogenic acid in a model system. *J. Agric. Food Chem.* **1990**, *38*, 1202-1204.
22. Narváez-Cuenca, C.-E.; Vincken, J.-P.; Gruppen, H., Identification and quantification of (dihydro) hydroxycinnamic acids and their conjugates in potato by UHPLC–DAD–ESI-MSⁿ. *Food Chem.* **2012**, *130*, 730-738.
23. Devkota, K. P.; Khan, M. T. H.; Ranjit, R.; Meli Lannang, A.; Samreen; Iqbal Choudhary, M., Tyrosinase inhibitory and antileishmanial constituents from the rhizomes of *Paris polyphylla*. *Nat. Prod. Res.* **2007**, *21*, 321-327.
24. Fu, B.; Li, H.; Wang, X.; Lee, F. S. C.; Cui, S., Isolation and identification of flavonoids in licorice and a study of their Inhibitory effects on tyrosinase. *J. Agric. Food Chem.* **2005**, *53*, 7408-7414.
25. Nerya, O.; Vaya, J.; Musa, R.; Izrael, S.; Ben-Arie, R.; Tamir, S., Glabrene and isoliquiritigenin as tyrosinase inhibitors from licorice roots. *J. Agric. Food Chem.* **2003**, *51*, 1201-1207.
26. Yokota, T.; Nishio, H.; Kubota, Y.; Mizoguchi, M., The inhibitory effect of glabridin from licorice extracts on melanogenesis and inflammation. *Pigm. Cell Res.* **1998**, *11*, 355-361.
27. Winters, A. L.; Minchin, F. R.; Michaelson-Yeates, T. P. T.; Lee, M. R. F.; Morris, P., Latent and active polyphenol oxidase (PPO) in red clover (*Trifolium pratense*) and use of a low PPO mutant to study the role of PPO in proteolysis reduction. *J. Agric. Food Chem.* **2008**, *56*, 2817-2824.
28. Kanade, S. R.; Paul, B.; Rao, A. G. A.; Gowda, L. R., The conformational state of polyphenol oxidase from field bean (*Dolichos lablab*) upon SDS and acid-pH activation. *Biochem. J.* **2006**, *395*, 551-562.
29. Mayer, A. M., Polyphenol oxidases in plants and fungi: Going places? A review. *Phytochemistry* **2006**, *67*, 2318-2331.
30. Pérez-Gilabert, M.; Morte, A.; García-Carmona, F., Histochemical and biochemical evidences of the reversibility of tyrosinase activation by SDS. *Plant Sci.* **2004**, *166*, 365-370.
31. Golbeck, J. H.; Cammarata, K. V., Spinach thylakoid polyphenol oxidase: isolation, activation, and properties of the native chloroplast enzyme. *Plant Physiol.* **1981**, *67*, 977-984.

SUPPORTING INFORMATION**Table S1.** Potato PPO purification scheme.

Step	Volume (mL)	Total activity (U)	Total protein (mg)	Specific activity (U/mg)	Activity yield (%)	Purification factor
CE	1460	1916	3510	0.55	100.0	1.0
AS	268	1428	1542	0.93	74.6	1.7
IEC	5	88	181	0.49	4.6	0.9
SEC	5	72	12	5.85	3.7	10.7

Chapter 6

General discussion

The research described in this thesis was aimed at (i) explaining the inhibitory mechanism of sulfite on enzymatic browning, by investigating its effect on reaction products of enzymatic browning and tyrosinase activity, and (ii) investigating whether two different PPOs responded similarly towards plant extracts potentially containing inhibitors of PPO. It was found that sulfite had a double inhibitory activity on enzymatic browning, initial browning was prevented by forming addition products with the enzymatically formed *o*-quinones, while in time tyrosinase was irreversibly inactivated by sulfite. Furthermore, we demonstrated that when screening for inhibitors of enzymatic browning the source of PPO used can have a considerable influence on the outcome of such a screening.

FORMATION OF SULFOPHENOLICS DURING FOOD PROCESSING

In **Chapter 2** the formation of different sulfophenolics in a sulfite-treated potato juice is described. It was demonstrated that PPO-mediated *o*-quinone formation was a prerequisite for the formation of sulfophenolics. In **Chapter 3** the effect of sulfite on the *in vitro* mushroom tyrosinase-catalyzed browning of chlorogenic acid was further studied, and compared to the effect of several other sulfur-containing compounds. This is the first time that mass spectrometric and NMR spectroscopic evidence of the formation of sulfophenolics during inhibition of enzymatic browning with sulfite is provided.

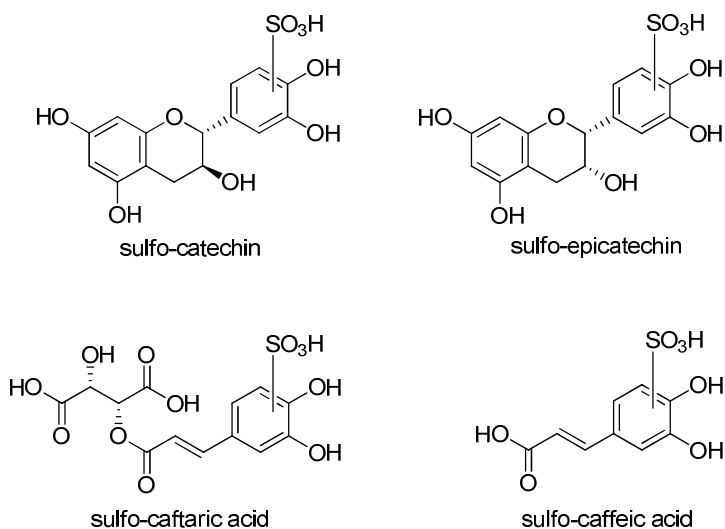


Figure 1. Sulfonated derivatives of different wine phenolics. Sulfonation occurred on either of the three available positions of the *o*-diphenolic ring.

The fact that sulfophenolics were both found during extraction of a sulfite-treated potato juice (**Chapter 2**), and in a model browning system (**Chapter 3**), raised the question

whether the formation of sulfophenolics might also be encountered in other food products in which sulfite is applied. In wine production, sulfite is applied during extraction of the juice from grapes. Since grapes are known to contain PPO (1) and a wide range of different phenolics (2), the system obtained when extracting grape juice for wine production bears resemblance to the system obtained in the industrial extraction of potato juice in the presence of sulfite, in terms of browning potential. Furthermore, an addition product of caftaric acid (an ester of caffeic acid and tartaric acid) with glutathione, referred to as 'grape reaction product', has been found in wine, in concentrations ranging from 6-49 mg/L (3-5). This product is formed by an addition reaction of glutathione present in grapes with the *o*-quinone resulting from enzymatic oxidation of caftaric acid. The PPO-mediated formation of grape reaction product indicates that during grape juice extraction PPO is active. Therefore, sulfophenolics could possibly also be formed during the production of wine.

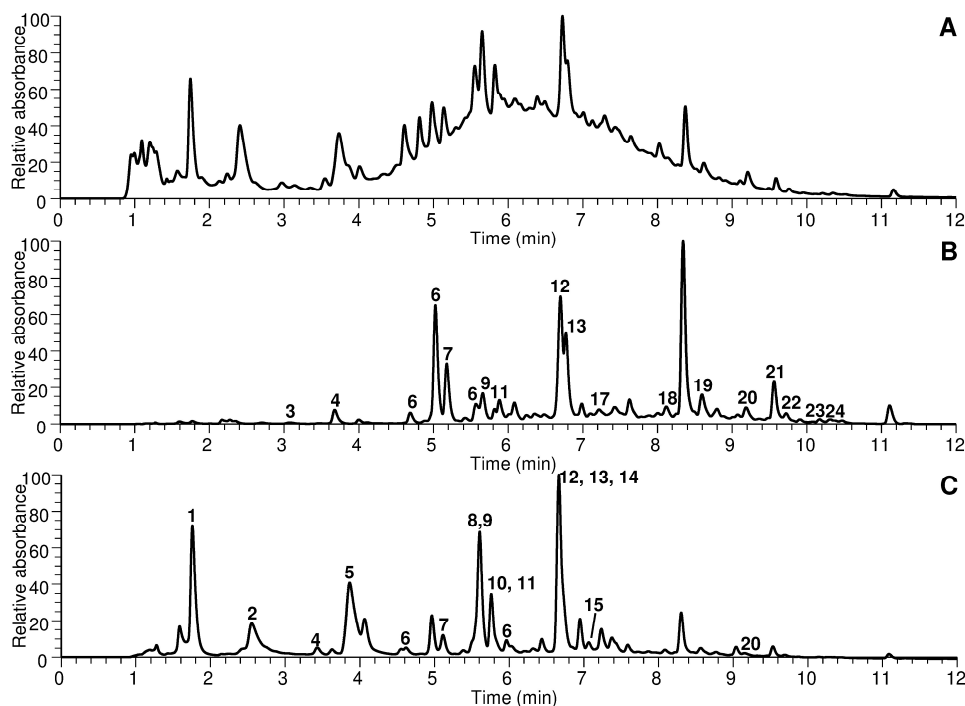


Figure 2. UV (280 nm) trace of RP-UHPLC analysis of crude wine (A), ethyl acetate pH 7 fraction (B) and ethyl acetate pH 2 fraction (C). Numbers refer to peak annotation in **Table 1**.

To investigate whether sulfophenolics could be produced from phenolics present in wine, the model system approach described in **Chapter 3** was used to prepare sulfonated standards. Caffeic acid, caftaric acid, catechin and epicatechin were used as representative

substrates, instead of chlorogenic acid. Using RP-UHPLC-MS (as described in **Chapter 3**), sulfonated derivatives of all these compounds were found (**Figure 1**), indicating that PPO substrates present in wine can be sulfonated via tyrosinase-catalyzed oxidation.

Wine contains a wide variety of phenolics, which can also be observed from the UV trace of RP-UHPLC analysis of a red wine sample (**Figure 2A**). A large hump is observed, with some peaks extending from it, indicating co-elution of many different compounds. In order to achieve a better identification of the phenolics in a red wine sample (Rioja 'Arbanta' 2009, Biurko Gorri, Bargaota, Spain), the sample was fractionated prior to analysis using sequential liquid-liquid extractions, as previously described (6)¹, resulting in two fractions ('ethyl acetate pH 2' and 'ethyl acetate pH 7'). The aqueous residue after the first ethyl acetate extraction contained anthocyanins, which are responsible for the red color of wine. It is known that sulfite can react with anthocyanins during wine production, resulting in decolorization of anthocyanins (**Figure 3**) (7). During aging, anthocyanins can react with several compounds to form more stable pigments, for instance by cross-linking reactions with flavan-3-ols (8).

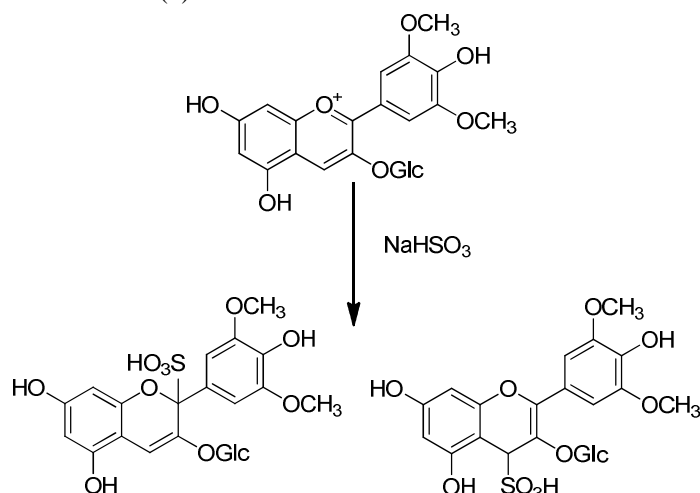


Figure 3. Reaction of sulfite with malvidin-3-O-glucoside (oenin), leading to decolorization of the anthocyanin.

RP-UHPLC-MS analysis of the resulting ethyl acetate fractions resulted in the annotation of 24 peaks, based on comparison of MS data with literature (**Figures 2B** and

¹ Dealcoholized wine was adjusted to pH 2 using 1 M HCl, after which liquid-liquid extraction with ethyl acetate (ratio 1:1) was performed. The resulting organic phase contained the phenolic compounds. To further separate the phenolics, the organic phase was dried and re-dissolved in 10 mM ammonium bicarbonate pH 7. At pH 7, phenolic acids will largely be present in dissociated form, making them more polar. Subsequent extraction with ethyl acetate resulted in an organic phase containing flavonoids ('ethyl acetate pH 7 fraction') and a water phase containing phenolic acids. To further purify phenolic acids, the water phase was adjusted to pH 2 using 1 M HCl, after which phenolic acids were extracted with ethyl acetate ('ethyl acetate pH 2 fraction').

2C, Table 1). Although the fractionation did not result in total separation of phenolic acids and other phenolics, the ethyl acetate pH 2 fraction was enriched in phenolic acids, while the ethyl acetate pH 7 fraction was enriched in flavonoids and resveratrol. Sulfophenolics were not found in either fraction, also not after specifically searching for their masses (mass of phenolic substrate + 80 a.m.u.) in MS data.

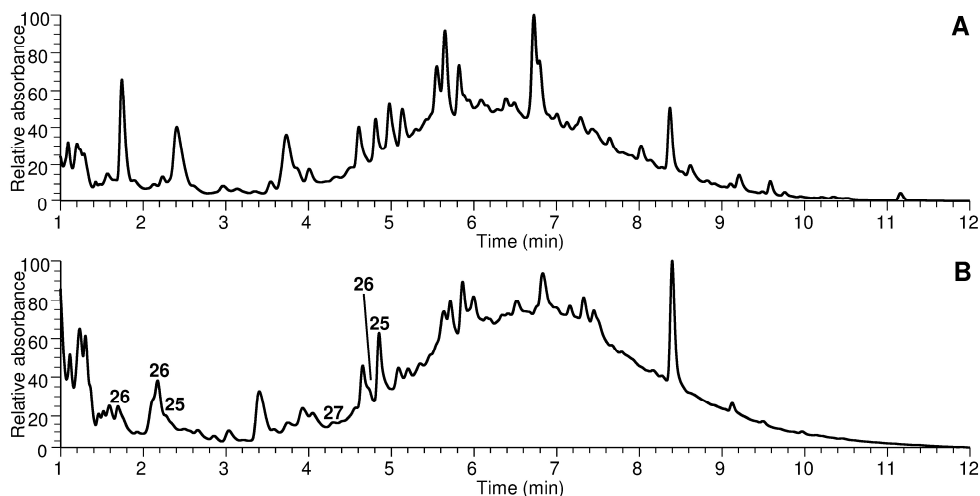


Figure 4. UV (280 nm) trace of RP-UHPLC analysis of wine (**A**) and wine incubated with mushroom tyrosinase (21 U/mL) (**B**). Sulfonated phenolics identified are numbered, numbers refer to **Table 1**.

Although it was found that wine phenolics can be sulfonated *in vitro* using mushroom tyrosinase, they were not found in the wine samples analyzed, while we were able to successfully analyze other phenolics in wine. These results indicate that formation of sulfophenolics during wine production is unlikely. Possibly, the activity of grape PPO was limited during the production of the wine analyzed, for instance due to suboptimal pH during manufacturing or inactivation of PPO by sulfite, analogous to the irreversible inactivation of mushroom tyrosinase that we observed (**Chapter 4**). It should be noted that we also did not find any grape reaction product, possibly because we investigated a red wine, while grape reaction product has most often been reported in white wine (5). In an experiment in which mushroom tyrosinase was added to red wine already containing sulfite, sulfonated derivatives of B-type procyanidin dimer, catechin and caffeic acid were found after incubation (**Figure 4**). These results indicated that in a wine matrix, active PPO would be able to oxidize phenolics, which in turn can react with the sulfite present. Another reason for not finding sulfophenolics in wine might be their possible instability during further processing. It might be speculated that sulfophenolics are formed during juicing of grapes in the presence of sulfite, but that they are unstable upon aging of wine. To further establish this, the stability of sulfophenolics should be studied.

Table 1. Tentative identification of peaks observed in RP-UHPLC-MS analysis of fractionated wine samples.

Peak	Tentative identification (reference)	[M-H] ⁻	MS ² [M-H] ⁻
1	Gallic acid (30,31)	169	125
2	Caftaric acid (30, 31)	311	179
3	Epigallocatechin (32)	305	260, 219, 179
4	Protocatechuic acid (31,33,34)	153	109
5	Coutaric acid (31)	295	163
6	B-type procyanidin dimer (31)	577	451, 425, 407, 289
7	Catechin (31,32)	289	245, 205
8	Vanillic acid (30,31)	167	152, 123
9	Caffeic acid (30,31)	179	135
10	Syringic acid(30,31)	197	182, 153
11	Epicatechin (31 32)	289	245, 205
12	<i>p</i> -Coumaric acid (30,31)	163	119
13	Ethyl gallate (31)	197	169, 125
14	Quercetin glucuronide (31)	477	301
15	Ferulic acid (31)	193	178, 149, 134
16	Myricetin glucoside (31)	479	317
17	Astilbin (31)	449	303
18	Myricetin (31)	317	179, 151
19	Trans-resveratrol (30,31)	227	185
20	Quercetin (31)	301	179, 151
21	Cis-resveratrol (30,31)	227	185
22	Ethyl caffeate (35)	207	179, 161, 135
23	Naringenin (31)	271	177, 151
24	Kaempferol (31)	285	257
25	Sulfonated B-type procyanidin dimer	657	369, 287
26	Sulfo-catechin	369	231, 289
27	Sulfo-caffeic acid	259	215, 179

COMPARING THE REACTIVITY OF NaHSO_3 , CYSTEINE AND GLUTATHIONE WITH *o*-QUINONES

Nucleophilic attack on enzymatically formed *o*-quinones was found to occur with NaHSO_3 , cysteine and glutathione (**Chapter 3**). There, only the formation of adducts in systems containing chlorogenic acid, mushroom tyrosinase and one sulfur-containing compound was described. To investigate which of these sulfur-containing compounds was most reactive with *o*-quinones, a competition experiment with NaHSO_3 , cysteine and glutathione was performed. Combinations of two or three of these sulfur-containing compounds (0.6 mM each) were simultaneously incubated (pH 6.5, adjusted using 0.1 mM NaOH, 25 °C) with catechin (0.3 mM) or caffeic acid (0.3 mM) and mushroom tyrosinase (21 U/mL). Reaction products were analyzed using RP-UHPLC-PDA-MS (as described in **Chapter 3**). The reaction products were identified based on MS analysis, and the relative amounts of the different products were determined based on UV peak area (at 280 nm), assuming comparable molar extinction coefficients for the different products formed. The results clearly indicated that cysteine has a higher tendency to form addition products when in direct competition with glutathione and NaHSO_3 (**Figure 5**). When catechin was incubated with combinations of NaHSO_3 , cysteine and glutathione or NaHSO_3 and cysteine, the sulfo-adduct represented less than 5 % of total reaction products, while cysteine-adducts represented 86 % or 97 %, respectively. When caffeic acid was incubated with NaHSO_3 , cysteine and glutathione or NaHSO_3 and cysteine, no sulfo-adduct was found at all, and cysteine adducts accounted for 95 % or 100 % of the reaction products. When the reactivity of only NaHSO_3 and glutathione was compared more sulfo-adduct was found, both for catechin (25 %) and for caffeic acid (14 %), but adduct formation with glutathione was preferred (75 % with catechin, 86 % with caffeic acid). When the reactivity of only cysteine and glutathione were compared, the relative amounts of cysteine and glutathione-adducts were 95 % and 5 %, respectively, for both catechin and caffeic acid.

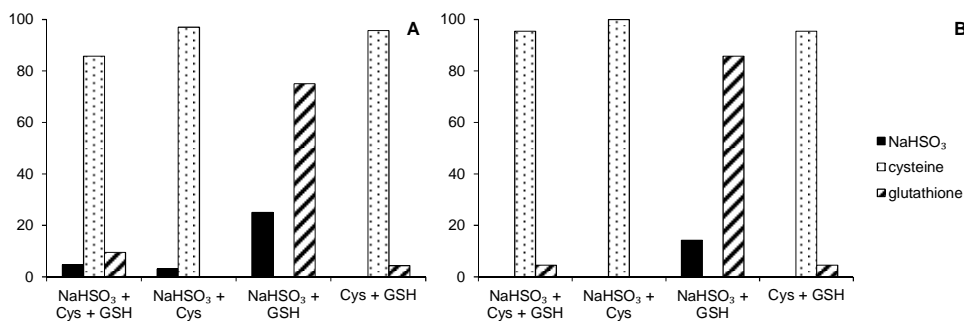


Figure 5. Relative amounts of reaction products formed upon incubation of catechin (**A**) or caffeic acid (**B**) with tyrosinase and different combinations of NaHSO_3 , cysteine (Cys) and glutathione (GSH). Amounts are expressed as percentages of total amount of products formed.

It should be noted that in case NaHSO₃ was used in these experiments, not all substrate was converted, due to inactivation of tyrosinase by NaHSO₃ (**Chapter 4**), while in the presence of only cysteine and glutathione all substrate was converted. Tyrosinase inhibition by NaHSO₃ was found to affect conversion of caffeic acid more than conversion of catechin. This probably indicated that catechin is a substrate with higher affinity for mushroom tyrosinase compared to caffeic acid, resulting in more substrate conversion during the time required for NaHSO₃ to inactivate tyrosinase. This might explain that sulfo-adducts were not found during incubation of caffeic acid with combinations of NaHSO₃ and cysteine. As the total amount of reaction products formed with caffeic acid is lower than with catechin, sulfo-caffeic acid that was potentially formed, could fall below the detection limit. To determine the ratio between the different reaction products after conversion of all substrate, the experiment could be repeated with sequential enzyme additions.

The results obtained demonstrate that of the three sulfur-containing compounds investigated, cysteine is most reactive with *o*-quinones, followed by glutathione and NaHSO₃. The fact that both thiols were more reactive than NaHSO₃ might be explained by the higher nucleophilicity of the thiol group, compared to the HSO₃⁻ ion. The oxygen surrounding sulfur in HSO₃⁻ has an electron withdrawing effect, in this way making the lone pair of electrons on sulfur less nucleophilic. The higher reactivity of cysteine compared to glutathione can probably be attributed to steric effects.

FEASIBILITY OF SULFITE REPLACEMENT WITH PLANT EXTRACTS

It was demonstrated that sulfite has a dual inhibitory mechanism on enzymatic browning: initial browning is prevented by trapping *o*-quinones in colorless sulfophenolics (**Chapters 2 and 3**), while in time mushroom tyrosinase was inactivated through covalent modification of an active site histidine residue (**Chapters 3 and 4**). This dual inhibitory mechanism makes sulfite a versatile inhibitor of browning, but it cannot be concluded which effect of sulfite is most important in the prevention of enzymatic browning. During the processing of potato juice, it is likely that the ability of sulfite to form sulfophenolics is the main mechanism at play. In sulfite-treated potato juice, almost all PPO substrates were found to be sulfonated, indicating that PPO was active, at least until most substrate was converted (**Chapter 2**). In wine, during the production of which sulfite is also used to prevent enzymatic browning, sulfophenolics were not found. This might be an indication that during wine making, the PPO inactivating effect of sulfite is more important.

Sulfite is a controversial additive to food, due to presumed health risks (9-11) and its reaction with vitamin B1 (12-14), and much research is dedicated towards finding natural alternatives (15-18). It is doubtful whether a natural inhibitor can be found that is as versatile as sulfite in its inhibitory effect on browning. As we demonstrated in **Chapter 5**, PPOs from different sources can respond completely different to inhibitors from plant

extracts, apparently indicating that inhibition is (at least to a certain extent) PPO-specific, which suggests that each raw material might require its own inhibitor. The application of plant extracts to inhibit browning might be further hampered by their influence on the taste of a product. Plant extracts are rich in phenolic compounds, which often have a bitter or astringent taste (19,20). Moreover, the phenolics present in plant extracts might also be substrates for PPO, in this way possibly increasing brown discoloration. Furthermore, many of the extracts used in our screening were colored themselves. The effects on taste and color could possibly be overcome by identifying and purifying the compound responsible for the inhibition observed with the plant extract. However, large scale purification of inhibitors from plant extracts would probably make application of such inhibitors economically unfeasible.

IMPACT OF UNRAVELING THE INHIBITORY MECHANISM OF SULFITE ON ENZYMATIC BROWNING

The knowledge obtained on inhibition of browning by sulfite might help in finding alternatives for sulfite. Possibly a natural sulfur-containing compound can be found that is capable of reacting in a similar way as sulfite, both with *o*-quinones (Chapters 2 and 3) and active site histidines (Chapter 4). In Chapter 3 some sulfur-containing compounds were investigated. It was found that reactions of the thiols cysteine and glutathione with *o*-quinones were similar to the reaction of sulfite with *o*-quinones. Although it was suggested that inactivation of mushroom tyrosinase occurred via nucleophilic addition of sulfite to a histidine residue in the active site, the nucleophiles cysteine and glutathione were not found to inactivate tyrosinase, even though thiols are more nucleophilic than sulfite. Possibly, their larger size in comparison to sulfite hinders the access of these thiols to the active site of tyrosinase. A thiol smaller than cysteine might offer opportunities in natural sulfite replacement. The reactivity of such a thiol with both *o*-quinones and tyrosinase remains to be established.

Another possibility by which the use of sulfite might be reduced, is to combine sulfite treatment with a method that delays browning. Two approaches that could be applied are temporarily inhibiting tyrosinase activity or temporarily preventing the formation of brown pigments. In the first approach, temporarily lowering the pH to a point sufficiently low for tyrosinase to be not catalytically active might be an option. In the meantime, a relatively small amount of sulfite might be able to irreversibly inactivate tyrosinase. For this strategy to be successful it is necessary to investigate the pH-dependence of irreversible inactivation by sulfite. Another consideration that needs to be taken into account is the possible influence of low pH on other properties of the product. For the second approach, ascorbic acid, which is known to delay browning (21), could be used. During the time required for sulfite to inactivate tyrosinase, ascorbic acid can prevent formation of brown pigments by reduction of the *o*-quinones formed. A factor that should be taken into account is the

competition between ascorbic acid and sulfite for reaction with the *o*-quinones formed. If sulfite would preferentially react with *o*-quinones, not enough sulfite might be present for inactivation of tyrosinase. Hence, the reactivity of sulfite with *o*-quinones relative to that of ascorbic acid should be determined. By fine-tuning the ratio of ascorbic acid and sulfite, it might be possible to considerably reduce the amount of sulfite currently needed, while achieving the same prevention of browning.

EXTRAPOLATION OF THE EFFECT OF SULFITE ON TYROSINASE-CATALYZED BROWNING TO OTHER PPOS AND LACCASE

The sulfonation of *o*-quinones during tyrosinase-catalyzed browning (**Chapters 2 and 3**) can very likely be extrapolated to inhibition of browning caused by other PPOs, as activity of all PPOs results in the formation of *o*-quinones. As discussed in the General Introduction of this thesis, enzymatic browning can also be induced by laccase (EC 1.10.3.2), which catalyzes the oxidation of *p*-diphenols and *o*-diphenols, resulting in *p*-quinones and *o*-quinones (22). It would be interesting to know whether a *p*-quinone could be sulfonated in a similar way as an *o*-quinone. It should, however, be taken into account that the laccase catalyzed quinone formation is different from that of PPO catalyzed quinone formation: laccase activity on a diphenolic substrate results in a radical, which can subsequently form the corresponding quinone, or react with other radicals to form polymers. In case radicals are polymerizing instead of forming quinones, reaction with sulfite is unlikely.

Considering that the type-3 copper center of PPOs is highly conserved among different species, it is likely that the reactivity of histidines in the active site of other PPOs with sulfite is similar to the observed reactivity of the active site of mushroom tyrosinase (**Chapter 4**). Mushroom tyrosinase has a thioether bond in the Cu-A site, which has also been found for other plant and fungal PPOs (1,23,24), while for bacterial PPOs a thioether has not been found (25,26). It would be interesting to see whether PPOs without the characteristic thioether can also be covalently inactivated by sulfite, perhaps the Cu-A site can also be modified in the absence of a thioether.

With respect to potential inactivation of laccases by sulfite, the differences between the laccase and PPO active sites have to be taken into account. While oxidation of *o*-diphenols in the type-3 copper center of PPO is characterized by concomitant reduction of oxygen (**Figure 3** in the General Introduction), the catalytic mechanism of laccases is more complex. Laccases have four copper ions, one of which is bound in a type-1 copper center, while the other three are bound in a combined, trinuclear type-2/type-3 copper center located inside the protein (27). The substrate to be oxidized binds close the type-1 copper center, after which an electron from the substrate is transferred to the trinuclear copper center, where reduction of oxygen to water takes place (28). Both in the type-1 copper center and in the trinuclear type-2/type-3 copper centers in laccase copper-coordinating histidine residues are present (**Figure 2** in the General Introduction). It

would be worthwhile to investigate whether the mechanism of covalent modification of a copper-coordinating histidine residue in mushroom tyrosinase (**Chapter 4**) can be extrapolated to either one or both of the two copper centers of laccase. A major aspect that might play a role is accessibility of the copper binding sites. Our results with mushroom tyrosinase demonstrated that inactivation by sulfite was prevented by presence of competitive inhibitors, indicating that the active site has to be accessible for sulfite to attach to a histidine residue (**Chapter 4**). The trinuclear copper center of laccase is more distant to the substrate binding site, buried inside the protein (29), and it is uncertain whether sulfite would be able to reach it. The type-1 copper center of laccase is closer to the substrate binding site (29), which is accessible for a wide variety of substrates, so it is more likely that sulfite would be able to access this site. Although the coordination of the single copper ion in this site is different from that of the two copper ions in mushroom tyrosinase, two histidine residues are involved. Possibly, one of these histidines can be covalently modified by sulfite, analogous to our observations in mushroom tyrosinase.

REFERENCES

1. Virador, V. M.; Reyes Grajeda, J. P.; Blanco-Labra, A.; Mendiola-Olaya, E.; Smith, G. M.; Moreno, A.; Whitaker, J. R., Cloning, sequencing, purification, and crystal structure of grenache (*Vitis vinifera*) polyphenol oxidase. *J. Agric. Food. Chem.* **2010**, *58*, 1189-1201.
2. Monagas, M.; Bartolomé, B.; Gómez-Cordovés, C., Updated knowledge about the presence of phenolic compounds in wine. *Crit. Rev. Food Sci. Nutr.* **2005**, *45*, 85-118.
3. Cheynier, V. F.; Trousdale, E. K.; Singleton, V. L.; Salgues, M. J.; Wylde, R., Characterization of 2-S-glutathionyl caftaric acid and its hydrolysis in relation to grape wines. *J. Agric. Food. Chem.* **1986**, *34*, 217-221.
4. Cejudo-Bastante, M. J.; Pérez-Coello, M. S.; Hermosín-Gutiérrez, I., Identification of new derivatives of 2-S-glutathionylcaftaric acid in aged white wines by HPLC-DAD-ESI-MSⁿ. *J. Agric. Food. Chem.* **2010**, *58*, 11483-11492.
5. Singleton, V. L.; Salgues, M.; Zaya, J.; Trousdale, E., Caftaric acid disappearance and conversion to products of enzymic oxidation in grape must and wine. *Am. J. Enol. Vitic.* **1985**, *36*, 50-56.
6. Ghiselli, A.; Nardini, M.; Baldi, A.; Scaccini, C., Antioxidant activity of different phenolic fractions separated from an Italian red wine. *J. Agric. Food. Chem.* **1998**, *46*, 361-367.
7. Berké, B.; Chèze, C.; Vercauteren, J.; Deffieux, G., Bisulfite addition to anthocyanins: revisited structures of colourless adducts. *Tetrahedron Lett.* **1998**, *39*, 5771-5774.
8. Wirth, J.; Morel-Salmi, C.; Souquet, J. M.; Dieval, J. B.; Aagaard, O.; Vidal, S.; Fulcrand, H.; Cheynier, V., The impact of oxygen exposure before and after bottling on the polyphenolic composition of red wines. *Food Chem.* **2010**, *123*, 107-116.
9. Bush, R. K.; Taylor, S. L.; Holden, K.; Nordlee, J. A.; Busse, W. W., Prevalence of sensitivity to sulfiting agents in asthmatic patients. *Am. J. Med.* **1986**, *81*, 816-820.
10. Lester, M. R., Sulfite sensitivity: significance in human health. *J. Am. Coll. Nutr.* **1995**, *14*, 229-32.
11. Riggs, B. S.; Harchelroad Jr, F. P.; Poole, C., Allergic reaction to sulfiting agents. *Ann. Emerg. Med.* **1986**, *15*, 77-79.
12. Combs Jr, G. F., Chapter 10 - Thiamin. In *The Vitamins (Fourth Edition)*, Academic Press: San Diego, CA, USA, 2012; pp 261-276.

13. Zoltewicz, J. A.; Kauffman, G. M.; Uray, G., A mechanism for sulphite ion reacting with vitamin B1 and its analogues. *Food Chem.* **1984**, *15*, 75-91.
14. Zoltewicz, J. A.; Uray, G., Thiamin: A critical evaluation of recent chemistry of the pyrimidine ring. *Bioorg. Chem.* **1994**, *22*, 1-28.
15. Chang, T.-S., An updated review of tyrosinase inhibitors. *Int. J. Mol. Sci.* **2009**, *10*, 2440-2475.
16. Kim, Y. J.; Uyama, H., Tyrosinase inhibitors from natural and synthetic sources: structure, inhibition mechanism and perspective for the future. *Cell. Mol. Life Sci.* **2005**, *62*, 1707-1723.
17. Loizzo, M. R.; Tundis, R.; Menichini, F., Natural and synthetic tyrosinase inhibitors as antibrowning agents: an update. *Compr. Rev. Food Sci. F* **2012**, *11*, 378-398.
18. Parvez, S.; Kang, M.; Chung, H.-S.; Bae, H., Naturally occurring tyrosinase inhibitors: mechanism and applications in skin health, cosmetics and agriculture industries. *Phytother. Res.* **2007**, *21*, 805-816.
19. Drewnowski, A.; Gomez-Carneros, C., Bitter taste, phytonutrients, and the consumer: a review. *Am. J. Clin. Nutr.* **2000**, *72*, 1424-1435.
20. Soares, S.; Kohl, S.; Thalmann, S.; Mateus, N.; Meyerhof, W.; De Freitas, V., Different phenolic compounds activate distinct human bitter taste receptors. *J. Agric. Food. Chem.* **2013**, *61*, 1525-1533.
21. Nappi, A. J.; Vass, E., Chromatographic analyses of the effects of glutathione, cysteine and ascorbic acid on the monophenol and diphenol oxidase activities of tyrosinase. *J. Liq. Chromatogr.* **1994**, *17*, 793 - 815.
22. Walker, J. R. L.; Ferrar, P. H., Diphenol oxidases, enzyme-catalysed browning and plant disease resistance. *Biotechnol. Genet. Eng. Rev.* **1998**, *15*, 457-498.
23. Klabunde, T.; Eicken, C.; Sacchetti, J. C.; Krebs, B., Crystal structure of a plant catechol oxidase containing a dicopper center. *Nat. Struct. Biol.* **1998**, *5*, 1084-1090.
24. Lerch, K., Primary structure of tyrosinase from *Neurospora crassa*. II. Complete amino acid sequence and chemical structure of a tripeptide containing an unusual thioether. *J. Biol. Chem.* **1982**, *257*, 6414-9.
25. Matoba, Y.; Kumagai, T.; Yamamoto, A.; Yoshitsu, H.; Sugiyama, M., Crystallographic evidence that the dinuclear copper center of tyrosinase is flexible during catalysis. *J. Biol. Chem.* **2006**, *281*, 8981-8990.
26. Sendovski, M.; Kanteev, M.; Ben-Yosef, V. S.; Adir, N.; Fishman, A., First structures of an active bacterial tyrosinase reveal copper plasticity. *J. Mol. Biol.* **2011**, *405*, 227-237.
27. Giardina, P.; Faraco, V.; Pezzella, C.; Piscitelli, A.; Vanhulle, S.; Sannia, G., Laccases: a never-ending story. *Cell. Mol. Life Sci.* **2010**, *67*, 369-385.
28. Solomon, E. I.; Augustine, A. J.; Yoon, J., O₂ Reduction to H₂O by the multicopper oxidases. *Dalton T.* **2008**, 3921-3932.
29. Rodgers, C. J.; Blanford, C. F.; Giddens, S. R.; Skamnioti, P.; Armstrong, F. A.; Gurr, S. J., Designer laccases: a vogue for high-potential fungal enzymes? *Trends Biotechnol.* **2010**, *28*, 63-72.
30. Vanhoenacker, G.; Villiers, A.; Lazou, K.; Keukeleire, D.; Sandra, P., Comparison of high-performance liquid chromatography — mass spectroscopy and capillary electrophoresis— mass spectroscopy for the analysis of phenolic compounds in diethyl ether extracts of red wines. *Chromatographia* **2001**, *54*, 309-315.
31. Hollecker, L.; Pinna, M.; Filippino, G.; Scrugli, S.; Pinna, B.; Argiolas, F.; Murru, M., Simultaneous determination of polyphenolic compounds in red and white grapes grown in Sardinia by high performance liquid chromatography–electron spray ionisation-mass spectrometry. *J. Chromatogr. A* **2009**, *1216*, 3402-3408.
32. Lazarus, S. A.; Adamson, G. E.; Hammerstone, J. F.; Schmitz, H. H., High-performance liquid chromatography/mass spectrometry analysis of proanthocyanidins in foods and beverages. *J. Agric. Food. Chem.* **1999**, *47*, 3693-3701.
33. Ricardo-da-Silva, J. M.; Rosec, J. P.; Bourzeix, M.; Mourgues, J.; Moutounet, M., Dimer and trimer procyanidins in Carignan and Mourvèdre grapes and red wines. *Vitis* **1992**, *31*, 55-63.

34. Lea, A. G. H., Reversed-phase gradient high-performance liquid chromatography of procyanidins and their oxidation products in ciders and wines, optimised by Snyder's procedures. *J. Chromatogr. A* **1980**, *194*, 62-68.
35. Celli, N.; Dragani, L. K.; Murzilli, S.; Pagliani, T.; Poggi, A., *In vitro* and *in vivo* stability of caffeic acid phenethyl ester, a bioactive compound of propolis. *J. Agric. Food. Chem.* **2007**, *55*, 3398-3407.

Summary

Enzymatic browning in foods occurs through the oxidation of phenolic compounds by polyphenol oxidases (PPOs), such as tyrosinase. Brown discoloration is a major quality issue in the processing of different foods and accounts for large economic losses in food industry. Sulfite is often used as an anti-browning agent, but its use is controversial due to presumed health risks and its detrimental effect on vitamin B1. Therefore, much research has been dedicated to finding alternatives. Surprisingly enough, despite its established use, the mechanism of browning inhibition by sulfite remains largely unknown, with different possible explanations proposed in literature. The aim of this thesis is to explain the inhibitory mechanism of sulfite on enzymatic browning in detail, by investigating its effects on reaction products of enzymatic browning and tyrosinase activity. Furthermore, two PPOs from different sources were used in a screening for potential inhibitory activity of plant extracts, to investigate whether they responded similarly.

Chapter 1 provides background information about different PPOs, their catalytic mechanism and some of their structural aspects. The mechanism of enzymatic browning is discussed, as well as different strategies to inhibit the formation of brown pigments.

Chapter 2 compares the effects of two commonly used anti-browning agents, sulfite and ascorbic acid, on the phenolic profile of potato juice. In the presence of ascorbic acid, two major compounds were obtained: 5-*O*-caffeoyl quinic acid (chlorogenic acid) and 4-*O*-caffeoyl quinic acid. In the presence of sulfite, their 2'-sulfo-adducts were found instead, the structures of which were confirmed by nuclear magnetic resonance spectroscopy and mass spectrometry. Applying a model system consisting of mushroom tyrosinase, chlorogenic acid and sodium hydrogen sulfite (NaHSO₃), it was demonstrated that sulfonation of chlorogenic acid occurred via tyrosinase-catalyzed *o*-quinone formation.

The same model system was used in **Chapter 3** to compare the effects of NaHSO₃ and other sulfur-containing inhibitors of enzymatic browning (cysteine, glutathione and dithiothreitol) on the tyrosinase-induced browning of chlorogenic acid. Development of brown color (spectral analysis), oxygen consumption, and reaction product formation (RP-UHPLC-DAD-MS) were monitored in time. It was found that the compounds showing anti-browning activity either prevented browning by forming colorless addition products with *o*-quinones of chlorogenic acid (NaHSO₃, cysteine, glutathione) or by inhibiting the catalytic activity of tyrosinase (NaHSO₃, dithiothreitol). NaHSO₃ was different from the other sulfur-containing compounds investigated, as it showed a dual inhibitory effect on browning. Initial browning was prevented by trapping the *o*-quinones formed in colorless addition products (sulfo-chlorogenic acid), while at the same time tyrosinase activity was inhibited in a time-dependent way, as was shown by pre-incubation experiments of tyrosinase with NaHSO₃. Furthermore, it was demonstrated that sulfo-chlorogenic acid and cysteinyl-chlorogenic acid were not inhibitors of mushroom tyrosinase.

In **Chapter 4**, the inhibition of tyrosinase activity by sulfite is addressed. Inactivation of mushroom tyrosinase by NaHSO₃ was found to be irreversible. By simultaneous incubation of tyrosinase with NaHSO₃ and a competitive tyrosinase inhibitor (tropolone or

kojic acid), it was demonstrated that NaHSO_3 acts in the active site of tyrosinase. RP-UHPLC-MSⁿ analysis of protease digests of NaHSO_3 -treated tyrosinase revealed peptides showing a characteristic neutral loss corresponding to the mass of SO_3 . Further fragmentation of these peptides revealed them to be homologous peptides containing two of the three histidine residues that form the copper-B binding site of mushroom tyrosinase isoforms PPO3 and PPO4. Peptides showing this neutral loss behavior were not found in the untreated control tyrosinase. Comparing the effect of NaHSO_3 on apo and holo-tyrosinase indicated that inactivation is facilitated by the active site copper ions. It was demonstrated that tyrosinase is inactivated by covalent modification of a single amino acid residue in the active site. Addition of sulfite most likely occurs on a copper-coordinating histidine residue, which is conserved in all PPOs.

Model systems are often used to screen for potential inhibitors of enzymatic browning. In **Chapter 5** the influence of the source of PPO used on the outcome of such a screening is addressed. Two different PPOs, mushroom tyrosinase (AbPPO) and potato PPO (StPPO), were used to screen 60 plant extracts for potential inhibitors of browning. Some plant extracts had different effects on the two PPOs: an extract that inhibited one PPO could be an activator for the other. As an example of this, the mate (*Ilex paraguariensis*) extract was investigated in more detail. In the presence of mate extract, oxygen consumption by AbPPO was found to be reduced more than 5-fold compared to a control reaction, whereas that of StPPO was increased more than 9-fold. RP-UHPLC-MS analysis showed that the mate extract contained a mixture of phenolic compounds and saponins. Upon incubation of mate extract with StPPO, phenolic compounds disappeared completely and saponins remained. Flash chromatography was used to separate saponins and phenolic compounds. It was found that the phenolic fraction was mainly responsible for inhibition of AbPPO and activation of StPPO. Activation of StPPO was probably caused by activation of latent StPPO by chlorogenic acid quinones. Our results show that screening approaches to find natural inhibitors should preferably be done with the target PPO.

Chapter 6 discusses the implications of our findings. The possible extrapolation of the observed sulfonation of phenolics to other food processes was investigated by analysis of wine, during the production of which sulfite is also used. Sulfophenolics were not found, suggesting that sulfonation of phenolics is not ubiquitous. The reactivity of the thiols cysteine and glutathione with *o*-quinones was compared to that of NaHSO_3 . Both thiols were found to be more reactive than NaHSO_3 . Furthermore, the possible extrapolation of the results found for the inhibition of tyrosinase-catalyzed browning by sulfite to other PPOs and laccases is discussed.

In conclusion, this thesis provides a molecular view on the inhibitory mechanism of sulfite on enzymatic browning. Sulfite slowly inactivates tyrosinase directly and irreversibly by covalent modification of the active site, whereas during the time span to effect this, reactive *o*-quinone products from residual tyrosinase activity are quenched by formation of sulfophenolics, which do not participate in browning anymore. Furthermore,

Summary

this thesis suggests that natural alternatives to replace more generic anti-browning agents, such as sulfite, are PPO specific.

Samenvatting

Enzymatische bruinkleuring in levensmiddelen vindt plaats via de oxidatie van fenolische verbindingen door polyfenol oxidases (PPOs), zoals tyrosinase. Bruinkleuring is een belangrijk kwaliteitsprobleem bij de verwerking van verschillende levensmiddelen en is verantwoordelijk voor grote economische verliezen in de levensmiddelenindustrie. Sulfit wordt vaak gebruikt als anti-bruiningsmiddel, maar het gebruik ervan is controversieel vanwege veronderstelde gezondheidsrisico's en zijn schadelijke effect op vitamine B1. Derhalve wordt veel onderzoek gewijd aan het vinden van alternatieven. Verrassend genoeg is, ondanks het wijdverbreide gebruik, het mechanisme waarmee sulfit bruinkleuring verhindert nog niet geheel bekend en worden er in de literatuur verschillende mogelijke verklaringen voorgesteld. Het doel van het in dit proefschrift beschreven onderzoek is het verklaren van het remmingsmechanisme van sulfit op enzymatische bruinkleuring, door de effecten van sulfit op de reactieproducten van enzymatische bruinkleuring en op de tyrosinase activiteit te onderzoeken. Daarnaast zijn PPOs van twee verschillende bronnen gebruikt in een screening voor remmers van bruining in plantenextracten, om te onderzoeken of beide PPOs vergelijkbaar reageren.

Hoofdstuk 1 geeft achtergrondinformatie over verschillende PPOs, hun katalytisch mechanisme en enkele van hun structurele eigenschappen. Het mechanisme van enzymatische bruinkleuring wordt besproken, evenals de verschillende strategieën om de vorming van bruine pigmenten te remmen.

Hoofdstuk 2 vergelijkt de effecten van twee veel gebruikte anti-bruiningsmiddelen, sulfit en ascorbinezuur, op het fenolische profiel van aardappelsap. In de aanwezigheid van ascorbinezuur werden twee componenten voornamelijk gevonden: 5-*O*-caffeoyl chinazuur (chlorogeenzuur) en 4-*O*-caffeoyl chinazuur. In aanwezigheid van sulfit werden in plaats daarvan hun 2'-sulfo-adducten gevonden, waarvan de structuur bevestigd is met behulp van kernspinresonantiespectroscopie en massaspectrometrie. Door middel van een modelsysteem bestaande uit champignon tyrosinase, chlorogeenzuur en natrium waterstof sulfit (NaHSO₃) wordt gedemonstreerd dat sulfonering plaatsvindt via tyrosinase gekatalyseerde *o*-chinon vorming.

Hetzelfde modelsysteem is in **Hoofdstuk 3** gebruikt om de effecten van NaHSO₃ en andere zwavelhoudende remmers van enzymatische bruinkleuring (cysteïne, glutathion en dithiothreitol) op tyrosinase geïnduceerde bruinkleuring van chlorogeenzuur te vergelijken. Ontwikkeling van bruine kleur (spectrale analyse), zuurstofverbruik en vorming van reactieproducten (RP-UHPLC-DAD-MS) werden gevolgd in de tijd. Er werd gevonden dat de verbindingen die bruining voorkomen dit deden door óf de vorming van kleurloze additieproducten met chinonen van chlorogeenzuur (NaHSO₃, cysteïne, glutathion) óf door het remmen van de katalytische activiteit van tyrosinase (NaHSO₃, dithiothreitol). NaHSO₃ was anders dan de andere onderzochte zwavelhoudende verbindingen, omdat het een dubbel remmend effect op bruining had. Initiële bruining wordt voorkomen door het wegvangen van de gevormde *o*-chinonen in kleurloze additieproducten (sulfo-chlorogeenzuur), terwijl tegelijkertijd tyrosinase activiteit op een tijdsafhankelijke

manier geremd wordt, zoals aangetoond werd door voorincubatie experimenten van tyrosinase met NaHSO_3 . Verder werd ook aangetoond dat sulfo-chlorogeenzuur en cysteïnyl-chlorogeenzuur geen remmers van champignon tyrosinase zijn.

In **Hoofdstuk 4** wordt de remming van tyrosinase activiteit door sulfiet behandeld. Gevonden werd dat de inactivatie van champignon tyrosinase door NaHSO_3 onomkeerbaar was. Door tyrosinase simultaan met NaHSO_3 en een competitieve tyrosinase remmer (tropolone of kojinezuur) te incuberen werd aangetoond dat NaHSO_3 werkzaam is in het actieve centrum van tyrosinase. RP-UHPLC-MSⁿ analyse van protease digesten van NaHSO_3 -behandeld tyrosinase onthulde peptiden die een karakteristiek neutraal verlies, overeenkomstig met de massa van SO_3 , vertoonden. Verdere fragmentatie van deze peptiden onthulde dat het homologe peptiden waren die twee van de drie histidine residuen bevatten die de koper-B bindingsplaats van de isovormen PPO3 en PPO4 van champignon tyrosinase vormen. Peptiden die dit neutrale verlies vertonen werden niet gevonden in een onbehandeld controlemonster. Het vergelijken van het effect van NaHSO_3 op apo- en holo-tyrosinase wees uit dat inactivatie wordt gefaciliteerd door de koper ionen in het actieve centrum. Aangetoond werd dat tyrosinase wordt geïnactiveerd door covalente modificatie van een enkel aminozuur residu in het actieve centrum. Additie van sulfiet vindt waarschijnlijk plaats aan een koper-coördinerend histidine residu, dat geconserveerd is in alle PPOs.

Modelsystemen worden vaak gebruikt om screenings voor potentiële remmers van enzymatische bruinkleuring uit te voeren. In **Hoofdstuk 5** wordt de invloed van de oorsprong van de gebruikte PPO op de uitkomst van zo'n screening behandeld. Twee verschillende PPOs, champignon tyrosinase (AbPPO) en aardappel PPO (StPPO), werden gebruikt om 60 plantenextracten te screenen voor potentiële remmers van bruinkleuring. Sommige plantenextracten hadden een verschillende uitwerking op de twee PPOs: een extract dat de ene PPO remde kon tegelijkertijd de andere PPO activeren. Als een voorbeeld hiervan is een mate (*Ilex paraguariensis*) extract in meer detail onderzocht. In de aanwezigheid van het mate extract werd het zuurstofverbruik van AbPPO meer dan vijfmaal verminderd ten opzichte van een controle reactie, terwijl het zuurstofverbruik van StPPO meer dan negenmaal toenam. RP-UHPLC-MS analyse wees uit dat het mate extract een mengsel van fenolische verbindingen en saponinen bevatte. Na incubatie van het mate extract met StPPO verdwenen de fenolische verbindingen volledig, terwijl de saponinen overbleven. Door middel van flash chromatografie werden saponinen en fenolische verbindingen van elkaar gescheiden. Gevonden werd dat vooral de fenolische fractie verantwoordelijk was voor remming van AbPPO en activatie van StPPO. Activatie van StPPO werd waarschijnlijk veroorzaakt door het activeren van latent StPPO door chinonen van chlorogeenzuur. Onze resultaten tonen aan dat het screenen om nieuwe remmers te vinden bij voorkeur dient te gebeuren met de PPO waarvoor de remmers uiteindelijk gebruikt zullen worden.

Hoofdstuk 6 bediscussieert de implicaties van de door ons gevonden resultaten. De mogelijke extrapolatie van de geobserveerde sulfonering van fenolen naar andere levensmiddelenprocessen werd onderzocht door middel van de analyse van wijn, waarbij in de productie ook sulfiet gebruikt wordt. Sulfofenolen werden niet gevonden, hetgeen suggereert dat sulfonering van fenolen niet alomtegenwoordig is. De reactiviteit van de thiolen cysteïne en glutathion met *o*-chinonen werd vergeleken met die van NaHSO₃. Beide thiolen waren reactiever dan NaHSO₃. Daarnaast wordt de mogelijke extrapolatie van de gevonden resultaten van remming van tyrosinase-gekatalyzeerde bruining door sulfiet naar andere PPOs en laccases besproken.

Samenvattend geeft dit proefschrift een moleculaire kijk op het remmingsmechanisme van sulfiet op enzymatische bruinkleuring. Langzaam inactiveert sulfiet tyrosinase direct en onomkeerbaar door covalente modificatie van het actieve centrum, terwijl in de tijd die hiervoor benodigd is reactieve *o*-chinonen, resulterend van resterende tyrosinase activiteit, weggevangen worden door de vorming van sulfofenolen, die niet meer kunnen reageren in de bruinkleuringsreactie. Daarnaast suggereert dit proefschrift dat natuurlijke alternatieven om generieke anti-bruiningsmiddelen zoals sulfiet te vervangen PPO specifiek zijn.

Acknowledgements

Alhoewel alleen mijn naam op het omslag van dit proefschrift prijkt, is het tot stand komen ervan niet slechts mijn verdienste, integendeel. Graag wil ik hier dan ook van de gelegenheid gebruik maken om hen die aan de totstandkoming ervan hebben bijgedragen te bedanken.

Allereerst Jean-Paul. Jou als co-promotor hebben is een voorrecht. Altijd weet je tijd te maken voor het bespreken van resultaten en manuscripten, desnoods aan de keukentafel in Renkum. Onze werkbesprekingen kenmerkten zich door een zeer ontspannen sfeer, waarbij tussen de serieuze discussies door altijd tijd was voor de nodige grappen. Mede dankzij jouw grenzeloos optimisme had ik na onze besprekingen vrijwel altijd een zonnigere kijk op de zaken dan ervoor. Ook heb ik goede herinneringen aan de gezamenlijke uitstapjes naar EU besprekingen en congressen.

Harry, bedankt voor je altijd scherpe en soms kritische inbreng bij het opschrijven van mijn resultaten. Jouw focus op de belangrijkste boodschap in mijn werk heeft mijn manuscripten zeker verbeterd. Ik zal de vraag ‘maar wat is nu de nieuwwaarde?’ dan ook niet snel vergeten.

Willem, Teunie en Adrie, als we er biochemisch even niet uitkwamen, of er weer eens oxygraafmetingen gedaan moesten worden, klopten we nooit tevergeefs aan in het Transitorium. Willem, als co-auteur van verschillende hoofdstukken van mijn proefschrift heb je je erg betrokken getoond. Bedankt voor jouw altijd snelle en zeer bruikbare op- en aanmerkingen bij mijn manuscripten. Teunie, bedankt voor het bespreken van resultaten en je hulp met de oxygraaf. Adrie, bedankt voor je hulp bij het maken van afbeeldingen van de active site van tyrosinase, waarmee je meteen een belangrijke bijdrage hebt geleverd aan het omslag van mijn proefschrift.

Stefano, thank you for working with us on the organic chemical aspects of our work, and for your contribution to chapter 4.

During my time as a PhD student I had the opportunity to supervise a number of BSc and MSc thesis students. Kuppu, Annewieke, Laurens, Wieteke, Jenna, Renske and Roelant, thank you very much for thinking with me and performing a lot of experiments. I hope your theses were a useful experience for you, I certainly learned a lot by supervising you.

Zonder apparatuur en chemicaliën geen onderzoek. Graag wil ik alle analisten bedanken voor het draaiende houden van apparatuur, het plaatsen van bestellingen, etc. In het bijzonder wil ik Mark bedanken voor de tijd die we samen hebben doorgebracht achter de LC-MS. Door de nodige problemen samen op te lossen heb ik veel geleerd. Naast experimentele uitdagingen zijn er soms ook organisatorische horden te nemen. Jolanda, bedankt voor je hulp bij deze zaken. En natuurlijk voor de altijd goed gevulde droppot.

A special thank you for Maxime and Annewieke, my paranymphs. Maxime, the past four years we were very much synchronized, from starting our thesis on the same day, till finishing the cover of our thesis in time, but it seems that you're going to overtake me on the very last day... Thank you very much for being my paranymph, as a doctor! Thank you even more for the great times we had in the lab and in the office, pulling jokes and having

good discussions on work and a range of other topics. Annewieke, ik vind het leuk dat zes maanden chlorogeenzuur en tyrosinase je er niet van hebben weerhouden nog vier jaar als aio met geoxideerde fenolen te gaan werken. Bedankt voor de lol in het lab, je eindeloze voorraad snoep, en natuurlijk dat je naast me wilt zitten tijdens mijn verdediging.

Finally, all the FCH colleagues that came and went during the past four years. It would be too much to name everyone here, but I thank you all for creating a great working atmosphere and for all the fun times we had during drinks, lab trips, PhD trips, dinners etc.

Tomas

About the author

CURRICULUM VITAE



Tomas F.M. Kuijpers was born on January 16th 1984 in Waalwijk, The Netherlands. After graduating from high school (Dr. Mollercollege, Waalwijk) in 2002, he started his studies in Food Technology at Wageningen University in 2003. His BSc degree was completed with a thesis on the potential antimicrobial properties of fermented soybeans at the Laboratory of Food Microbiology. His MSc degree in Food Biotechnology was completed with a thesis at the Laboratory of Food Chemistry, working on the induction and analysis of estrogenic compounds in soybeans. An industrial internship was performed at Dyadic Netherlands (Wageningen, The Netherlands), focusing on the purification and characterization of hemicellulases and pectinase from a fungal expression system. After graduation, Tomas worked as a researcher at the Laboratory of Food Chemistry for three months, before starting the work described in this PhD thesis in June 2009. Currently, Tomas is working as a researcher at the Laboratory of Food Chemistry.

Contact: tomas.kuijpers@gmail.com

PUBLICATIONS

Simons, R.; Vincken, J.-P.; Bohin, M.C.; **Kuijpers, T.F.M.**; Verbruggen, M.A.; Gruppen, H. Identification of prenylated pterocarpan and other isoflavonoids in *Rhizopus* spp. elicited soya bean seedlings by electrospray ionisation mass spectrometry. *Rapid Commun. Mass Spectrom.*, **2011**, *25*, 55-65

Narváez-Ceunca, C.-E., **Kuijpers, T.F.M.**, Vincken, J.-P., de Waard, P., Gruppen, H. New insights into an ancient anti-browning agent: formation of sulfo-phenolics in sodium hydrogen sulfite treated potato extracts. *J. Agric. Food. Chem.* **2011**, *59*, 10247-10255

Kuijpers, T.F.M., Narváez-Ceunca, C.-E., Vincken, J.-P., Verloop, A.J.W., van Berkel, W.J.H., Gruppen, H. Inhibition of enzymatic browning of chlorogenic acid by sulfur-containing compounds. *J. Agric. Food. Chem.* **2012**, *60*, 3507-3514

Kuijpers, T.F.M., Gruppen, H., Sforza, S., van Berkel, W.J.H., Vincken, J.-P. The anti-browning agent sulfite inactivates *Agaricus bisporus* tyrosinase through covalent modification of the copper-B site. *Accepted, FEBS J.*, **2013**

Kuijpers, T.F.M., van Herk, T., Vincken, J.-P., Janssen, R.H., Narh, D.L., van Berkel, W.J.H., Gruppen, H. Potato and mushroom polyphenol oxidase activities are differently modulated by natural plant extracts. *Submitted*

OVERVIEW OF COMPLETED TRAINING ACTIVITIES

Discipline specific activities

Conferences and meetings

- Oxizymes, Leipzig, Germany, 2010
- 26th international conference on polyphenols[†], Florence, Italy, 2012
- Oxizymes[‡], Marseille, France, 2012

Courses

- Graduate course advanced organic chemistry (ORC), Wageningen, The Netherlands, 2009-2010
- Advanced food analysis[†] (VLAG), Wageningen, The Netherlands, 2010
- Ion trap operations course, (Thermo Scientific), London, United Kingdom, 2011
- Food and biorefinery enzymology (VLAG), Wageningen, The Netherlands, 2011

General courses

- PhD introduction week (VLAG), Baarlo, The Netherlands 2010
- Philosophy and ethics of food sciences and technology (VLAG), Wageningen, The Netherlands, 2010
- Techniques for writing and presenting scientific papers (WGS), Wageningen, The Netherlands 2012
- Presentation skills, WUR language services, Wageningen, The Netherlands, 2012
- Teaching and supervising thesis students, Wageningen University, The Netherlands 2012

Optionals

- Preparation PhD research proposal, Wageningen, The Netherlands, 2009
- Food Chemistry study trip, Ghent, Belgium, 2009
- Food Chemistry PhD trip, Switzerland and Italy[‡], 2010
- Food Chemistry PhD trip, Singapore and Malaysia[‡], 2012
- Food Chemistry seminars, Wageningen, The Netherlands, 2009-2013
- Food Chemistry colloquia, Wageningen, The Netherlands, 2009-2013

[†] Poster presentation; [‡] Poster and oral presentations

VLAG: Graduate School for Nutrition, Food Technology, Agrobiotechnology and Health Sciences

WGS: Wageningen Graduate Schools

ORC: Laboratory of Organic chemistry, Wageningen University

The work described in this thesis was performed at the Laboratory of Food Chemistry, Wageningen University, The Netherlands. This research was financially supported by the Commission of the European Communities within the Seventh Framework Programme for research and technological development (FP7), Grant Agreement No. 226930.

Financial support from Wageningen University for printing this thesis is gratefully acknowledged.

This thesis was printed by GVO Drukkers en Vormgevers B.V. / Ponsen & Looijen, Ede,
The Netherlands

Edition: 275 copies

Tomas F.M. Kuijpers, 2013